A comparison of atmospheric CO_2 capture with steel slags in Mexico and the United Kingdom.

José Porfirio Del Ángel Lozano.
GUID: XXXXXXXX
Email: XXXXXXXX@research.gla.ac.uk
School of Geographical and Earth Sciences.
Supervisor: Dr John MacDonald.
Co-supervisor: Dr Alice Macente.

Abstract.

The continuous increase of greenhouse gas emissions, particularly CO_2, has prompted considerable concern and research towards decreasing their impact within the environment. Efforts to reduce CO_2 emissions have been developed with the aim of avoiding further increases in global temperature, one of the main repercussions of increased greenhouse gas emissions, and affecting the planetary balance. From this, carbon capture and storage, through mineral carbonation using iron and steel slags, could represent a solution for CO_2 emissions offsetting, while also repurposing of an industrial waste material.

The research work described within this thesis aims to address the environmental challenges related to excessive atmospheric CO_2, by investigating carbon removal strategies, focusing on the utilisation of iron and steel manufacturing slags for CO_2 sequestration, while efficiently repurposing industrial waste. The research will be structured around three main objectives. Firstly, it will assess the CO_2 capturing rates of legacy slags from Monclova, Mexico, and Ravenscraig, Scotland, using x-ray tomography and 3D data analysis. Secondly, it will estimate the volume of legacy iron and steel slags in Mexico through mapping former and current steelmaking locations, to calculate the CO_2 sequestration capacity of the country. Thirdly, it will evaluate the cementitious properties of legacy slags from England, Mexico, and Scotland for potential reutilization in sustainable concrete production. Through chapters II, III, and IV, the thesis aims to extend the understanding of mineral carbonation of iron and steel manufacturing slags to mitigate carbon dioxide emissions.

This research highlighted the key role of humidity along passive mineralisation of CO_2 within slag heaps, as the amount of carbonated CO_2 quantified in Scottish slags was double that of Mexican slags. Within the 273 K tonnes of slags stockpiled across Mexico, 5.7 K tonnes of CO_2 have been mineralised; and there is an estimated potential of 160 K tonnes of CO_2 that can be captured through enhanced carbonation. Potential pozzolanic behaviour were found in legacy iron and steel slags from England, Mexico and Scotland, where Blast Furnace and Basic Oxygen Furnace slags showed higher reactivity than Electric Arc Furnace slags, however further research is needed to determined their capacity to be used as replacement for Ordinary Portland Cement. The findings from this research aim to extend the understanding on iron and steel slags and their wider use for environmental remediation and a source of materials for various industrial fields, not only correlated to steel manufacturing.

University of Glasgow

College of Science and Engineering

Statement of Originality to Accompany Thesis Submission

Name: José Porfirio Del Angel Lozano

Registration Number: XXXXXXXXX

I certify that the thesis presented here for examination for a PhD degree of the University of Glasgow is solely my own work other than where I have clearly indicated that it is the work of others (in which case the extent of any work carried out jointly by me and any other person is clearly identified in it) and that the thesis has not been edited by a third party beyond what is permitted by the University's PGR Code of Practice.

The copyright of this thesis rests with the author. No quotation from it is permitted without full acknowledgement.

I declare that the thesis does not include work forming part of a thesis presented successfully for another degree.

I declare that this thesis has been produced in accordance with the University of Glasgow's Code of Good Practice in Research.

I acknowledge that if any issues are raised regarding good research practice based on review of the thesis, the examination may be postponed pending the outcome of any investigation of the issues.

Signature: …… ……

Date: ……March 31st, 2024……

Acknowledgment.

In 2019, my PhD journey started with the intention of conducting research to make a positive contribution to my home country. After four years filled with both remarkable experiences and challenges, I am happy the thesis is finally complete. It not only contains the findings from the research work completed but also reflects all the knowledge and experiences gained throughout these years.

I feel so proud of the work done in the past few years and grateful for all the people involved in this journey, thank you all…

I would like to express my gratitude to Dr John MacDonald, my supervisor, for his invaluable support, patience and guidance through the entire process of completing this research project. His experience and advice were key in completing this huge step. A massive thank you for always give me your time and always helped me to keep my focus in continuing my PhD.

Thank you to Dr Alice Macente, co-supervisor within the project, who always was keen to help and contribute, while sharing knowledge and advice. Thank you!

Thank you to the School of Geography and Earth Sciences and the University of Glasgow for making this experience even better than I expected! Thank you to all the staff and colleagues that made this time so enjoyable and full of new experiences. If I had the chance to start my PhD again, I will always be choosing Glasgow University.

Thank you to the "Consejo Nacional de Ciencia y Tecnología (CONACyT) for your valuable support during my studies.

Thank you to all my PGR friends in the Molema building and in the East Quad, I will always have in my memory the coffee mornings and our chats in the office, I am sure you all will be amazing researchers.

Thank you to my mom, my dad, and my always cheerful sister, who shared their love and joy with me at every stage of this journey. Thank you to all my family for continuously expressing how proud you were of me pursuing my PhD and for your unwavering support. I am happy to say that from now onwards I will be joining all family gatherings as the thesis is done!

Thank you to all my dear friends from all around the world. Your support has been invaluable during these challenging times. Your encouragement and humour have helped me stay grounded and positive. I am grateful for your friendship and for the laughter you've brought into my life.

A very special thank you to my dear ones that are no longer in this world, you are missed here.

Thank you all for being part of this experience! Muchas gracias!

Sincerely

José Porfirio Del Angel Lozano.

Table of content.

List of figures.

List of tables.

Abbreviations.

CCUS	Carbon Capture Utilisation and Storage
CCS	Carbon Capture and Storage
CCU	Carbon Capture and Utilisation
CO_2	Carbon Dioxide
BF	Blast Furnace (slag).
BOF	Basic Oxygen Furnace (slag).
EAF	Electric Arc Furnace (slag).
LF	Ladle Furnace (slag).
GGBFS	Ground Granulated Blast Furnace (slag).
GHG	Greenhouse gases
SCM	Supplementary Cementitious Material.
SS	Steel slag.
XCT	X-ray Computed Tomography.
XRD	X-ray Diffraction.

Chapter I. Introduction.

1.1 Context of the Research Project.

1.1.1 Definition of the Problem.

The continuous increase in the levels of greenhouse emissions have given rise to global concern on the escalating impact these could have on the atmosphere and the planetary environment. The European Commission, in their most recent report, indicated that global greenhouse gas emissions measured for 2022 increased 1.4% since 2021 (Crippa et al., 2023), with a total of 53.8 Gt CO_{2eq} in 2022, from which CO_2 represented 71.6%, CH_4 21%, N_2O 4.8% and F-gases 2.6%. The impact of greenhouse gases on the climate is undeniable, and every year the world continues to face an increase in the severity of climate events, for instance extended dry seasons, above/below normal temperatures, extreme rainfall, floods, etc. This demonstrates the need to develop remediation strategies centred on the reduction of emissions. Extended efforts on decreasing carbon dioxide continue to grow but are still limited in their scope to solve the environmental problem.

In this context, it is fundamental to find strategic solutions to mitigate these above normal levels of greenhouse gases, mainly targeting increasing emissions of carbon dioxide, where industrial activities play a main role as major contributors to the release of greenhouse gases to the atmosphere. As reported by the National Oceanic and Atmospheric Administration (2023), atmospheric CO_2 emissions were 417.06 ppm on their 2022 measurements, which is 50% higher than pre-industrial levels. In particular, energy production, transportation and the manufacturing of cement, steel and chemicals are considered principal sources of the increasing levels of atmospheric CO_2.

Carbon capture and storage has demonstrated great potential to strategically offset excessive CO_2 from industry and the atmosphere (International Energy Agency, 2023). Within the carbon capture technologies, the mineral carbonation approach using iron and steel slags has shown suitable characteristics to be implemented not only as a carbon removal technology, but also as a waste management option (Baras et al., 2023).

1.1.2 Project Outline.

This thesis aims to contribute within the environmental context provided, by conducting research for the development of extended carbon removal efforts and strategies, particularly where slags from iron and steel manufacturing can facilitate CO_2 sequestration, while serving as an efficient option for industrial waste management. Therefore, this work will focus on three key objectives below, which will be further developed within chapters two, three, and four.

1. To provide underpinning knowledge on the CO_2 capturing rates of legacy slags to be used for carbon removal in the context of Mexico and Scotland. This will involve the quantification of carbonated CO_2 within slags from Monclova, Mexico and Ravenscraig, Scotland, using x-ray tomography, 3D data analysis and the assessment of the potential parameters influencing carbonation reaction at both contrasting sites.

2. To estimate the volume of legacy iron and steel slags accumulated in Mexico by mapping former and current steelmaking locations using Quantum Geographic Information System (*QGIS*) and historical records of the steel industry evolution from the country. This inventory of Mexican iron and steel slag resources would enable calculation of the CO_2 sequestration capacity of the country to facilitate their wider utilisation.

3. To evaluate cementitious properties of legacy slags from England, Mexico and Scotland for their potential reutilisation in cement replacement for sustainable concrete. Reactivity and hydraulic behaviour are evaluated using x-ray diffraction, isothermal calorimetry and thermogravimetric analysis to better understand the kinetics of the iron and steel slags when used as supplementary cementitious materials under controlled conditions.

The thesis seeks to increase the understanding of mineral carbonation of iron and steel manufacturing slags in the context of minimising carbon dioxide in the atmosphere. In chapter two, the utility of slag for passive carbonation is evaluated as a carbon removal technology in Scotland and Mexico, while chapter 3 builds on this by determining the potential of legacy slag in Mexico as a resource of carbon dioxide removal. Chapter 4 explores the potential of Mexican and UK slags for a different context for reducing net CO_2 emissions from industry, in this case as a replacement for Ordinary Portland Cement.

1.2 Literature Review.

1.2.1 Introduction.

The current environmental context is mostly defined by the excessive greenhouse gas emissions on the atmosphere and the influence these have on global warming and climate change. Anthropogenic emissions of greenhouse gases (*GHG*) such as CO_2 are accelerating global climate change, impacting ecosystems and biodiversity (Roy et al., 2023; Thonemann et al., 2022a). The strong correlation between GHG and anthropogenic activities is considered the origin of the current environmental imbalance. Unfortunately, human evolution, particularly, in relation to industrial development, has produced over 1.5 trillion tons of carbon dioxide since the beginning of industrialization. Pre-industrial CO_2 emissions were estimated around 280 ppm, that is ~ 38 % less than the latest 417.06 ppm (2022) measured by the National Oceanic and Atmospheric Administration (2023), demonstrating the rapid increase in CO_2 concentrations in the atmosphere within a narrow period.

This current overview on the global environmental context reinforces the need to achieve Net-Zero by 2050 (Davies & Hastings, 2022). The short-term achievements on mitigation strategies for environmental issues will determine the upcoming context on the variation of temperature and climate patterns derived from high GHG levels, making clear that efforts towards decarbonising technologies and the transition into a more sustainable way of life is needed (Roy et al., 2023). This transition should involve significant efforts to reduce fossil fuels by utilising renewable energy sources such as wind, solar, hydroelectric, geothermal, etc.(Davies & Hastings, 2022). Furthermore, there a need to reach communal agreements on international policy making and promote circular economy, to provide a uniform global perspective on environmental legislation (Davies & Hastings, 2022). There is need to improve research and technology in all the sectors involved, supporting a collective approach to reduce greenhouse gas emissions, particularly CO_2, where carbon capture utilisation and storage should play a key role in reducing atmospheric CO_2 concentration.

1.2.2 Carbon Capture Utilisation and Storage fundamentals.

Carbon removal technologies began in the mid-20th century, as a response to the early concern about increasing levels of CO_2 and their influence on global temperature rise. The understanding of the environmental disruption enabled initial remediation efforts, from where the earliest versions of current carbon capture technologies emerged.

In this way, Carbon Capture Utilisation and Storage (*CCUS*) is the consolidation of methods and technologies to capture CO_2 emissions, either from the atmosphere or from anthropogenic point sources, for utilisation implications or permanent storage. Although Carbon Capture Utilisation and Storage (*CCUS*) includes diverse carbon removal options as reported from Thonemann et al. (2022a), it is common to find variations on the acronym used:

- **CCUS** (*carbon capture utilisation and storage*) is used for decarbonising methods with human intervention, where some of the captured CO_2 has a further use, e.g., industrial facilities or mineral carbonation, and some is stored, e.g. in geological formations.
- **CCS** (*carbon capture and storage*) implies CO_2 capture for long-term storage in geological formations.
- **CCU** (*carbon capture and utilisation*) is focused on capturing CO_2 for commercial aims, e.g., in the chemical or pharmaceutical industry.

The operational scope of CCUS is diverse and highly adaptable, involving the removal of carbon dioxide from industrial processes or human intervention on natural CO_2 sequestration mechanisms to maximise their capturing rates. CO_2 is separated from gaseous streams within industrial processes (*e.g., power generation or manufacturing*) using pre-combustion, post-combustion or oxy-fuel methods. It is then compressed and transported for wider utilisation or into permanent storage sites such as depleted hydrocarbons reservoirs or saline formations. In the second approach, examples of the Earth's natural mechanisms to absorb atmospheric CO_2 are photosynthesis, oceanic carbon uptake or mineral carbonation (*mineral/rock weathering*) of metal oxides and silicate compounds, precipitating CO_2 into stable carbonates.

Carbon Capture facilities have gained wider acceptance as key contributors to the remediation efforts to avoid the 1.5 to 2 °C increase on global temperature by 2050. Currently, 45 Mt of CO_2 are being captured each year by the 40 operating facilities installed across the globe (Herzog, 2023). This is consistent with the information provided by the International Energy Agency report (2023) where it is mentioned that the amount of CCUS facilities will be doubled by 2030 with a capturing potential up to 125 Mt of CO_2 per year. Although carbon capture and storage methods have proven their efficiency, it is also valuable to explore all carbon sequestration technologies such as: ocean, biological, geological or mineral carbonation (Yadav & Mehra, 2017) (*see Figure 1*). Within mineral carbonation, the use of geomaterials as a CO_2 sequestration approach could simultaneously contribute to better waste management of high calcium/magnesium/silicon industrial by-products like fly-ash or steel slags.

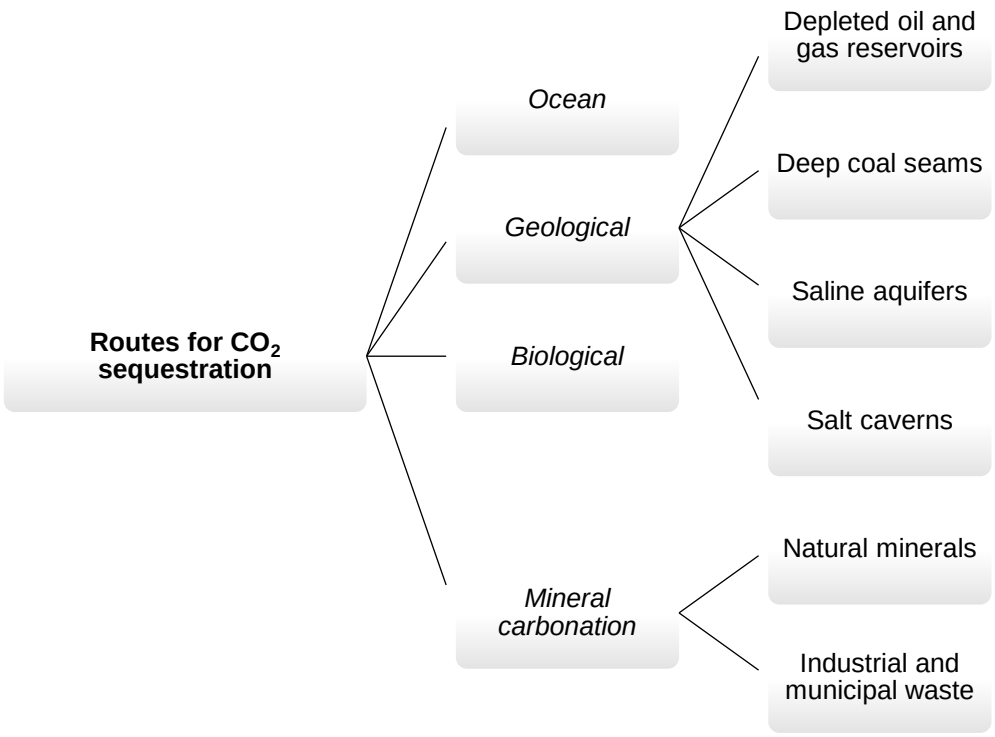

Figure 1 *Summary of CO_2 sequestration routes, based in literature from Yadav & Mehra (2017).*

1.2.3 Mineral carbonation.

Mineral carbonation is the conversion of atmospheric carbon dioxide into stable carbonate compounds. This carbon sequestration reaction can occur passively (no human intervention) within geological timescales on natural magnesium/calcium silicates or metal oxides, where atmospheric CO_2 reacts with the alkaline compounds, precipitating into solid stable carbonates like calcite (*$CaCO_3$*), dolomite (*$Ca0.5MgO{\cdot}5CO_3$*), magnesite (*$MgCO_3$*) or siderite (*$FeCO_3$*) (Olajire, 2013). Also known as mineral weathering, passive mineral carbonation of alkaline compounds has captured more than ~39,000,000 Gt of CO_2 over geologic time (Oelkers & Cole, 2008) on geogenic materials such as ultramafic rocks (*serpentine, peridotite rocks, olivine*) or calcium-silicate minerals (*wollastonite*) (Thonemann et al., 2022a).

Mineral carbonation also can occur actively, as a human-intervened process, where the mineral weathering reaction is accelerated in a controlled environment under supervised conditions. Active mineral weathering has shown high performance adaptability, as metal oxides and calcium/magnesium silicates derived from industry showed suitable reactivity to be reactants during the controlled mineralization of CO_2 (Gao et al., 2023).

There has also been interest in the wider utilisation of the carbonated products, for instance as a supplementary construction material (Meijssen et al., 2023). A separate approach on mineral carbonation mechanisms is defined by where the process takes place, whether in-situ or ex-situ; during in-situ carbonation CO_2 is injected into underground alkaline sources with suitable reactivity characteristics (B. Wang et al., 2021).

This mineral carbonation approach involves a preliminary assessment on the site to assure the subsurface is adequate to inject CO_2 and permeability conditions are in place (Olajire, 2013). Ex-situ carbonation is performed above ground where the mineralization reaction between the alkaline compound and atmospheric CO_2 occurs in a controlled environment (Stokreef et al., 2022; B. Wang et al., 2021). Studies have shown that in both mineral carbonation approaches, some industrial by-products such as iron and steel slags have shown higher reactivity when compared to natural materials, supporting this sequestration method as a strategic solution for CO_2 emissions decrease and better waste management from related industries. Figure 2 summarizes ex-situ mineral carbonation methods.

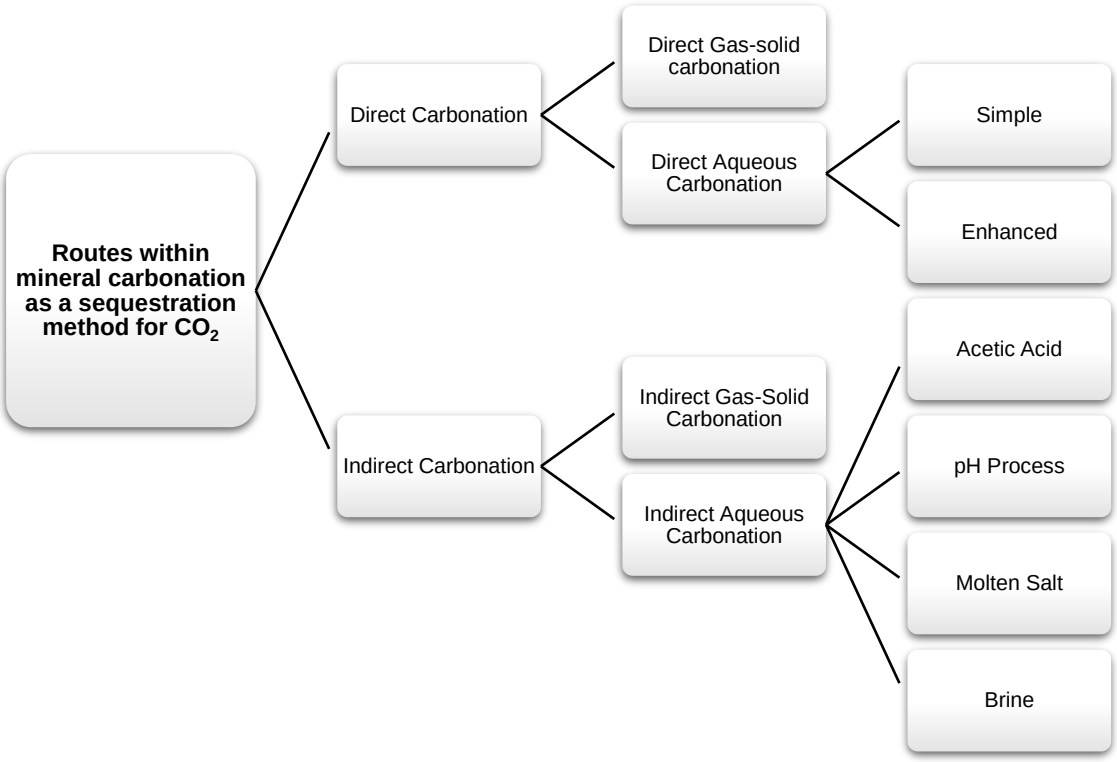

Figure 2 *Ex-situ mineral carbonation methods based in the work from Yadav & Mehra (2017).*

1.2.3.1 Mineral carbonation thermodynamics.

Mineral carbonation involves different chemical reactions dependent on the kinetics of the alkaline compound reacting with carbon dioxide; this carbonation process might occur in a single or multiple stages within a direct (*fluid-mediated/aqueous carbonation*) or indirect reaction. The general mineral carbonation process is described in *Reaction 1* below (Stokreef et al., 2022), where a metal oxide (*MO*), commonly Calcium, Magnesium, Iron, reacts with gaseous carbon dioxide to produce a stable carbonate compound in an exothermic reaction.

Reaction 1.

$$MO_{(s)} + CO_{2(g)} \rightarrow MCO_{3(s)} + heat$$

Reaction 2 is a generalised reaction for the mineral weathering reaction of calcium and magnesium silicates occurring in nature (Rahmanihanzaki & Hemmati, 2022):

Reaction 2.

$$(Ca,\ Mg)SiO_{3(s)} + CO_{2(g)} \rightarrow (Ca,\ Mg)CO_{3(s)} + SiO_{2(s)}$$

The chemical composition of the metal oxides determines the amount of heat released during the mineral carbonation reaction, for instance magnesium oxides reacting with atmospheric CO_2 heat release is -118 kJ/mol and for calcium oxide mineral carbonation the heat released is -179kJ/mol. See *Reaction 3.*

Reaction 3.

$$MgO_{(s)} + CO_{2(g)} \rightarrow MgCO_{3(s)}\ (\Delta H_r = -118\frac{kJ}{mol})$$

$$CaO_{(s)} + CO_{2(g)} \rightarrow CaCO_{3(s)}\ (\Delta H_r = -179\frac{kJ}{mol})$$

The thermodynamics of mineral carbonation indicates solid carbonates formation is favoured when pressure and temperature parameters are both increased, and when water is present as a catalyst medium; when this reaction occurs at environmental conditions the conversion time from gas to solid is longer than when performed under controlled conditions (Q. Wang, 2019).

1.2.3.2 Mineral carbonation using industrial waste.

Mineral carbonation is a highly adaptable process with suitable thermodynamics for actively sequestering atmospheric CO_2; these characteristics in addition to the abundance of alkaline waste from industry creates an advantageous scenario for the technology to succeed. Metal oxides and calcium/magnesium silicates derived from industry such as gypsum, red mud, steel slags and fly ash, have shown suitable properties to react with atmospheric CO_2 under controlled conditions to produce stable carbonates (Miao et al., 2023; B. Wang et al., 2021). For instance, iron and steel slags have shown carbonation rates of up to 360 kg of CO_2 per ton of slag (W. Liu et al., 2021). This not only will contribute to reducing the steel industry carbon footprint, it also could provide an extended mitigation solution to reduce global CO_2 levels in the atmosphere.

Although the alkaline characteristics of steel slag provide a favourable reactant to mineralize CO_2, there are existent gaps to fill on the active utilisation of mineral carbonation, as carbonation rates of steelmaking slag are dependent on the composition, steel making method used, and post processing conditions among other factors (Rahmanihanzaki & Hemmati, 2022). Thus, further understanding on the reaction mechanisms and external factors influencing the carbonation of the slag is needed. This to set mineral carbonation of iron and steel slag as a feasible option to mitigate carbon dioxide emissions and provide better solid waste management for industry (Thonemann et al., 2022b).

1.2.4 Iron and steel slag fundamentals.

Ferrous (*from iron and steel making*) slags are alkaline byproducts resultant of the melting of iron ores, limestone or dolomite (*flux*) and coke (*fuel and reductant*) for iron and steel making (Piatak et al., 2015a). The production methods employed determine the type and composition of the slag (Jiang et al., 2018; Thomas et al., 2018); characteristics such as a dark glassy appearance, porous structure or a colour range in between black and brown with shades of grey are visual indicators of slag (Jiang et al., 2018). Such characteristics are also determined during the cooling process of the slag; while rapid cooling processes produce an amorphous structure, slower cooling processes or the addition of heat treatment create slags with crystalline properties (Yildirim & Prezzi, 2011). Moreover, within the slag's morphology, porosity becomes of significance by providing a distinctive structure for mineral carbonation to occur within the pores of the rock (Li et al., 2022).

Slag mineralogy is partly determined by the production process and the chemistry of the raw materials. Mineral phases found in slags have variable chemical properties chemical properties, however common phases identified through mineralogical analysis by X-Ray Diffraction (*XRD*) include: olivine group phases ($Ca, Fe, Mg, Mn)_2SiO_4$, larnite (β-Ca_2SiO_4), monticellite ($CaMgSiO_4$), forsterite (Mg_2SiO_4) (Piatak et al., 2015b); or as considered by Li et al. (2022), there are some basic phases for instance found in most steel slags, for instance, tricalcium silicate (C_3S), dicalcium silicate (*e.g.,* β-C_2S, α-C_2S, *and* γ-C_2S), dicalcium ferrite (C_2F), and the inert RO phase ($MgO{\cdot}xFeO$).

Although chemical, mineralogical and morphological properties of the ferrous slags are determined by the smelting route followed (*BOF, EAF, BF*), the main composition of slags is based on high calcium and magnesium silicates (*olivine and melilite groups*), oxides and significant levels of Fe, Ca and Al. Pure metals, intermetallic compounds, sulfides and calcite are also found in lower proportions (Piatak et al., 2015b; Yildirim & Prezzi, 2011).The understanding of the variations in these properties is key to explore their potential utilisation, for instance as supplementary construction materials or for CO_2 sequestration.

1.2.5 Types of iron and steel slags.

There are different types of slags with variable compositions, based on their production and post-processing methods (Liu et al., 2019). For instance blast furnace (*BF*) slag is originated during the initial stage of the process when iron ore is blended with scrap steel on the blast furnace for ironmaking; subsequent processing of steel making based on the final product requirements like steel type or grade will define the slag properties and classification. Steel making slags are classified by the furnace used: Basic Oxygen Furnace (*BOF*), Electric Arc Furnace (*EAF*) or Ladle Furnace (*LF*) (Yildirim et al., 2023). There are additional slag classifications like open-hearth (no longer common) or ground granulated blast furnace slag (*GGBFS*) whose characteristics are defined by post-processing methods used on blast furnace slags.

A schematic of the main phases of iron and steel manufacturing is illustrated within Figure 3, offering a brief summary of the raw materials and showing how the operation evolves, where molten iron is produced to further derived in different grades of steel. Slags are also produced during the different stages, as previously mentioned.

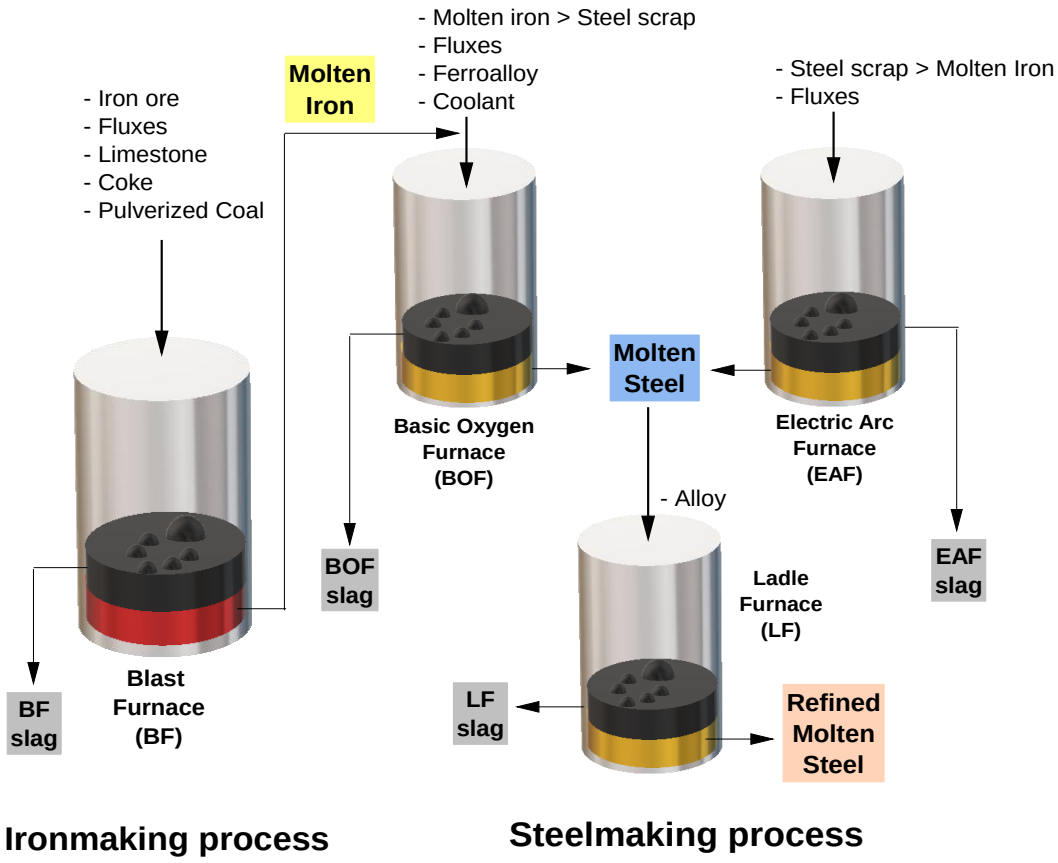

Figure 3 *Schematic of iron and steel production (modified from the illustration by Piatak et al. (2015b)).*

1.2.5.1 Blast Furnace slag (BF).

Blast Furnace (*BF*) slag is produced during the molten and metal refining phase during iron making (Piatak et al., 2019). The production method, where between 300 to 1000 kg of BF slag are produced per tonne of iron (Chen et al., 2021), starts by the addition of Fe ore, coke and fluxes (*limestone or dolomite*) into a blast furnace, from which pig iron is produced (*molten Fe*) and as a byproduct BF slag is formed (Piatak et al., 2015b). This chemistry of BF slags typically involves Al_2O_3, FeO, K_2O, MgO, MnO, Na_2O among other component traces (Barabanshchikov et al., 2020; Piatak & Ettler, 2021c).

Once the slag is produced, the post-processing methods followed could be slow cooling under open-air conditions, which gives crystalline characteristics and a porous structure within the slag. Or involving the use of water in moderate amounts as post-processing route, determining a porous crystalline and glassy characteristics (Ghorbani et al., 2023; Piatak et al., 2015b).

Furthermore, faster cooling methods, such as pelletizing or granulating, produce blast furnace slags in the form of glassy and porous pellets. For example, granulated BF slags are characterized by vitrified granules, which enhance the strength of concrete blends over decades (Moranville-Regourd et al., 2019). Within these BF slags, slow cooling slags have shown beneficial characteristics for reutilisation as construction aggregates, while BF pelletized and moderate water-cooling slags are only suitable for lightweight construction purposes, due to low density properties (Piatak et al., 2015b).

1.2.5.2 Ground Granulated Blast Furnace slag (GGBFS).

Ground Granulated Blast Furnace slags (*GGBFS*) are studied for their feasibility to act as a partial replacement for Ordinary Portland Cement (*OPC*) in concrete blends (Barabanshchikov et al., 2020). This slag type is derived from the post-processing of Blast Furnace (BF) slags through a rapid quenching method using water or steam (Piatak & Ettler, 2021a). This cooling route produces granular products with glassy characteristics that are ground to produce a fine powder to be used as supplementary cementitious material due to its amorphous nature (Wang & Suraneni, 2019). Chemical composition of this slag involves calcium silicates, calcium aluminates and calcium ferrites; although it has an amorphous nature, some traces of crystalline fukalite ($Ca_4Si_2O_6(CO_3)\ (OH)_2$) is commonly found (Wang & Suraneni, 2019). Among other properties, the hydraulic reactivity of GGBFS enables their use as cementitious material, as when part of a concrete blend, the material contributes to strength and durability (Snellings et al., 2023; Suraneni & Weiss, 2017).

1.2.5.3 Basic Oxygen Furnace slag (BOF).

Above 1600 °C within a Basic Oxygen converter where steel scraps and pig iron are added, Basic Oxygen Furnace (*BOF*) slag is produced as a residual component from steel manufacturing (Ragipani et al., 2021). Lime (*CaO*) and dolomite ($Mg\ Ca\ (CO_3)_2$) are commonly added in the mixture as chemical removal agents for sulphur and phosphorous content (Piatak et al., 2015b; Piatak & Ettler, 2021a). As part of the process, BOF slags are removed and post-processed (cooling), typically following an air-cooling method, where characteristics of the slag would be impacted, such as mineral composition, phase and particle size and also the degree of crystalline structure developed during cooling (Chang et al., 2011; Humbert & Castro-Gomes, 2019; Shi, 2004).

The composition of air-cooled BOF slags as documented by Ragipani et al. (2021) is as follows: CaO: 42–55%, SiO_2: 12–18%, Fe: 14–20%, MgO: 5–8%, MnO: ≤5.0%, Al_2O_3: ≤3.0% Ca_2SiO_4, $3CaO.P_2O_5$, $Ca_2Fe_2O_5$, CaO, MgO, (Mg, Fe, Mn) O.

If water-cooling is applied as a post-processing route for BOF slags, the result is a low glass content with higher amounts of tricalcium silicates and free lime (Li et al., 2022). When BOF slags cooled, physical characteristics typically are dense and granular texture with visible pores in the surface, where chemical composition is dependent on the raw materials, steel production method used and the cooling process selected (Polettini et al., 2016). Based on its properties, BOF slags are suitable for its use in construction as aggregates, in pavement structures or in sustainable concrete production (O'Connor et al., 2021). An additional use that BOF slags have are for soil remediation based on its high calcium content (Humbert & Castro-Gomes, 2019). Moreover, iron and phosphorus metal extraction can occur in BOF slags. In terms of carbonation potential, Eloneva et al. (2008) calculated that a potential ~170 million tonnes of CO_2 can be sequestrated in steel making slags (*BOF and EAF*), which is 0.6% of the total CO_2 emitted annually from the iron and steel industry.

1.2.5.4 Electric Arc Furnace slag (EAF).

Besides BOF slags, Electric Arc Furnace slags (*EAF*) are considered primary steel making slags. EAF slags are derived from steel production using electric arcs or mini mills to melt steel scraps (*from recycling*) and convert it into high-quality steel (Andersson et al., 2023). The melting process involves electricity generation from the electric arcs which converts the steel scraps into molten steel, then lime or dolomite is added during the process before starting the refining step, where decarburization and dephosphorization happens (Piatak et al., 2015b, 2019).

Cooling procedures used for EAF slags are open-air (*slow cooling*) methods giving a crystalline nature with a dense structure and glassy texture. Physical characteristics of colour normally ranged between dark grey or black (Yadav & Mehra, 2017). Recently, rapid quenching cooling methods have been applied to EAF slags for developing amorphous characteristics and suitable properties for its utilisation in concrete mixtures (Muhmood et al., 2009).

Ragipani et al. (2021) reports the chemical composition and primary mineral phases of EAF slags as follows: CaO: 25–40%, SiO_2: 10–17%, Fe: 18–29%, MgO: 4–15%, Al_2O_3: 4–7%, MnO: ≤6.0%; Ca_2SiO_4, Ca_2Al ($AlSiO_7$), Ca_3Mg $(SiO_4)_2$, (Mg, Fe, Mn) O, Fe_2O_3.

Based on their calcium and magnesium content, EAF slags are considered for CO_2 sequestration through mineral carbonation procedures and are valuable sources for metal extraction (*iron and manganese*) and within agribusiness due to its liming properties for soil stabilization in agriculture (Liapis & Papayianni, 2015; Rojas & Sánchez De Rojas, 2004).

1.2.5.5 Ladle Furnace (LF).

Ladle Furnace slags derive from a secondary process of steel refinement (Piatak et al., 2015b). As previously mentioned BOF and EAF slags are produced during the primary stage of the operation and further to this, if needed, the steel is treated to achieve high grade properties, involving the removal of exceeding sulphur, oxygen, nitrogen, hydrogen, and other impurities; from this, ladle furnace slag is produced (Guo et al., 2018). There is limited information about the chemical composition of ladle furnace slags, as it is highly variable and dependant on the grade of processing implemented; normally they presented lower amounts of FeO and higher content of Al_2O_3 and CaO, when compared to BOF and EAF slags (Ragipani et al., 2021). Data on the mineralogical properties of Ladle Furnace slags is still quite limited, but it is known that polymorphs of C_2S are typically the main phase (Piatak et al., 2021). As with the other slag types, ladle slags are used for metal recovery, within the construction industry and for soil treatments; however, the utilisation potential of this secondary produced slag remains less explored (Piatak & Ettler, 2021b, 2021c).

1.2.5.6 Open-hearth Furnace slags.

Open-hearth procedures have been mainly replaced by EAF and BOF routes in recent times (Piatak et al., 2015b). The way steel was produced through this procedure involved the melting of pig iron and scrap steel into an open-hearth furnace operated by waste gases from molten Fe to generate temperatures above 2000°C (Kiselev & Bodyagin, 2004).The addition of lime and dolomite was common for impurities removal (Piatak et al., 2015b). Chemical composition of slags produced from these operations contained SiO_2, Al_2O_3, Fe_2O_3, FeO, TiO_2 and high levels of Cr_2O_3 and MnO, pure iron and iron oxides (Anashkin et al., 2007; Kiselev & Bodyagin, 2004). Phases found in open-hearth slags documented by Zaichuk & Belyi (2012) showed magnesioferrite (*$MgFe_2O_4$*) and magnesiowustite (*(MgFe)O*), merwinite (*3CaO MgO $2SiO_2$*), afwillite (*$3CaO\ 2SiO_2\ 3H_2O$*). Open-hearth slag utilization efforts mainly focus in the recovery of cast iron from remaining slag deposits (Anashkin et al., 2007).

1.2.6 Iron and steel slag utilisation.

As documented by Ragipani et al. (2021), the global production of steel is near 1700 million tonnes per year, from which 237 metric tonnes of steel slags are generated. In the scenario that in the next 10 years the production of steel increases to 2000 million tonnes of steel per annum, the mass of slag produced would be 270 million tonnes approximately. This represents a considerable tonnage of material for potential re-utilisation.

Across time, iron and steel slags have been used as an aggregate in road construction, based on its strength and hardness properties, contributing to increasing the durability of the infrastructure when implemented in pavements (Naidu et al., 2020; Wang, 2016). Within its application in the construction field, an extensive use of these by-products was involved in the production of concrete, as aggregates with favourable results in terms of physical and mechanical properties for the mixture (O'Connor et al., 2021; Shi, 2004). The use of slags as supplementary cementitious materials continues to evolve, as it was proven that it enhanced the performance of concrete, improving its durability and reducing heat generation during the hydration phase of the blend (Snellings et al., 2023; Suraneni et al., 2019). However extended research within this application is needed to better understand the behaviour of the material when applied for extensive building purposes (Snellings & Scrivener, 2016), and to better manage its contribution to the sustainability transition of concrete production by reducing the demand for Portland cement (Suraneni & Weiss, 2017).

Beyond its properties for construction, iron and steel slags have also been applied in the agricultural sector as a soil conditioner (O'Connor et al., 2021; Reddy et al., 2019). Due to its calcium and magnesium content, the slags helped to neutralize soil acidity and provide essential nutrients for plant growth and improving soil fertility (Ferrara et al., 2023). Over time, iron and steel slags were also utilized in the manufacturing of mineral wool insulation, due to its fibrous structure and adequate properties for thermal insulation (Piatak et al., 2015b; Renforth et al., 2009). Furthermore, the hardness and abrasive characteristics of iron and steel slags made them useful for sandblasting procedures (Brand & Fanijo, 2020).

In recent decades, research into the use of iron and steel slags for carbon sequestration has grown significantly (Thonemann et al., 2022a). The dual nature of slag reutilisation, serving both as a waste management solution and an environmental opportunity to decrease net CO_2 emissions, makes iron and steel slags a promising option for converting atmospheric CO_2 into stable carbonates through mineral carbonation (Dri et al., 2014; Romanov et al., 2015).

Current research is now focused in further studying the kinetics of the carbonation reaction, the potential parameters influencing the CO_2 sequestration and exploring how to accelerate the process without increasing its energy demand and costs (Chang et al., 2012; Costa et al., 2007; Polettini et al., 2016; Ukwattage et al., 2017).

Overall, lab-scale experiments have shown that the time of carbonation can be accelerated if iron and steel slags are exposed to an environment with abundant CO_2, under controlled conditions of pressure, temperature, pH and humidity (Ko et al., 2015; Nielsena et al., 2020). However, there is limited knowledge involving passive carbonation occurring in slag heaps, where the CO_2 sequestration is performed with no human intervention (Mayes et al., 2018; Riley et al., 2020).

This approach of mineral carbonation using iron and steel slags for environment remediation can lead to a circular economy scheme of the waste material, where it is not only used for environmental purposes, but can also be further applied within any of the fields mentioned previously, where slags properties have shown feasible outcomes (Riley et al., 2020). For instance, once the slags show a high degree of carbonation, they can be re-utilised as supplementary cementitious material, serving as an aggregate replacement in the production of Ordinary Portland Cement, reducing the level of environmental impact within this industry while facilitating CO_2 removal from the atmosphere (Snellings et al., 2023; Suraneni et al., 2019). Therefore, there is a need to further explore the opportunities iron and steel slags can provide in various fields, also considering global markets or locations with less experience in the matter, as could be the case of Mexico, where the use of iron and steel slags is on hold (Hasanbeigi et al., 2016; Mercado Fernandez & Baker, 2022), and where there is a great potential to develop a cost-effective carbon sequestration solution, contributing to a more sustainable production method for the concrete industry.

1.3 Aim and Thesis Structure

The thesis presented aims to explore the repurposing of iron and steel slags as a strategic solution for CO_2 removal. It also investigates their properties for further utilization within the construction industry, in the context of Mexico and the United Kingdom. The thesis is structured into five chapters:

Chapter I: 'Introduction' serves as an introductory approach, providing fundamental knowledge on the mineral carbonation of iron and steel slags and their potential utilisation.

Chapter II: 'A comparison of atmospheric CO_2 capture with steel slags in Mexico and the United Kingdom', describes the findings in the quantification of CO_2 in BOF slags from Monclova, Mexico and Ravenscraig Scotland, and discusses which factors might determine the contrasting CO_2 volumes within the slags studied.

Chapter III: 'Geospatial evaluation of legacy iron and steel slag sites in Mexico for CO_2 sequestration', connects the discussion of Chapter II and IV by completing a volume estimation of slag deposits in Mexican territory with a land use analysis for slag utilisation in feasible industries.

Chapter IV: 'Utilisation of legacy iron and steel slag as sustainable construction materials', describes the results from the assessment of iron and steel slags from England, Mexico and Scotland and their potential to be used as supplementary cementitious materials within the scope of sustainable concrete production.

Chapter V: 'Conclusions and future work', provides a summary of the findings from the three experimental chapters (*II, III, IV*) and discusses further research opportunities involving the utilisation of legacy iron and steel slags as a mitigation method for the global increase of CO_2 emissions, while providing an option for efficient waste management.

References.

Anashkin, N. S., Polyakov, N. S., Usov, M. A., & Polyakov, V. N. (2007). Use of processed open-hearth dump slag for production of cast iron. *Steel in Translation*, *37*(1), 5–6. https://doi.org/10.3103/S0967091207010020

Andersson, A., Isaksson, J., Lennartsson, A., & Engström, F. (2023). Insights into the Valorization of Electric Arc Furnace Slags as Supplementary Cementitious Materials. *Journal of Sustainable Metallurgy*. https://doi.org/10.1007/s40831-023-00778-y

Barabanshchikov, Y., Usanova, K., Akimov, S., & Bílý, P. (2020). Low heat concrete with ground granulated blast furnace slag. *IOP Conference Series: Materials Science and Engineering*, *896*(1). https://doi.org/10.1088/1757-899X/896/1/012098

Brand, A. S., & Fanijo, E. O. (2020). A review of the influence of steel furnace slag type on the properties of cementitious composites. In *Applied Sciences (Switzerland)* (Vol. 10, Issue 22, pp. 1–27). MDPI AG. https://doi.org/10.3390/app10228210

Chang, E. E., Chen, C. H., Chen, Y. H., Pan, S. Y., & Chiang, P. C. (2011). Performance evaluation for carbonation of steel-making slags in a slurry reactor. *Journal of Hazardous Materials*, *186*(1), 558–564. https://doi.org/10.1016/j.jhazmat.2010.11.038

Chang, E. E., Pan, S. Y., Chen, Y. H., Tan, C. S., & Chiang, P. C. (2012). Accelerated carbonation of steelmaking slags in a high-gravity rotating packed bed. *Journal of Hazardous Materials*, *227–228*, 97–106. https://doi.org/10.1016/j.jhazmat.2012.05.021

Chen, Z., Cang, Z., Yang, F., Zhang, J., & Zhang, L. (2021). Carbonation of steelmaking slag presents an opportunity for carbon neutral: A review. In *Journal of CO2 Utilization* (Vol. 54). Elsevier Ltd. https://doi.org/10.1016/j.jcou.2021.101738

Costa, G., Baciocchi, R., Polettini, A., Pomi, R., Hills, C. D., & Carey, P. J. (2007). Current status and perspectives of accelerated carbonation processes on municipal waste combustion residues. In *Environmental Monitoring and Assessment* (Vol. 135, Issues 1–3, pp. 55–75). https://doi.org/10.1007/s10661-007-9704-4

Crippa, M., Guizzardi, D., Schaaf, E., Monforti-Ferrario, F., Quadrelli, R., Risquez Martin, A., Rossi, S., Vignati, E., Muntean, M., Brandao De Melo, J., Oom, D., Pagani, F., Banja, M., Taghavi-Moharamli, P., Köykkä, J., Grassi, G., Branco, A., San-Miguel, J., & European Commission. Joint Research Centre. (2023). *GHG emissions of all world countries : 2023.*

Davies, A. J., & Hastings, A. (2022). Quantifying greenhouse gas emissions from decommissioned oil and gas steel structures: Can current policy meet NetZero goals? *Energy Policy*, *160*. https://doi.org/10.1016/j.enpol.2021.112717

Dri, M., Sanna, A., & Maroto-Valer, M. M. (2014). Mineral carbonation from metal wastes: Effect of solid to liquid ratio on the efficiency and characterization of carbonated products. *Applied Energy*, *113*, 515–523. https://doi.org/10.1016/j.apenergy.2013.07.064

Eloneva, S., Teir, S., Salminen, J., Fogelholm, C. J., & Zevenhoven, R. (2008). Steel converter slag as a raw material for precipitation of pure calcium carbonate. *Industrial and Engineering Chemistry Research*, *47*(18), 7104–7111. https://doi.org/10.1021/ie8004034

Ferrara, G., Belli, A., Keulen, A., Tulliani, J. M., & Palmero, P. (2023). Testing procedures for CO2 uptake assessment of accelerated carbonation products: Experimental application

on basic oxygen furnace steel slag samples. *Construction and Building Materials*, *406*. https://doi.org/10.1016/j.conbuildmat.2023.133384

Gao, W., Zhou, W., Lyu, X., Liu, X., Su, H., Li, C., & Wang, H. (2023). Comprehensive utilization of steel slag: A review. In *Powder Technology* (Vol. 422). Elsevier B.V. https://doi.org/10.1016/j.powtec.2023.118449

Ghorbani, S., Stefanini, L., Sun, Y., Walkley, B., Provis, J. L., De Schutter, G., & Matthys, S. (2023). Characterisation of alkali-activated stainless steel slag and blast-furnace slag cements. *Cement and Concrete Composites*, *143*. https://doi.org/10.1016/j.cemconcomp.2023.105230

Guo, J., Bao, Y., & Wang, M. (2018). Steel slag in China: Treatment, recycling, and management. In *Waste Management* (Vol. 78, pp. 318–330). Elsevier Ltd. https://doi.org/10.1016/j.wasman.2018.04.045

Hasanbeigi, A., Arens, M., Cardenas, J. C. R., Price, L., & Triolo, R. (2016). Comparison of carbon dioxide emissions intensity of steel production in China, Germany, Mexico, and the United States. *Resources, Conservation and Recycling*, *113*, 127–139. https://doi.org/10.1016/j.resconrec.2016.06.008

Herzog, H. (2023, January 20). *Carbon Capture*. MIT Climate Portal.

Humbert, P. S., & Castro-Gomes, J. (2019). CO2 activated steel slag-based materials: A review. In *Journal of Cleaner Production* (Vol. 208, pp. 448–457). Elsevier Ltd. https://doi.org/10.1016/j.jclepro.2018.10.058

International Energy Agency. (2023, July 11). *Carbon capture, utilisation and storage*. Energy System.

Jiang, Y., Ling, T. C., Shi, C., & Pan, S. Y. (2018). Characteristics of steel slags and their use in cement and concrete—A review. In *Resources, Conservation and Recycling* (Vol. 136, pp. 187–197). Elsevier B.V. https://doi.org/10.1016/j.resconrec.2018.04.023

Kiselev, V. N., & Bodyagin, E. A. (2004). *USE OF CONCENTRATE PREPARED FROM DISCARDED OPEN-HEARTH SLAG TO MAKE ALLOYED IRON FOR INGOT MOLDS SCIENCE, TECHNOLOGY, INDUSTRY* (Vol. 48, Issue 1).

Ko, M. S., Chen, Y. L., & Jiang, J. H. (2015). Accelerated carbonation of basic oxygen furnace slag and the effects on its mechanical properties. *Construction and Building Materials*, *98*, 286–293. https://doi.org/10.1016/j.conbuildmat.2015.08.051

Li, Ling, T. C., & Pan, S. Y. (2022). Environmental benefit assessment of steel slag utilization and carbonation: A systematic review. In *Science of the Total Environment* (Vol. 806). Elsevier B.V. https://doi.org/10.1016/j.scitotenv.2021.150280

Liapis, I., & Papayianni, I. (2015). Advances in chemical and physical properties of electric arc furnace carbon steel slag by hot stage processing and mineral mixing. *Journal of Hazardous Materials*, *283*, 89–97. https://doi.org/10.1016/j.jhazmat.2014.08.072

Liu, W., Teng, L., Rohani, S., Qin, Z., Zhao, B., Xu, C. C., Ren, S., Liu, Q., & Liang, B. (2021). CO2 mineral carbonation using industrial solid wastes: A review of recent developments. In *Chemical Engineering Journal* (Vol. 416). Elsevier B.V. https://doi.org/10.1016/j.cej.2021.129093

Liu, Z., Zhang, D. wang, LI, L., Wang, J. xiang, Shao, N. ning, & Wang, D. min. (2019). Microstructure and phase evolution of alkali-activated steel slag during early age.

Construction and Building Materials, *204*, 158–165. https://doi.org/10.1016/j.conbuildmat.2019.01.213

Mayes, W. M., Riley, A. L., Gomes, H. I., Brabham, P., Hamlyn, J., Pullin, H., & Renforth, P. (2018). Atmospheric CO2 Sequestration in Iron and Steel Slag: Consett, County Durham, United Kingdom. *Environmental Science and Technology*, *52*(14), 7892–7900. https://doi.org/10.1021/acs.est.8b01883

Meijssen, M., Marinello, L., di Bella, C., Gasós, A., & Mazzotti, M. (2023). Industrial demonstration of indirect mineral carbonation in the cement and concrete sector. *Journal of Environmental Chemical Engineering*, *11*(5). https://doi.org/10.1016/j.jece.2023.110900

Mercado Fernandez, R., & Baker, E. (2022). The sustainability of decarbonizing the grid: A multi-model decision analysis applied to Mexico. *Renewable and Sustainable Energy Transition*, *2*, 100020. https://doi.org/10.1016/j.rset.2022.100020

Miao, E., Du, Y., Zheng, X., Zhang, X., Xiong, Z., Zhao, Y., & Zhang, J. (2023). CO2 sequestration by direct mineral carbonation of municipal solid waste incinerator fly ash in ammonium salt solution: Performance evaluation and reaction kinetics. *Separation and Purification Technology*, *309*. https://doi.org/10.1016/j.seppur.2023.123103

Moranville-Regourd, M., Kamali-Bernard, S., & Hewlett, P. (2019). Cements made from blastfurnace slag. In *Lea's Chemistry of Cement and Concrete* (pp. 469–507). Elsevier. https://doi.org/10.1016/B978-0-08-100773-0.00010-1

Muhmood, L., Vitta, S., & Venkateswaran, D. (2009). Cementitious and pozzolanic behavior of electric arc furnace steel slags. *Cement and Concrete Research*, *39*(2), 102–109. https://doi.org/10.1016/j.cemconres.2008.11.002

Naidu, T. S., Sheridan, C. M., & van Dyk, L. D. (2020). Basic oxygen furnace slag: Review of current and potential uses. In *Minerals Engineering* (Vol. 149). Elsevier Ltd. https://doi.org/10.1016/j.mineng.2020.106234

National Oceanic and Atmospheric Administration. (2023, April 5). *Greenhouse gases continued to increase rapidly in 2022*. NOAA News and Features.

Nielsena, P., Booneb, M. A., Horckmansa, L., Snellingsa, R., & Quaghebeura, M. (2020). Accelerated carbonation of steel slag monoliths at low CO2 pressure – microstructure and strength development. *Journal of CO2 Utilization*, *36*(36), 124–134.

O'Connor, J., Nguyen, T. B. T., Honeyands, T., Monaghan, B., O'Dea, D., Rinklebe, J., Vinu, A., Hoang, S. A., Singh, G., Kirkham, M. B., & Bolan, N. (2021). Production, characterisation, utilisation, and beneficial soil application of steel slag: A review. *Journal of Hazardous Materials*, *419*. https://doi.org/10.1016/j.jhazmat.2021.126478

Oelkers, E. H., & Cole, D. R. (2008). Carbon Dioxide Sequestration A Solution to a Global Problem. *Elements*, *4*(5), 305–310. https://doi.org/10.2113/gselements.4.5.305

Olajire, A. A. (2013). A review of mineral carbonation technology in sequestration of CO2. In *Journal of Petroleum Science and Engineering* (Vol. 109, pp. 364–392). Elsevier B.V. https://doi.org/10.1016/j.petrol.2013.03.013

Piatak, N. M., & Ettler, V. (2021a). *4 Chemistry in the Environment Series No. 2 Metallurgical Slags: Environmental Geochemistry and Resource Potential Edited by*. www.rsc.org

Piatak, N. M., & Ettler, V. (2021b). *51 Chemistry in the Environment Series No. 2 Metallurgical Slags: Environmental Geochemistry and Resource Potential Edited by*. www.rsc.org

Piatak, N. M., & Ettler, V. (2021c). *94 Chemistry in the Environment Series No. 2 Metallurgical Slags: Environmental Geochemistry and Resource Potential Edited by*. http://books.rsc.org/books/edited-volume/chapter-pdf/1617876/bk9781788018876-00194.pdf

Piatak, N. M., Ettler, V., Kierczak, J., & Piatak B A, N. M. (2021). *25 Chemistry in the Environment Series No. 2 Metallurgical Slags: Environmental Geochemistry and Resource Potential Edited by 4.1 Introduction Weathering of Slags*. www.rsc.org

Piatak, N. M., Parsons, M. B., & Seal, R. R. (2015a). Characteristics and environmental aspects of slag: A review. In *Applied Geochemistry* (Vol. 57, pp. 236–266). Elsevier Ltd. https://doi.org/10.1016/j.apgeochem.2014.04.009

Piatak, N. M., Parsons, M. B., & Seal, R. R. (2015b). Characteristics and environmental aspects of slag: A review. In *Applied Geochemistry* (Vol. 57, pp. 236–266). Elsevier Ltd. https://doi.org/10.1016/j.apgeochem.2014.04.009

Piatak, N. M., Seal, R. R., Hoppe, D. A., Green, C. J., & Buszka, P. M. (2019). Geochemical characterization of iron and steel slag and its potential to remove phosphate and neutralize acid. *Minerals*, *9*(8). https://doi.org/10.3390/min9080468

Polettini, A., Pomi, R., & Stramazzo, A. (2016). Carbon sequestration through accelerated carbonation of BOF slag: Influence of particle size characteristics. *Chemical Engineering Journal*, *298*, 26–35. https://doi.org/10.1016/j.cej.2016.04.015

Ragipani, R., Bhattacharya, S., & Suresh, A. K. (2021). A review on steel slag valorisation: Via mineral carbonation. In *Reaction Chemistry and Engineering* (Vol. 6, Issue 7, pp. 1152–1178). Royal Society of Chemistry. https://doi.org/10.1039/d1re00035g

Rahmanihanzaki, M., & Hemmati, A. (2022). A review of mineral carbonation by alkaline solidwaste. In *International Journal of Greenhouse Gas Control* (Vol. 121). Elsevier Ltd. https://doi.org/10.1016/j.ijggc.2022.103798

Reddy, K. R., Gopakumar, A., & Chetri, J. K. (2019). Critical review of applications of iron and steel slags for carbon sequestration and environmental remediation. In *Reviews in Environmental Science and Biotechnology* (Vol. 18, Issue 1, pp. 127–152). Springer Netherlands. https://doi.org/10.1007/s11157-018-09490-w

Renforth, P., Manning, D. A. C., & Lopez-Capel, E. (2009). Carbonate precipitation in artificial soils as a sink for atmospheric carbon dioxide. In *Applied Geochemistry*. www.ianfarmerassociates.co.uk

Riley, A. L., MacDonald, J. M., Burke, I. T., Renforth, P., Jarvis, A. P., Hudson-Edwards, K. A., McKie, J., & Mayes, W. M. (2020). Legacy iron and steel wastes in the UK: Extent, resource potential, and management futures. *Journal of Geochemical Exploration*, *219*. https://doi.org/10.1016/j.gexplo.2020.106630

Rojas, M. F., & Sánchez De Rojas, M. I. (2004). Chemical assessment of the electric arc furnace slag as construction material: Expansive compounds. *Cement and Concrete Research*, *34*(10), 1881–1888. https://doi.org/10.1016/j.cemconres.2004.01.029

Romanov, V., Soong, Y., Carney, C., Rush, G. E., Nielsen, B., & O'Connor, W. (2015). Mineralization of Carbon Dioxide: A Literature Review. In *ChemBioEng Reviews* (Vol. 2, Issue 4, pp. 231–256). Wiley-Blackwell. https://doi.org/10.1002/cben.201500002

Roy, S., Rautela, R., & Kumar, S. (2023). Towards a sustainable future: Nexus between the sustainable development goals and waste management in the built environment. In *Journal of Cleaner Production* (Vol. 415). Elsevier Ltd. https://doi.org/10.1016/j.jclepro.2023.137865

Shi, C. (2004). *Steel Slag-Its Production, Processing, Characteristics, and Cementitious Properties*. https://doi.org/10.1061/ASCE0899-1561200416:3230

Snellings, R., & Scrivener, K. L. (2016). Rapid screening tests for supplementary cementitious materials: past and future. *Materials and Structures/Materiaux et Constructions*, *49*(8), 3265–3279. https://doi.org/10.1617/s11527-015-0718-z

Snellings, R., Suraneni, P., & Skibsted, J. (2023). Future and emerging supplementary cementitious materials. *Cement and Concrete Research*, *171*. https://doi.org/10.1016/j.cemconres.2023.107199

Stokreef, S., Sadri, F., Stokreef, A., & Ghahreman, A. (2022). Mineral carbonation of ultramafic tailings: A review of reaction mechanisms and kinetics, industry case studies, and modelling. In *Cleaner Engineering and Technology* (Vol. 8). Elsevier Ltd. https://doi.org/10.1016/j.clet.2022.100491

Suraneni, P., Hajibabaee, A., Ramanathan, S., Wang, Y., & Weiss, J. (2019). New insights from reactivity testing of supplementary cementitious materials. *Cement and Concrete Composites*, *103*, 331–338. https://doi.org/10.1016/j.cemconcomp.2019.05.017

Suraneni, P., & Weiss, J. (2017). Examining the pozzolanicity of supplementary cementitious materials using isothermal calorimetry and thermogravimetric analysis. *Cement and Concrete Composites*, *83*, 273–278. https://doi.org/10.1016/j.cemconcomp.2017.07.009

Thomas, C., Rosales, J., Polanco, J. A., & Agrela, F. (2018). Steel slags. In *New Trends in Eco-efficient and Recycled Concrete* (pp. 169–190). Elsevier. https://doi.org/10.1016/B978-0-08-102480-5.00007-5

Thonemann, N., Zacharopoulos, L., Fromme, F., & Nühlen, J. (2022a). Environmental impacts of carbon capture and utilization by mineral carbonation: A systematic literature review and meta life cycle assessment. In *Journal of Cleaner Production* (Vol. 332). Elsevier Ltd. https://doi.org/10.1016/j.jclepro.2021.130067

Thonemann, N., Zacharopoulos, L., Fromme, F., & Nühlen, J. (2022b). Environmental impacts of carbon capture and utilization by mineral carbonation: A systematic literature review and meta life cycle assessment. In *Journal of Cleaner Production* (Vol. 332). Elsevier Ltd. https://doi.org/10.1016/j.jclepro.2021.130067

Ukwattage, N. L., Ranjith, P. G., & Li, X. (2017). Steel-making slag for mineral sequestration of carbon dioxide by accelerated carbonation. *Measurement: Journal of the International Measurement Confederation*, *97*, 15–22. https://doi.org/10.1016/j.measurement.2016.10.057

Wang. (2016). Slag use in cement manufacture and cementitious applications. In *The Utilization of Slag in Civil Infrastructure Construction* (pp. 305–337). Elsevier. https://doi.org/10.1016/b978-0-08-100381-7.00013-6

Wang, B., Pan, Z., Cheng, H., Zhang, Z., & Cheng, F. (2021). A review of carbon dioxide sequestration by mineral carbonation of industrial byproduct gypsum. In *Journal of Cleaner Production* (Vol. 302). Elsevier Ltd. https://doi.org/10.1016/j.jclepro.2021.126930

Wang, Q. (2019). *76 Inorganic Materials Series No. 2 Post-combustion Carbon Dioxide Capture Materials Edited*. www.rsc.org

Wang, & Suraneni. (2019). Experimental methods to determine the feasibility of steel slags as supplementary cementitious materials. *Construction and Building Materials*, *204*, 458–467. https://doi.org/10.1016/j.conbuildmat.2019.01.196

Yadav, S., & Mehra, A. (2017). Experimental study of dissolution of minerals and CO2 sequestration in steel slag. *Waste Management*, *64*, 348–357. https://doi.org/10.1016/j.wasman.2017.03.032

Yildirim, I. Z., Balunaini, U., & Prezzi, M. (2023). Strength-Gain Characteristics and Swelling Response of Steel Slag and Steel Slag–Fly Ash Mixtures. *Journal of Materials in Civil Engineering*, *35*(8). https://doi.org/10.1061/jmcee7.mteng-14823

Yildirim, I. Z., & Prezzi, M. (2011). Chemical, mineralogical, and morphological properties of steel slag. *Advances in Civil Engineering*, *2011*. https://doi.org/10.1155/2011/463638

Zaichuk, A. V, & Belyi, Y. I. (2012). *WASTES INTO PRODUCTION BLACK CERAMIC PIGMENTS BASED ON OPEN-HEARTH SLAG* (Issue 3).

Chapter II. Potential for the utilisation of mineral carbonation using steel slag as a solution to decrease atmospheric CO_2 levels.

2.1 Introduction.

Greenhouse gases, mainly carbon dioxide, are key drivers of inherent global temperature increase, from the greenhouse effect, and climate disruption generating environmental disparity. Thus, a need for formulating strategic solutions to remove CO_2 emissions from the atmosphere is essential to mitigate global warming and climate change effects on the planet. Carbon sequestration is a reliable way to safely capture CO_2 through different removal approaches, like industrialized methods or the adaptation of natural CO_2 sequestration reactions like mineral carbonation. In this context, understanding the mineral carbonation of industrial by-products (*e.g., steel slag*) as a carbon removal technology offers a promising opportunity for both CO_2 removal and the environmental repurposing of waste materials.

Steel slag, a by-product of steel manufacturing, has been identified as a suitable candidate for mineral carbonation due to its alkaline nature. This process not only facilitates the sequestration of atmospheric CO_2 but also holds potential applications in the production of supplementary cementitious materials. Considering this context, it is fundamental to study the factors influencing the mineralisation rate of legacy steel slag and the amount of atmospheric CO_2 that can be captured for optimizing this decarbonization strategy.

The content of the following chapter describes the use of x-ray tomography (XCT) in the quantification of mineralised CO_2 in steel slags that passively carbonated in Monclova, Mexico and Ravenscraig, Scotland. By comparing the volumes of carbonated CO_2 quantified in both sets of legacy slags, the following sections explore the methodologies used for XCT analysis, present the quantification results and discuss the implications of external conditions on the capturing potential of legacy steel slags to carbonate atmospheric CO_2.

Preliminary findings indicate that humidity plays a decisive role in enhancing the carbonation process, overshadowing other parameters such as temperature and time. This insight challenges prior assumptions about the influence of temperature on carbonation kinetics and suggests that moisture availability is a primary driver of CO_2 uptake in passive carbonation systems. The findings presented in this chapter highlight the role of environmental conditions in determining the carbonation potential of steel slags, with significant implications for future decarbonization strategies.

2.2 Literature Review.

2.2.1 Mineral carbonation of atmospheric CO_2 on legacy steel slag.

Mineral carbonation, using steel slags for atmospheric CO_2 uptake, is a promising option involving carbon removal potential and industrial waste reutilisation. Furthermore, its growing acceptance also relies upon the wide availability of slags and its suitability for mineralising CO_2, based on the slag alkaline composition. Findings from Mo (2018) and Teir et al. (2007) indicated high reactivity of steel slags when in the presence of carbon dioxide, based on the Ca, Mg and Fe content. Thus, higher levels of Ca and Mg in steel slags facilitate the carbonation of CO_2 (Mo, 2018). Pan et al. (2013) also reported that calcium and magnesium silicate phases favoured the accelerated carbonation of CO_2. Pan et al. (2013) propose the general reaction (*Reaction 4*) for mineral carbonation of steel slags, where magnesium and calcium silicates react with CO_2 producing calcium/magnesium carbonates, where the conversion into calcium carbonates or calcite ($CaCO_3$) is favoured.

Reaction 4.

$$(CaO,\ MgO)_x(SiO_2)_y(s) + x\ CO_2(g) \rightarrow x(Ca,\ Mg)CO_3(s) + ySiO_2(s)$$

While literature evidence focuses on understanding the influence of steel slag properties, such as type, composition, particle size, age, etc., on mineral carbonation, there is less documented research on external conditions that might influence the mineralisation rates of carbon dioxide (Piatak et al., 2015a; Shi, 2004; Thomas et al., 2018; Yildirim & Prezzi, 2011). Thus, if the production of 1 tonne of steel generates between 130 to 200 Kg of slags(Rahmanihanzaki & Hemmati, 2022), commonly disposed on the manufacturing site surroundings, it is highly probable that temperature variation, seasonal weather, anthropogenic activities, among other external variables have an impact on the slag composition or the kinetics of CO_2 capturing rates during the carbonation reaction (Romanov et al., 2015).

Therefore, by comparing volumes of captured CO_2 between slags from Monclova, Mexico and Ravenscraig, Scotland, where carbonation occurred with no human intervention and under very different environmental conditions, this chapter aims to explore whether environmental factors like water content, temperature variation, atmospheric pressure or pH could also have a determining role in the mineralisation of CO_2 happening passively in slag heaps. This will increase knowledge on how CO_2 capturing rates and slag properties are influenced by external conditions and will provide better understanding on the challenges of scaling up the technology, whose main drawback is that is relies on carbonation time.

2.2.1.1 Mineral carbonation time.

Time as a parameter, is of significance when analysing the carbonation of steel slags, either if the reaction is classified as passive or accelerated, as the length of the reaction is related to the process efficiency and is a variable giving the scope for external factors to have an impact on the slag characteristics and determine mineralisation rates within the material (Baras et al., 2023; Chen et al., 2021). Either passive or accelerated, both carbonation routes contribute to the mitigation of atmospheric CO_2, where the main differentiator in between is the time (Chang et al., 2012; Santos et al., 2013). Accelerated carbonation is a process engineered by human intervention, where the precipitation of carbon dioxide into stable carbonates occurs rapidly under controlled conditions and is normally employed at industrial scale with an efficient sequestration rate of CO_2 emissions (Ko et al., 2015).

While accelerated carbonation offers an immediate benefit of CO_2 capture, passive carbonation occurs with no human intervention over decadal periods and does not involve process manipulation or monitoring (Pullin et al., 2019). In passive carbonation, the reaction relies on environmental conditions and the material properties (*e.g. iron and steel slags*). In nature, mineral carbonation occurs over extended timescales (Chukwuma et al., 2021), which is considered a main drawback on its use for carbon removal, as currently decreasing carbon emissions within the least time possible is imperative (Costa et al., 2007) and longer capturing periods are also related to higher costs. The reaction length between the alkaline material (*e.g., magnesium/calcium silicates, metal oxides*) and atmospheric CO_2 is derived from the slow contact mechanisms between the slag surface and gaseous CO_2 to be sequestrated (Georgakopoulos et al., 2016). Those mechanisms are directly influenced by parameters such as: temperature, pressure and humidity, extending the reaction over hundreds or thousands of years (Stewart et al., 2018); therefore, by understanding these parameters and their role in mineral carbonation occurring passively, the time and the reaction kinetics could be adapted to specific contexts as a CO_2 sequestration option.

2.2.1.2 External influence on passive CO_2 mineralisation on legacy steel slag.

The following review was completed, by exploring how environment conditions, e.g., temperature, rainfall (*water presence*) pressure, altitude, among others, interact over mineralisation of CO_2 in steel slags. This is to shed light on CO_2 capturing volumes differing during the comparison between Mexican and Scottish slags quantified over this chapter.

2.2.1.2.1 Temperature.

Research under controlled conditions indicate that temperature is a variable with contrasting effects on the reaction kinetics of mineral carbonation (Mo, 2018). Increasing temperatures between 150-175°C are ideal to produce Ca leachate, which is beneficial for carbonate formation within alkaline compounds; on the contrary above 175°C solubility properties of carbon dioxide are decreased (Quaghebeur et al., 2015). Those temperatures are less likely to occur as ambient conditions but provide an overview of the reaction-ideal thermodynamics (Klein & Garrido, 2011). On the contrary, lower temperatures would have a negative impact on the reaction kinetics, slowing down mineral carbonation and affecting the solubility of silicates and other mineral phases contained in the slags, (Quaghebeur et al., 2015).

Studies conducted on stockpiled slags passively carbonating under ambient conditions indicate an exothermic behaviour during mineral carbonation (Liu et al., 2021; Olajire, 2013; Stokreef et al., 2022); this was also reported by Baras et al. (2023) and Huijgen et al. (2005) whose research also indicate feasible carbonation kinetics between 25 to 50 °C. This temperature is suitable to increase reactivity of Ca-bearing phases of the slag, enabling an accelerated carbonate formation and avoiding drawbacks on the solubility of carbon dioxide in the presence of water. Therefore, CO_2 sequestration in slags is more likely to occur at ambient temperature between 25 to 50 °C.

2.2.1.2.2 Rainfall.

As in the case of temperature, the presence of water positively impacts the kinetics of mineral carbonation of steel slag, either in a controlled (*artificial*) environment or under exterior conditions, where water acts as a solvent on the carbonation reaction, facilitating the sequestration of carbon dioxide. During mineral carbonation water serves to “transport” CO_2 through the porous structure of the slag, enabling the interaction of both reactants: steel slag and carbon dioxide (Baras et al., 2023; Georgakopoulos et al., 2016; Klein & Garrido, 2011). Mineral carbonation occurring passively in an open-air location may not always have a moisture source nearby, but this does not stop the carbonation reaction from occurring, it just increases the reaction time (Huijgen et al., 2005). The carbonation of atmospheric CO_2 in a context where water (*moisture*) is abundant has been documented. For example, Mayes et al. (2018a) describes the precipitation into carbonates from the mineral silicate weathering of iron and steel slags sourced from the drainage water of a slag pile.

The study from Ghacham et al. (2016) conducted at ambient temperature, explored different arrangements of liquid/solid ratio during mineral carbonation, concluding that 10:1 is the optimal ratio resulting in higher sequestration of carbon dioxide. Although Baras et al. (2023) agrees that capturing rates increase in the presence of moisture, their work also found that excessive amounts of water might block the slag pores preventing CO_2 diffusion. Overall, water in the form of rainfall acts as a catalyst medium to enhance the natural carbonation within stockpiled slags by increasing the dissolution of CO_2 within the minerals (Sorrentino et al., 2023); this increases the process efficiency resulting in higher rates of atmospheric CO_2 mineralization (Wang et al., 2018).

2.2.1.2.3 Atmospheric pressure and altitude.

Outdoor mineral carbonation of steel slags is subject to atmospheric pressure influence which is highly related to altitude of the location. These factors and their impact on carbonation of atmospheric CO_2 happening in slag heaps remains mostly unexplored. Evidence held on pressure as a variable affecting capturing rates of steel slag has mostly been studied over controlled carbonation experiments, where pressure levels exceeded Earth atmospheric conditions (Rushendra Revathy et al., 2016).

The higher the altitude, the lower the atmospheric pressure (Mattila et al., 2012), thus slag heaps carbonating in higher-altitude locations would slow CO_2 sequestration rates. However, as passive carbonation normally occurs at ambient conditions of atmospheric pressure, its influence is not as determinative as temperature or moisture over the kinetics of the reaction (Luo & He, 2021; Mattila et al., 2012), but it does play a role in facilitating the penetration of CO_2 into slag pores, enhancing surface contact and further sequestration (Baras et al., 2023).

2.2.1.2.4 Additional environmental conditions.

Having an alkaline pH in the immediate environment of where slags are passively carbonating has been found as beneficial on their mineral carbonation reaction by increasing the solubility of calcium ions and the likelihood of carbonate precipitation such as $CaCO_3$ and $MgCO_3$ (Bonenfant et al., 2008). The impact of high-pH environment (*drainage water*) was also reported by Mayes et al. (2018a), whose geochemistry analysis on water streams supported CO_2 sequestration based on the presence of carbonates formed by steel slag weathering.

2.2.2 Overview of mineral carbonation of legacy steel slag as a decarbonizing technology.

While the use of steel slags represents a feasible option to reverse the environmental impact from excessive CO_2 emissions released into the atmosphere, particularly from fields like steel production, which is one of the largest industrial sectors contributing approximately 7% of the global total CO_2 emissions (Roy et al., 2023), there still much to accomplish to globally scale up mineral carbonation as a carbon capture and storage option. From this perspective, Yadav et al. (2017) in their work provided a conclusive summary of operational factors, where further research is necessary, starting with exploring various ways to accelerate reaction times in mineral carbonation processes using iron and steel slags. They also documented that a reduction in operational and technological cost of CO_2 capture (*any of the CCS/CCUS options*) will increase the adoption of this carbon removal option in a wider perspective. They also pointed out the need in reducing energy consumption related to the procedures and the importance to find feasible utilisation options for the carbon capture products, including sequestered CO_2 or carbonated steel slags.

Consistent to the overview from Yadav et al. (2017), a more recent evaluation on mineral carbonation parameters to improve, or to focus research on, is summarized in the work from Baras et al. (2023) and Luo et al. (2021). These studies agreed to suggest that wider and more detailed cost-effectiveness studies are necessary to drastically reduce energy costs in carbon removal projects at industrial scale; this literature also highlighted the importance to develop high-added value products from carbonation procedures, e.g. the use of carbonated slags in the production of sustainable supplementary cementitious materials for the construction industry.

The literature also explored the benefits of maximizing carbonation methods such as ultrasonic enhancement (to increase chemical reaction rate and mass transfer) or improving slags chemical composition by composite calcination. Aligned to the recorded data from Baras et al. (2023) and Luo et al. (2021), the work from Liu et al. (2021) also recommend the use of wastewater from various sources to facilitate mineral carbonation of slags, as this adds a circular economy element to the process, and is more sustainable than using fresh water, a limited resource globally. Potential drawbacks of using wastewater for slag carbonation enhancement might include the need for additional water treatments to remove heavy metals or other unsuitable components, regulatory implications, and possible alterations to the physical or chemical characteristics of slags during the carbonation reaction (Gao et al., 2023; Luo & He, 2021).

The wider overview of using mineral carbonation of legacy slags from steel industry agreed on the need to further explore aspects of the reaction to reduce the length of the mineralisation of atmospheric CO_2 and to develop further steps in the utilisation of the carbonated rocks to promote a circular economy, where industrial wastes are repurposed into a CO_2 emissions mitigation strategy.

2.2.3 Utilisation potential of mineral carbonation with steel slags to decrease atmospheric CO_2 levels. Case studies Mexico and Scotland.

This chapter aims to explore the mineral carbonation reaction of legacy steel slags that carbonated passively in two contrasting locations with very different weather and environmental parameters. Study sites in Monclova, Mexico, and Ravenscraig, Scotland set a feasible context to compare CO_2 capture while evaluating how external conditions influence the mineralisation of atmospheric CO_2. The utilisation of legacy slags and their capacity to mineralise CO_2 is still a growing opportunity in Mexico. The upscaling of mineral carbonation has not yet been considered as a carbon removal option, as current efforts are focused on decarbonizing electrical, metal, chemical and cement industries using CCS as cited by Mercado Fernandez et al. (2022), Castrejon et al. (2018) and Vega-Ortiz et al. (2021), or the use of Sr and Ba alkaline solutions to form carbonates studied by Cruz Navarro et al. (2020).

CCUS technologies in Mexico are increasingly looking to develop new approaches to decrease carbon emissions (Mota-Nieto et al., 2023), but the specifics of passive mineral carbonation on legacy slags have not been yet explored. The UK has significantly researched mineral carbonation of legacy slags, where geospatial evaluation was completed over slag heaps to calculate the volume of available alkaline material to estimate CO_2 sequestration potential (Riley et al. (2020). Also, the kinetics of passive mineral carbonation in slag heaps were documented by Pullin et al. (2019) and Mayes et al. (2018a), whose research also presented the influence of moisture (water) increasing carbonate formation during mineral weathering.

Progress in the UK can be used as guidance to address the potential of Mexico in the use of mineral carbonation as a carbon removal option. The volume quantification of carbonated CO_2 in legacy steel slags from both countries, will be beneficial to better understand the implications of the local environment influencing CO_2 sequestration rates during passive mineral carbonation. As a result, this chapter seeks to use a new approach to quantifying CO_2 mineralised on steel slag and to assess the influence of environment (*climatic factors*) on determining the volume of CO_2 captured in slags that passively carbonated in Mexico and Scotland.

2.3 Methodology.

2.3.1 Carbonation context of legacy steel slags: Mexico and Scotland.

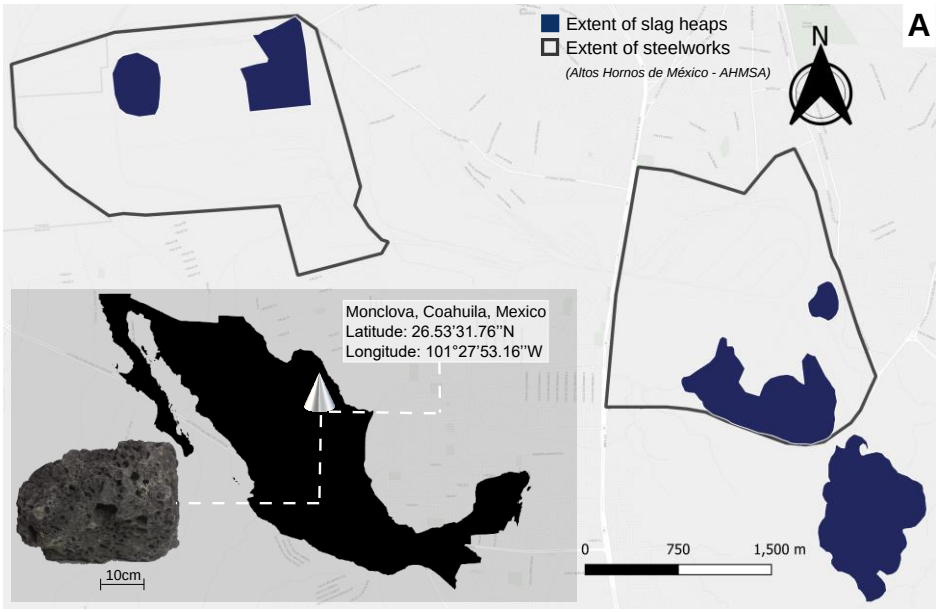

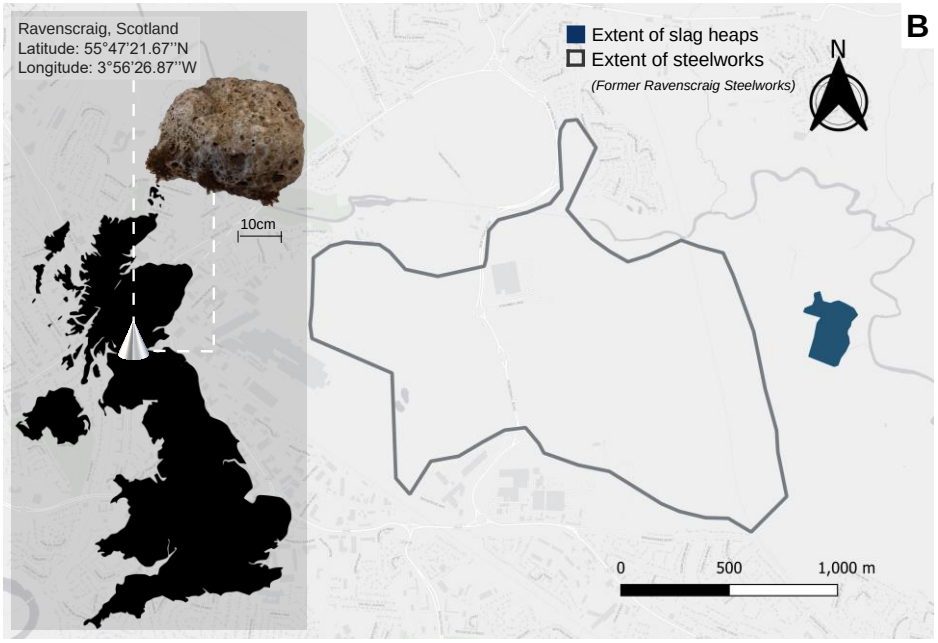

Figure 4 *Location maps of Altos Hornos de Mexico in Monclova, Mexico (a) and former Ravenscraig Steel Works in Scotland (b).*

Legacy slags studied in this chapter were originated in Monclova, Mexico and Ravenscraig, Scotland, respectively; this background provided a suitable setting to explore the influence of local environment on CO_2 sequestration rates occurring passively in steel slag heaps, as climatic context from both locations differ. Figure 4 shows the location of the slag heaps in Mexico (a) and Scotland (b).

2.3.1.1 Ravenscraig, Scotland, United Kingdom.

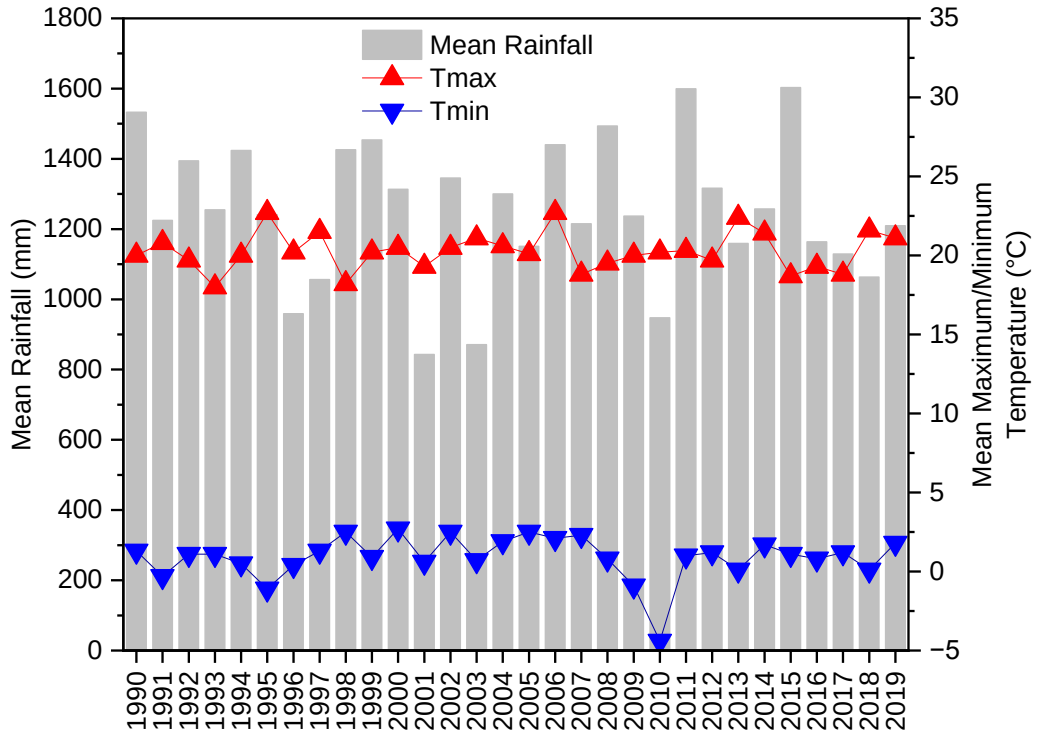

Figure 5 *Summary of mean temperature and rainfall conditions during carbonation time in Ravenscraig, Scotland.*

Scottish steel slags were collected from the former steel manufacturing site of Ravenscraig Steel Works (*Colvilles Ltd*) located near Motherwell, within the Lanarkshire Council area, in Scotland (*Elevation: 109m/ Latitude: 55°47'21.67''N/ Longitude: 3°56'26.87''W*). Steel production using Basic Oxygen Furnaces in the site started in 1964 until the closing of the Steel Works in 1990 (Hume, 2007). Slags from steel production were stockpiled since 1964 in the area nearby and remained carbonating up to present date.

For this research, samples were collected from the surface of the slag heap, thus ~29 years of passive carbonation is assumed, considering slag from the heap surface was dumped nearer the closing date in 1990. The collection site experiences variable climate conditions along the year, for example historical records from the Met Office UK (2023) indicate that for 2019 (*collection year*) temperature variation was between 2.5 to 22 °C with the rainfall average measurement was 1254 mm per year and average humidity was ~80% throughout the year (Met Office UK, 2023). A summary of rainfall and mean temperature occurring in Ravenscraig, Scotland between 1990 to 2019 is presented in Figure 5.

2.3.1.2 Monclova, Coahuila, Mexico.

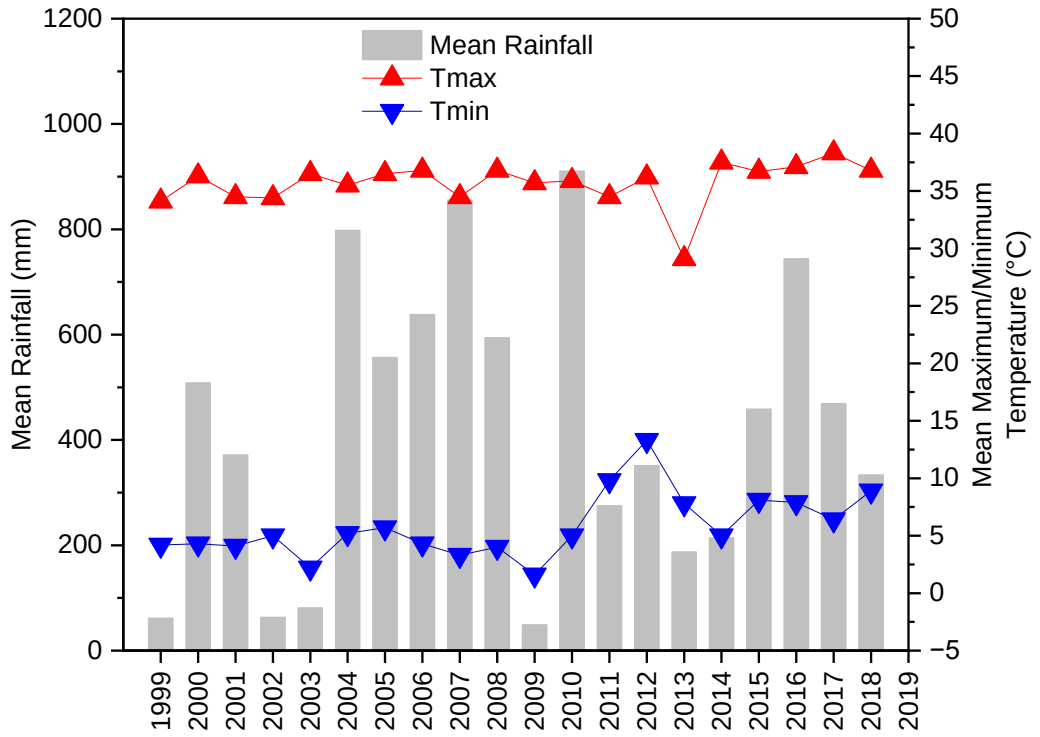

Figure 6 *Summary of mean temperature and rainfall conditions during carbonation time in Monclova, Mexico.*

Mexican steel slag samples were provided by Altos Hornos de Mexico, one of the largest steel producers in the country, with an overall production of 5.5 Mt in 2020 (AHMSA, 2020). The site was opened in 1941, using EAF, BOF and BF methods for iron and steel production and remains in operation since then, is located in the city of Monclova, in the northern region of Coahuila, Mexico. The altitude of the site is ~ 622 m above sea level. Once produced, BOF slag is disposed in the immediate area within the industrial site, is stockpiled a rotation scheme

based on the year of production and is left there for open-air carbonation. BOF slags for this research were produced in 1999 and 2009, with ~20 and ~10 years of carbonation period respectively. The environmental conditions of the collection site (*Latitude: 26.53'31.76''N / Longitude: 101°27'53.16''W*) are semi-aridic, with an average annual temperature of 22.4°C with maximum temperatures reaching 37.6°C and minimum of 6.4°C; average rainfall is 425 mm a year, mostly during summer months, with sporadic thunderstorms that most of the times end up in floods; humidity is in the region of around 50% throughout the year (Servicio Meteorológico Nacional, 2023). A summary of the temperature variation and rainfall occurring in Monclova, Coahuila, Mexico between 1999 to 2018 is presented in Figure 6, above.

2.3.1 Preliminary work on legacy steel slag sampled for CO_2 quantification.

The slag pieces representative from Mexico and Scotland were preserved under airtight conditions to avoid further mineral carbonation before CO_2 volume quantification. The sampled slags (*16 pieces*) were classified from A to P as shown in Table 1, where a summary of key information of the samples is also provided.

Table 1. Classification of sampled legacy steel slags used for mineralised CO_2 quantification.

Sample code	Collection site	Steel slag type	Steel slag age
A	Ravenscraig, Scotland	Basic Oxygen Furnace (BOF)	1964-1990
B	Ravenscraig, Scotland	Basic Oxygen Furnace (BOF)	1964-1990
C	Ravenscraig, Scotland	Basic Oxygen Furnace (BOF)	1964-1990
D	Ravenscraig, Scotland	Basic Oxygen Furnace (BOF)	1964-1990
E	Ravenscraig, Scotland	Basic Oxygen Furnace (BOF)	1964-1990
F	Ravenscraig, Scotland	Basic Oxygen Furnace (BOF)	1964-1990
G	Ravenscraig, Scotland	Basic Oxygen Furnace (BOF)	1964-1990
H	Ravenscraig, Scotland	Basic Oxygen Furnace (BOF)	1964-1990
I	Monclova, Mexico	Basic Oxygen Furnace (BOF)	2009-2019
J	Monclova, Mexico	Basic Oxygen Furnace (BOF)	2009-2019
K	Monclova, Mexico	Basic Oxygen Furnace (BOF)	1999-2019
L	Monclova, Mexico	Basic Oxygen Furnace (BOF)	1999-2019
M	Monclova, Mexico	Basic Oxygen Furnace (BOF)	1999-2019
N	Monclova, Mexico	Basic Oxygen Furnace (BOF)	1999-2019
O	Monclova, Mexico	Basic Oxygen Furnace (BOF)	1999-2019
P	Monclova, Mexico	Basic Oxygen Furnace (BOF)	1999-2019

2.3.2 Legacy steel slag preparation for X-ray computed tomography analysis.

Preparation of legacy steel slag samples, illustrated in Figure 7, involved first sectioning the samples into ~1.5 cm width slices, to further cut representative cubes of ~1 cm per side, including contrasting phases of mineral carbonation along inner and outer pores to avoid bias on the computed tomography analysis. The sectioning of the steel slag pieces into cubic samples for XCT was completed and documented for each sample (*A to P*) by using (*in this order*) a Contempo 24" Lapidary Saw, a Logitech CS10 Cut-Off and Trim Saw with diamond-tipped grinding blade and the ATM GmbH Brillant 220 Cut-Off Machine; this equipment enabled cutting the samples into small sections, before producing (*~1 cm per side*) cubes. Humidity removal was performed after sectioning the sixteen steel slag samples into cubes in a MMM Group Vacucell (*VU*) vacuum at 50°C under atmospheric pressure for 4 hours.

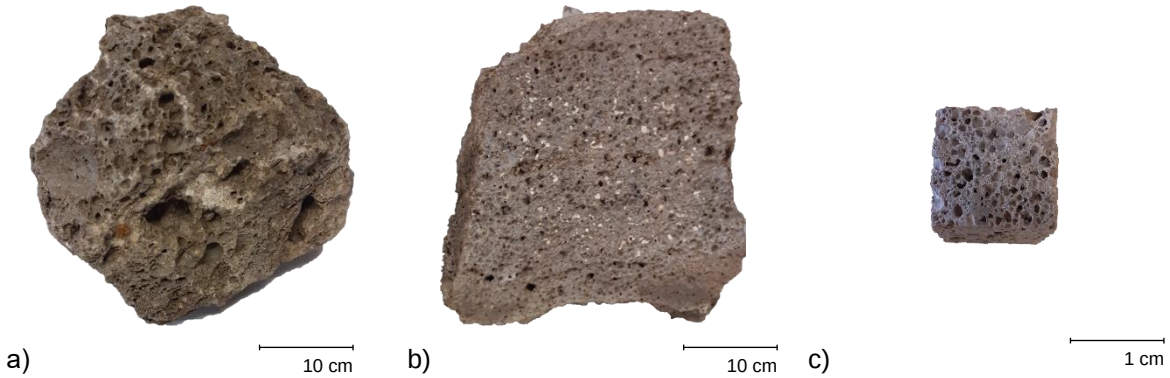

Figure 7 *Illustrative images showing the transition of steel slag samples during sectioning in preparation for x-ray computed tomography. a) initial rock b) ~1.5 cm width slices c) cubes of ~1 cm per side.*

2.3.3 X-ray computed tomography.

X-ray computed tomography was performed individually over sixteen legacy steel slag cubic samples (*A to P*) using a Nikon XT H 225/320 LC system equipped with a Deben CT 10kN cell located at the Advanced Materials Research Laboratory at University of Strathclyde, Scotland. The outcome of the computed tomography analysis over steel slag cubes was sixteen data sets containing 3000 to 3500 2D radiographs, to be potentially used to render 3D visualizations of the samples or perform reconstructive and segmentation analysis over the 2D elements.

In this case, preliminary assessment of the scanning was completed, from which around 1000 to 1500 slices were selected from the original dataset, as these slices presented suitable characteristics for image processing using Avizo system (*Version 9.3.0* | *4.5.0 NVIDIA 353.62* | *GeForce GTX TITAN X/PCIe/SSE2*) and further CO_2 quantification. Following preparation actions for image processing and to keep uniformity on the processing of the data sets from XCT analysis, the sixteen sets of scanned material were portioned into blocks of 500 slices each (*sub-volumes*), to keep a manageable working size, adequate visualization and facilitating 3D reconstruction when performing image processing on Avizo.

2.3.4 Image processing of x-ray computed data for CO_2 quantification on legacy steel slag samples using Avizo system.

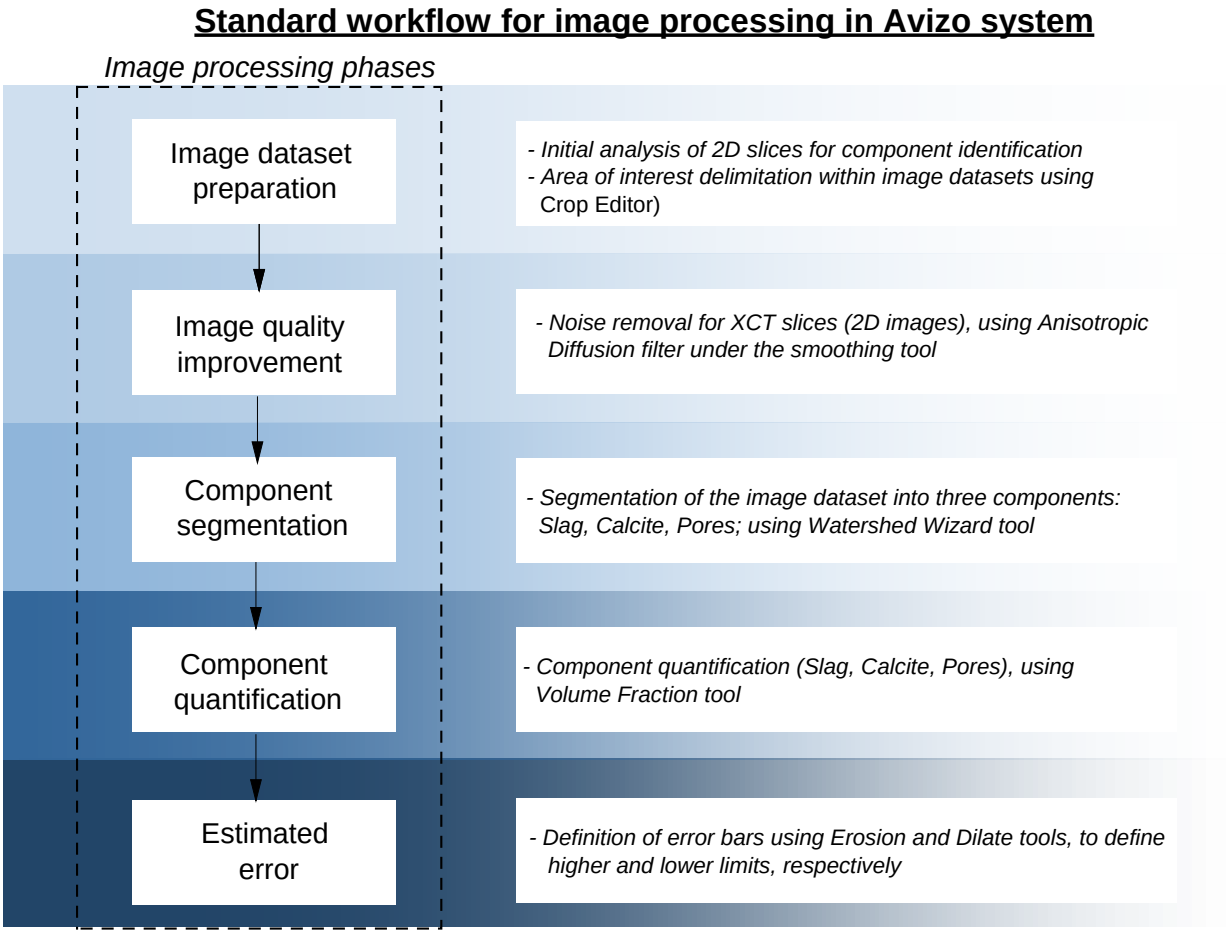

Figure 8 *Standard workflow for image processing in Avizo system, applied for CO_2 quantification within legacy steel slags.*

The image processing for CO_2 quantification of XCT scanned steel slag involved the treatment of the resulted 2D radiographs using Avizo system. See Figure 8.

To complete this action, a standard processing workflow involving the modules and tools available on the software was developed by following Avizo Users Guide 2019 (Thermo Fisher Scientific, 2019); the working plan involved four main processing steps:

- Firstly, by initiating the quantification procedure with a preparation of the image dataset, which included a deep analysis on the images and selecting an area of interest with suitable characteristics for CO_2 quantification.

- The second step was quality improvement of the 2D image datasets, implicating the modification of exposure parameters to facilitate the definition and visualization of the materials constituting the samples.

- The third step was component segmentation, where based on the capacity of the software to define a threshold over the digitalized steel slag, a separation and categorization of the pixels associated to each phase forming the steel slag was generated enabling identification of the phases of interest.

- The fourth step on the workflow was to measure the volume each of the segmented components occupied inside the samples. An additional step was completed to create error bars to validate quantification results. The actions completed along with the parameters involved in each step of the image data set processing workflow are detailed in the following subsections of the document.

2.3.4.1 Area of interest selection.

The first step on the processing workflow of legacy steel slag radiographs involved an initial review on the characteristics of the 2D slices forming the data set to process any identified irregular areas that might generate noise on the measurement or possible visualization inaccuracies from the digitalized samples. To complete this action, the *"Crop Editor"* tool from Avizo, through its command window, enabled the modification of the initial index values to shape the sample into a cubic form; this step was also necessary to remove areas or empty spaces that affected further quantification actions.

The significance of this initial step is to promote uniformity along the samples studied and avoid any bias on subsequent steps like segmentation, where empty space or irregularities on the dataset could be mistaken as a phase of interest.

2.3.4.2 Quality improvement of image datasets.

The second step on the image processing of x-ray imaged legacy steel slag cubes involved noise removal and component differentiation on the 2D radiographs; this to facilitate the delimitation of the edges between the materials of interest, simplifying a subsequent segmentation process. Figure 9 illustrates the process of improving image quality in a 2D radiograph, identifying components of interest, and presenting segmentation results in 2D and 3D format.

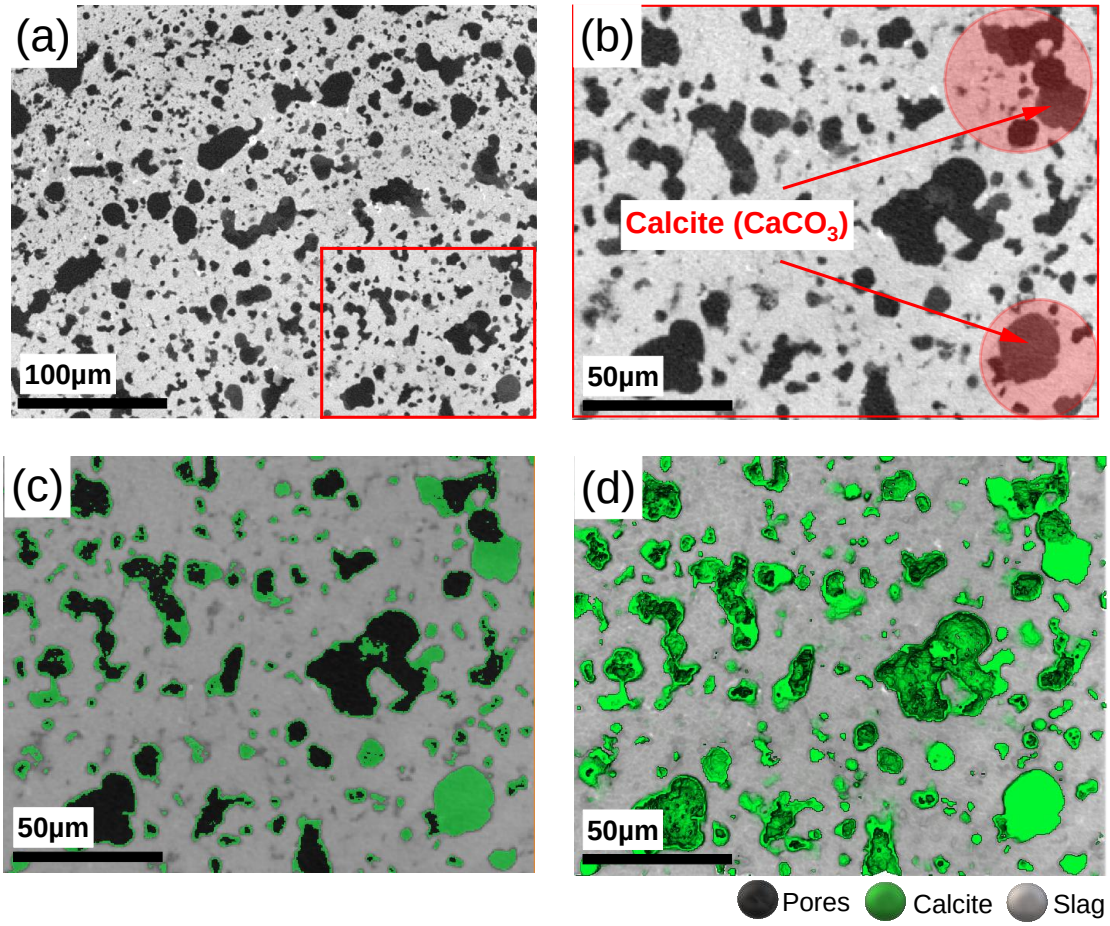

Figure 9 *XCT slice reconstruction using Avizo. a) Full image filtered. Magnified area of interest: calcite identification (b); 2D segmented components (c): Pores (black), Calcite (green), Slag (grey); (d) 3D segmented components: Calcite (green), Slag (grey).*

The component differentiation between the materials involved testing diverse filtering options within the smoothing filter classification offered by the Avizo system. The selection of the anisotropic diffusion filter was based on literature from Ferreria et al. (2018) and by conducting several attempts on testing filter options using the *'filter sandbox'* tool, which provided an overview of smoothing and denoising results under different parameters arrangements.

Therefore, anisotropic diffusion was the most feasible option based on the high performance offered on clearing the visual noise on the image datasets and enabling a delimitation of the components within the material without compromising segmentation and quantification results.

2.3.4.3 Component segmentation.

Segmentation was a key step in the processing of x-ray computed images to estimate the amount of mineralised carbon dioxide present on the legacy steel slags studied. The module used to complete this procedure was watershed wizard, an advantageous tested route to segment and quantify different materials coexisting in a sample. As seen in Figure 10, the segmented components: slag (*a*) and calcite (*b*) were divided to further measure the fraction of the volume each occupied within the steel slag sample.

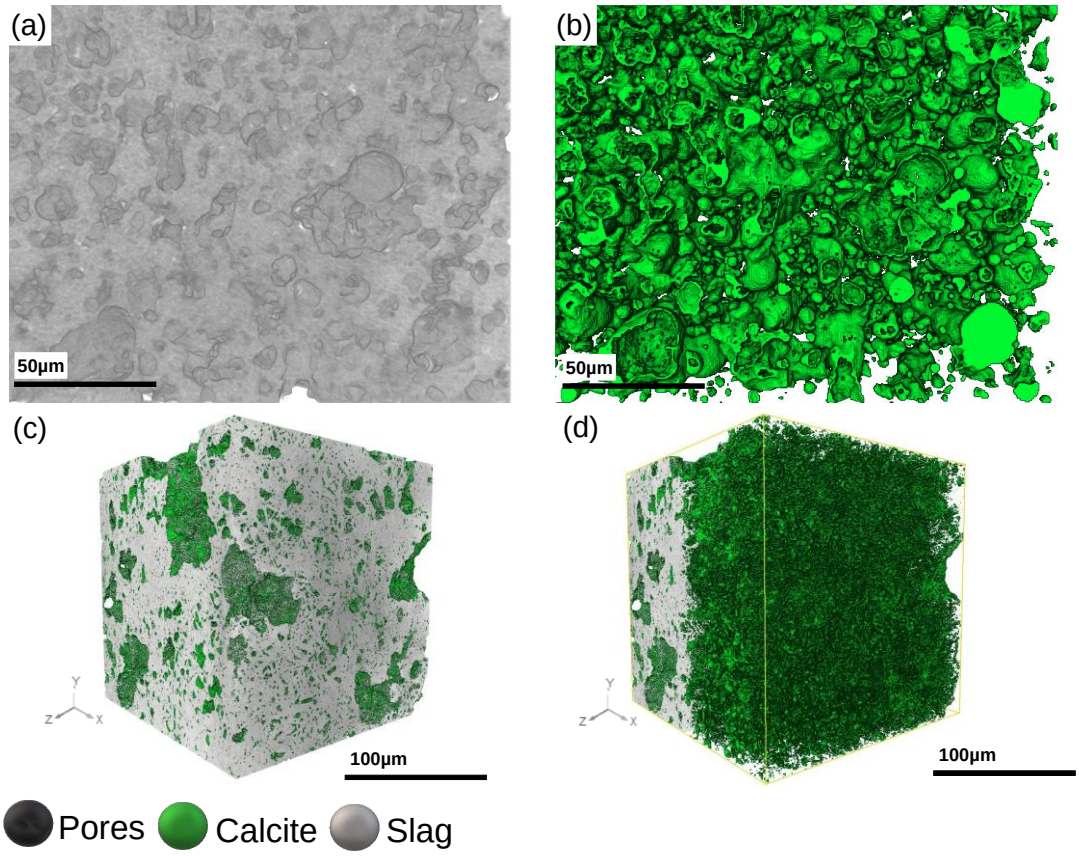

Figure 10 *Component segmentation of a steel slag sample: (a) Slag, (b) Calcite; 3D view of the slag: (c) full image, showing the interaction between slag (grey) and calcite (green) and (d) render of the inside view of the calcite component within the sample.*

To perform the watershed route, it is necessary to initially guide the software on the understanding of the materials to segment, by assigning each material or phase of interest to a pixel along the greyscale of the 2D radiographs. The initial pixel to component assignment was done based on the natural density differential existing between the steel slag constituents, which enabled definition of three components of interest (*calcite, pores and slag*) over the 2D radiographs, where black areas indicated porosity (*pores*) and empty space around the cubic sample rendered, areas coloured in different shades of grey made visible the solid fraction forming the steel slag (*Al_2O_3, CaO, FeO, K_2O, MgO, MnO, S, SiO_2,TiO_2*) (Piatak et al., 2015b) and pale grey or white coloured spots on the edges of the sample and between pores (*black*) and the grey areas showed the mineralised CO_2 as calcite.

The three components coexisting within the steel slag sample were identified by adjusting the gradient threshold parameters in representative slices using the watershed wizard tool. This process involved selecting characteristic pixels on the 2D images representing the components to be segmented, guiding the software to apply the treatment across the entire dataset. The segmentation of these three components determined the proportion of each within the total volume of the sample, thus facilitating further quantification.

2.3.4.4 CO_2 quantification.

The quantification of mineralised CO_2 on the legacy steel slag studied involved completing the image processing of the samples through Avizo, using the volume fraction module to conduct an interpretation of the labelled voxels computed during the segmentation step and counting them. This action calculated the volume fraction (*vol.%*) each segment (*calcite, pores, slag*) represented from the total volume of the sample. Then, with better understanding on the volumetric distribution of the constituents in the sample, the volume fraction (*vol.%*) corresponding to the calcite component was converted into mass units using *Equation 1*, where volume data derived from XCT analysis and the density of calcite ($CaCO_3$) used was ρ_{CaCO_3}=2.71 g/cm^3 from Mineralogical Society of America (2024).

Equation 1.

$$mass_{CaCO_3} = Volume_{\ CaCO_3} * \ \rho_{CaCO_3}$$

Where:

- Mass $_{CaCO_3}$: is the calculated mass of the component (calcite) from the sample studied (g).
- Volume $_{CaCO_3}$: Volume of calcite ($CaCO_3$) within the steel slag sample (cm^3). See equation 1.1 below.
- Density $_{CaCO_3}$: 2.71 g/cm^3 from (Mineralogical Society of America, 2024).

To calculate the volume of calcite ($CaCO_3$), *Equation 1.1* was used, involving the total volume of each of the steel slag samples, derived from XCT measurement, multiplied by the Volume fraction (Vol.%) obtained from the processing of each sample through Avizo.

Equation 1.1.

$$Volume\ _{CaCO_3} = Vol.\%_{CaCO_3} * Volume\ of\ steel\ slag\ cube.$$

Once the mass of each phase was calculated, the subsequent action was to estimate the mass of carbon dioxide (*CO_2*) mineralised within the calcite phase using the molecular mass from both compounds (*CO_2 and $CaCO_3$*) and the known mass of the calcite (*$CaCO_3$*) fraction. *Equation 2* illustrate the calculations completed.

Equation 2.

$$\frac{Mass_{CO_2}}{Molecular\ mass_{CO_2}} = \frac{Mass_{CaCO_3}}{Molecular\ mass_{CaCO_3}}$$

$$Mass_{CO_2} = \frac{Mass_{CaCO_3}}{Molecular\ mass_{CaCO_3}} * Molecular\ mass_{CO_2}$$

Where:

- Mass CO_2: is the mass of carbon dioxide (CO_2) to be estimated (g).
- Mass $CaCO_3$: is the mass of the calcite ($CaCO_3$) component (g) Equation 1 (above).
- Molecular mass CO_2: 44g/mol.
- Molecular mass $CaCO_3$: 100 g/mol.

The mass of carbon dioxide within the calcite component was calculated for the scanned block processed; quantified CO_2 mineralised on steel slag was normalized as grams of CO_2 per grams of steel slag (*involving the total weight of the scanned block*). A final step during the quantification of mineralised CO_2 on steel slag is expressing the results as kilograms per tonne of steel slag, a common practice on related literature for standardizing data. Following this methodology, unit conversion was completed as a final step on the processing of the sixteen legacy steel slag samples. The calculations performed are detailed below on *Equation 3*:

Equation 3

$$\frac{mass_{CO_2}}{g_{Steel\ slag}} = \left(\frac{1000000\ g_{Steel\ slag}}{1\ tonne_{Steel\ slag}}\right) * \left(\frac{1\ Kg_{CO_2}}{1000\ g_{CO_2}}\right) = Quantified\ CO_2\ expressed\ in\ \frac{Kg_{CO_2}}{tonne_{Steel\ slag}}$$

Where:

- Mass CO_2 per gram of steel slag: is the estimated mass of carbon dioxide mineralised per gram of steel slag.

2.3.4.5 Determination of the ranges for maximum and minimum values.

The determination of upper and lower boundaries during the image processing of x-ray computed steel slag facilitates accurate volume fraction calculation for each segment of interest (*slag, pores and calcite*) to quantify the total CO_2 mineralized in each sample. The process involved adding an interactive thresholding module to define the maximum and minimum values that segmented phases can attain. This action contributes in maintaining consistent binarization logic (to categorize the interior and exterior materials in the sample) across the three segmented phases. As reported in Macente et al. (2019), the modules (*dilation and erosion*) enabled estimation of values above and below of the computed volume fraction resulting from the image processing, generating the error boundaries needed to assure validation on the quantification results.

During the binarization of the segmented phases of the samples processed, the utilisation of the dilation module helped in filling the space that was not covered by the watershed wizard tool during segmentation step. During this process, the erosion module was employed to refine the boundaries of the segmented areas by removing any irrelevant features or noise that could have been not suitable for the volume fraction measurement. This enhanced that the final segmented phases were well-defined, resulting in accurate CO_2 quantification over the image analysis of the segments of interest: slag, pores and calcite. A volume fraction module was attached to compute the resulting values and *Equations 1, 2 and 3* (*see section 2.4.4.4 above*) were used to calculate CO_2 amount and complete a conversion to mass units.

2.3.4.6 X-ray diffraction XRD.

X-ray diffraction was conducted on four of the sixteen legacy steel slag samples studied to corroborate the presence of atmospheric carbon dioxide mineralised as calcite ($CaCO_3$). The four samples were prepared under 105 µm and then analysed for qualitative x-ray diffraction (*XRD*) (*Malvern Panalytical Empyrean; Cu Kα radiation; reflection geometry 5-80°2Θ; step size 0.0131°*). High Score Plus software (*Malvern Panalytical B.V. version 5.1a (5.1.1.30138)*) was used to conduct the crystallographic analysis after XRD performance.

2.4 Results.

2.4.1 X-ray diffraction (XRD).

X-ray diffraction analysis was conducted to the determine presence of calcite ($CaCO_3$) (*component of interest when performing CO_2 quantification*) before x-ray computed tomography and further image processing. Figure 11 shows the crystalline behaviour of diffraction patterns from samples A, B, J, K where characteristic peaks corresponding to calcite ($CaCO_3$) were identified. This validated the presence of calcite, where mineralised CO_2 is solidified passively over the carbonation periods. The presence of other mineral phases inherent to Basic Oxygen Furnace slag, such as akermanite ($Ca_2MgSi_2O_7$) were also identified, showing an expected composition on the samples tested (Piatak et al., 2015b) regardless of their collection background.

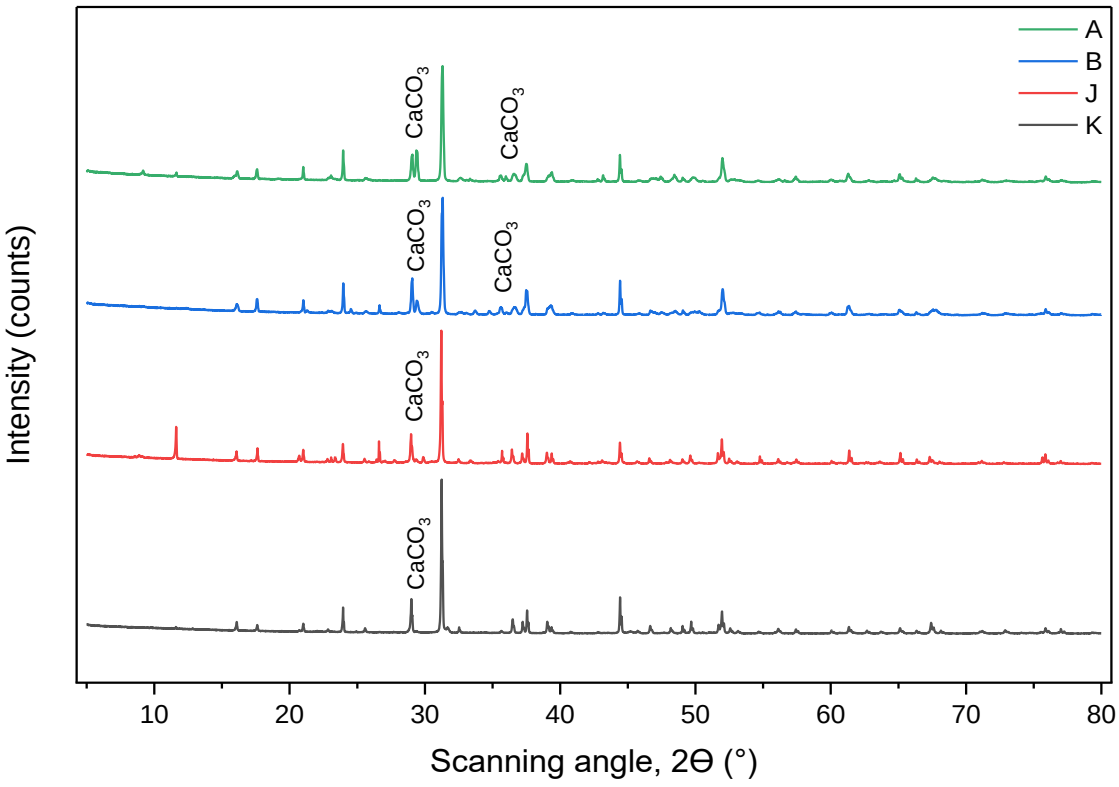

Figure 11 *Qualitative x-ray diffraction analysis (XRD) for legacy steel slag collected in Mexico and Scotland.*

2.4.2 Volume fraction of segmented components.

Figure 12 shows the average volume fraction of each component (*Pores, Calcite, Slag*) in the sixteen legacy steel slag cubes labelled from A to P. Data categorized from A to H illustrate the Scottish steel slag samples, showing the volume fraction of Pores, Calcite and Slag components represented in terms of percentage. On average the Slag component is 66.5% with a minimum volume fraction of 50% (*sample H*) and a maximum value around 77% (*sample F*). The Pores component is variable, with an average fraction of the volume of 24.86%, having 13% as the lowest vol.% on sample F and 43% as a maximum value on sample H. This was expected based on the results from slag component distribution on both slag cubes tested, showing a significant difference on the component distribution along the Scottish slags. Calcite volume fraction (*component of interest*) as expected was the lowest value among the three components within the total samples analysed, the average fraction corresponding to this Calcite was 8.63% with a maximum value of 11% calculated on sample E and with a minimum of 6% from sample B. Steel slag cubes E, F and G also presented 10% of vol.% which is close to the maximum limit calculated in sample E (*11%*). Close to the average volume fraction calculated for calcite component (*8.63%*), steel slag cubes A, B, C, H with computed fractions of the total volume of 8, 6, 7, 7 vol.% respectively.

Mexican steel slag presented lower average calcite volume fraction over the eight samples analysed. The processed slag (*samples I to P*) showed an average of 3.25 vol.% on the calcite component; sample I and J were the lowest computed, both with 1 vol.%; sample K showed a 2 vol.% and close to the average measured value, samples M, N had 3 Vol.% of mineralised CO_2 as $CaCO_3$. In samples I, J and K, the segmented slag volume fraction was I=75, J=78, K=77 vol.% respectively with an average of 76.6 vol.%; Pore volume fraction measurement results were similar with an average of 21.66% and specific values of: I=24, J=21 and K=20 vol.%. Samples M and N showed average calcite phases as mentioned earlier but had differences on the distribution of pore and slag components. The slag component in sample N was 66 vol.%, which was lower than that processed for sample M (*70 vol.%*); sample N (*30 vol.%*) then showed higher porosity compared to sample M (*27 vol.%*) which was the same as porosity found on sample L, where corresponding values on slag and calcite components were 69 vol.% and 4 vol.% respectively. From the eight Mexican slag cubes processed, sample P showed the highest volume fraction of calcite with 7 vol.%; this was above average and was evident on visual analysis of the sample. Slag and pore components on sample P were 67 vol.% and 26 vol.% correspondingly.

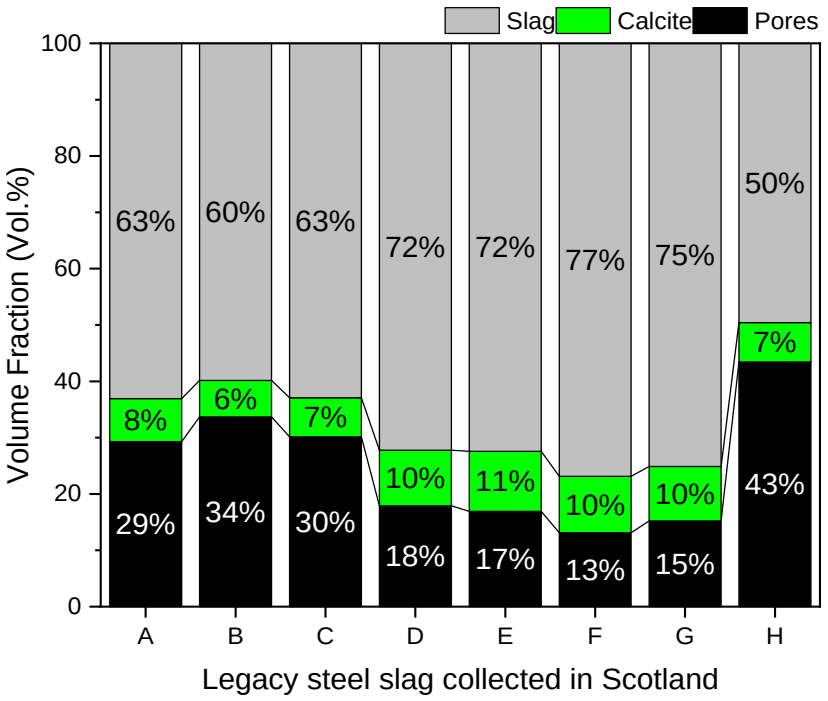

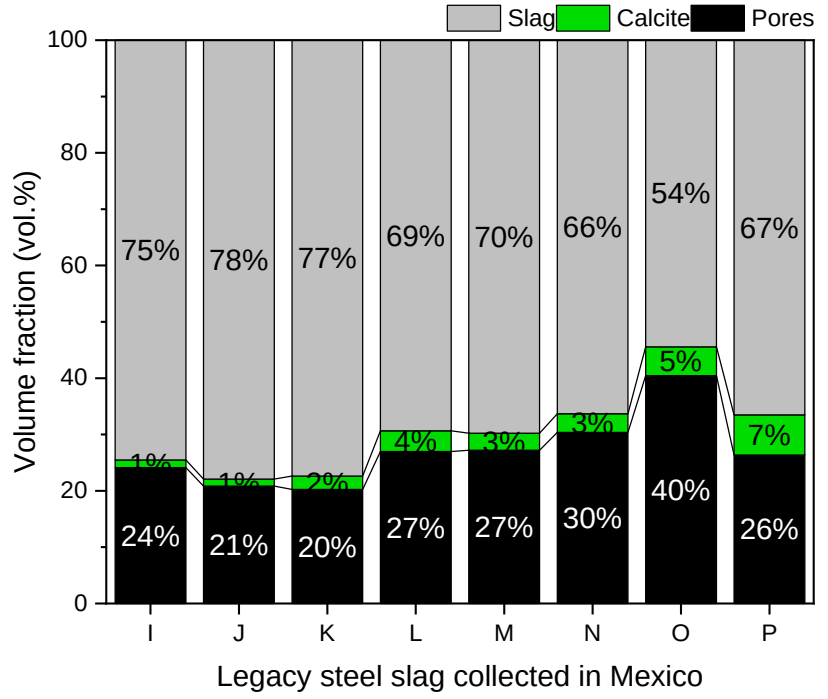

Figure 12 *Average volume fraction of segmented components (Calcite, Pores, Slag) on steel slags from Mexico and Scotland.*

2.4.3 Content of mineralised CO_2: Comparing $CaCO_3$ volumes between loads.

Scanned slag samples (A to P) obtained from XCT were composed of 1000 slices each. These slices were then divided into sub-volumes (or loads) consisting of 500 slices each, facilitating image processing in Avizo software. This method aimed to quantify mineralized CO_2 precipitated as calcite ($CaCO_3$) in each scanned slag cube, while enabled to compare if the volumes of $CaCO_3$ were similar between both loads. Analysis of calcite component volumes (cm^3) indicated that Scottish slag samples (A to H) showed mostly consistent values of calcite across sub-volumes. The only slight variation was shown in samples A, B, G and H where the calculated difference between sub-volumes was below 0.03 cm^3. Mexican slags (*I to P*) showed equivalent volumes of carbonated CO_2 as calcite with no major differences between sub-volumes in each processed sample. The calculated volume difference between sub-volumes is summarized on Table 2 and Figure 10.

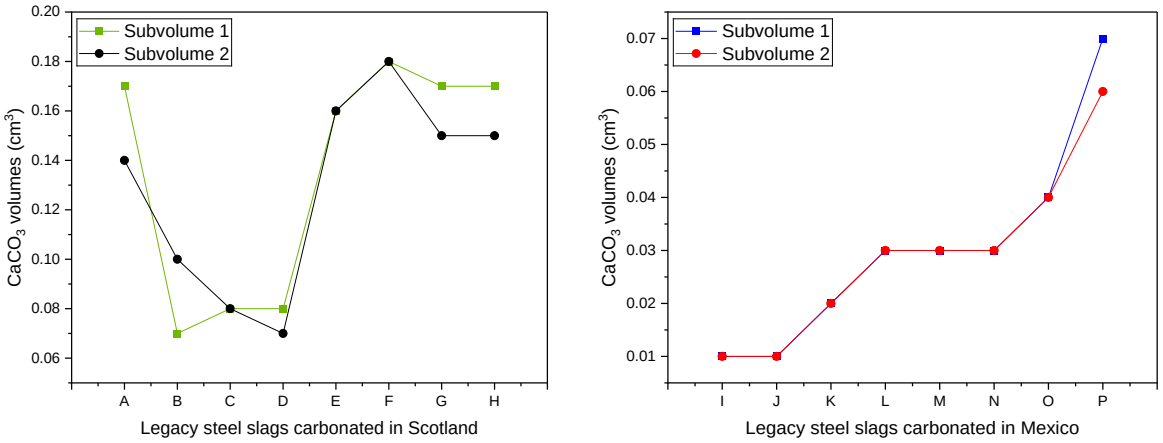

Figure 13 *$CaCO_3$ volumes comparison between sub-volumes of steel slag samples: Mexico and Scotland.*

Table 2. $CaCO_3$ volumes comparison between steel slags sub-volumes: Mexico and Scotland.

Comparison between $CaCO^3$ volumes in each sub-volume corresponding to steel slag samples A to P. Expressed in cm^3.																
	Scottish steel slag samples								**Mexican steel slag samples**							
	A	**B**	**C**	**D**	**E**	**F**	**G**	**H**	**I**	**J**	**K**	**L**	**M**	**N**	**O**	**P**
S1*	0.17	0.07	0.08	0.08	0.16	0.18	0.17	0.17	0.01	0.01	0.02	0.03	0.03	0.03	0.04	0.07
S2*	0.14	0.10	0.08	0.07	0.16	0.18	0.15	0.15	0.01	0.01	0.02	0.03	0.03	0.03	0.04	0.06

2.4.4 Quantified CO_2 (Kg) per tonne of legacy steel slag: Mexico and Scotland.

Slags from Scotland showed higher rates of carbon dioxide sequestrated than Mexican steel slags. Average CO_2 quantified in kilograms per tonne of steel slag is presented in Figure 14, comparing the sixteen samples processed (*A to P*). Within the slags from Ravenscraig (*A to H*), the minimum value quantified of carbonated CO_2 was 42 $KgCO_2$/tonne $_{Steel\ Slag}$ in sample B and the maximum volume quantified of mineralised CO_2 was 60 $KgCO_2$/tonne $_{Steel\ Slag}$ from sample E; the calculated average of carbon dioxide precipitated in Scottish samples was 54 Kg of CO_2 per tonne of legacy steel slag. The quantification analysis of CO_2 in slags from Monclova, Mexico (*I to P*) showed on average 21 Kg of CO_2 per tonne of slag; in Mexican slags, minimum values of CO_2 measured were of 6 Kg of CO_2/tonne $_{Steel\ Slag}$ (*sample J*) and the maximum of 51 Kg of CO_2/tonne $_{Steel\ Slag}$ (*sample P*). The plot also shows the estimated error (*error bars*) for each of the sixteen samples quantified from Mexico and Scotland, this is further detailed in section 2.4.4.1, by providing the higher and lower limits or error bars calculated for each of the samples using the Avizo system.

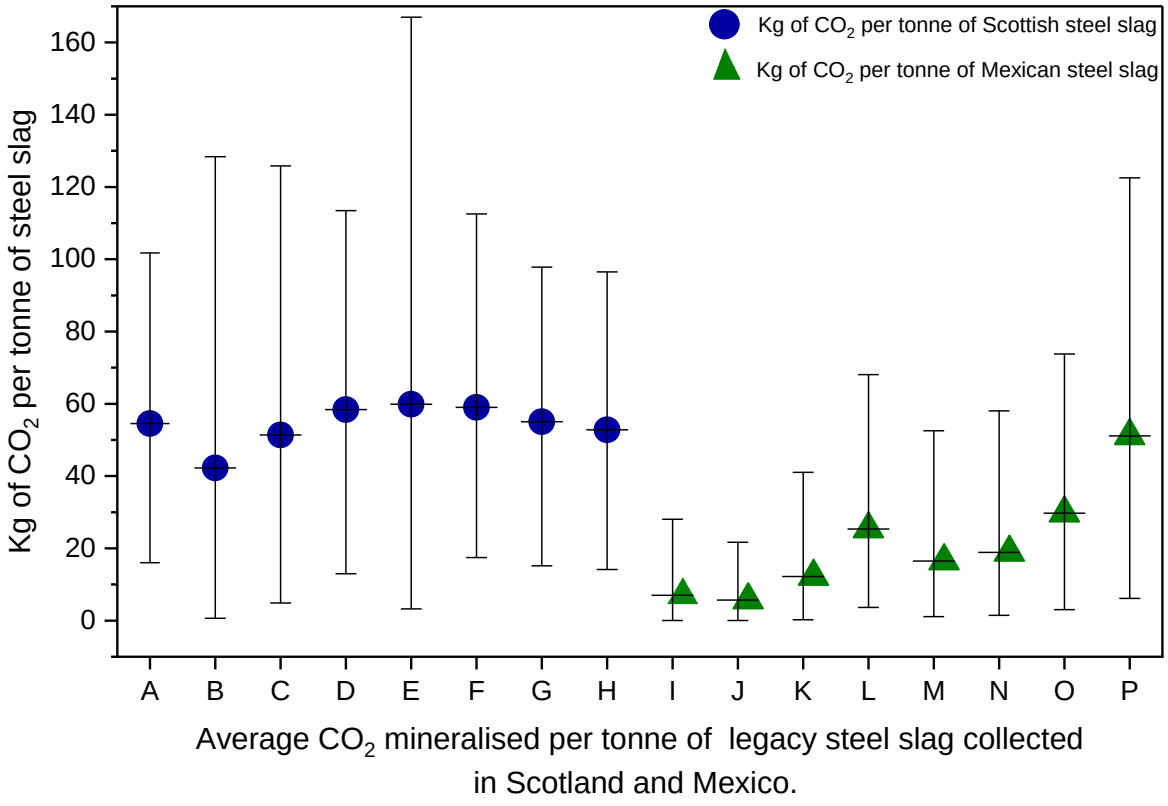

Figure 14 *Comparison between Mexico and Scotland on average CO_2 quantified on legacy steel slag.*

2.4.4.1 Error bars of quantified CO_2 (Kg) per tonne of legacy steel slag: Erosion and Dilation.

The estimated error (*error bars*) over the sixteen steel slag samples was calculated using erosion and dilation tools from the Avizo system, where the resulting volume fraction values provided error bars (*higher and lower*) limits as a validation guidance on segmentation and phase volume fraction procedures. This was also illustrated in Figure 14, providing the error bars for the quantified CO_2 in each steel slag sample from Mexico and Scotland.

Error bars were applied in a conservative way. Therefore, from the sixteen slag samples studied, sample E (*Scotland*) presented the higher volume of quantified CO_2 with 60 $kgCO_2/tonne_{\ Steel\ Slag}$, maximum (+) and minimum (-) error limits were calculated using erosion and dilation tools from Avizo system, resulting in a higher limit or maximum volume of 167 $kgCO_2/tonne_{\ Steel\ Slag}$ (*dilation*) and a lower limit or minimum calculated volume of 3 $kgCO_2/tonne_{\ Steel\ Slag}$ (*erosion*). The same procedure was done for the rest of the samples, e.g., sample J (*Mexico*), which had the lowest average CO_2 of 6 $kgCO_2/tonne_{\ Steel\ Slag}$, and a calculated error range of 0.04 $kgCO_2/tonne_{\ Steel\ Slag}$ (*for the lower limit (erosion)*) to 21 $kgCO_2/tonne_{\ Steel\ Slag}$ for the higher limit (*dilation*).

Within the eight steel slags processed from Ravenscraig, Scotland, the lower CO_2 volumes quantified were Sample A, B, C and H. Mineralised CO_2 measured for sample A was 54 $kgCO_2/tonne_{\ Steel\ Slag}$, and the calculated error range for this sample was within 16 (*lower limit*) and 102 (*higher limit*) $kgCO_2/tonne_{\ Steel\ Slag.}$ Carbonated CO_2 measured in sample B was 42 $kgCO_2/tonne_{\ Steel\ Slag}$ with error bars between 1 to 129 $kgCO_2/tonne_{\ Steel\ Slag}$. Quantified for sample C, in this order, quantified CO_2, lower and higher limits for error bars: 51, 5, 126 $kgCO_2/tonne_{\ Steel\ Slag.}$ The volume of CO_2 from sample H was 53 $kgCO_2/tonne_{\ Steel\ Slag}$ with lower and higher limits of calculated error between 14 to 97 $kgCO_2/tonne_{\ Steel\ Slag.}$

Mexican slag cubes with lower quantified CO_2 levels were as follows: sample I had 7 kg CO_2/tonne of steel slag with an error range of 0.3 kg CO_2/tonne (*lower limit*) to 28 kg CO_2/tonne (*upper limit*). Sample K had 12 kg CO_2/tonne of steel slag, with a lower error limit of 0.3 kg CO_2/tonne due to erosion and an upper error limit of 41 kg CO_2/tonne due to dilation. For sample M, the average CO_2 volume was 16 kg CO_2/tonne of steel slag, with error bars ranging from 1.1 kg CO_2/tonne to 43 kg CO_2/tonne.

The mass of CO_2 calculated for sample N was 19 kg CO_2/tonne of steel slag, with a lower error limit of 1.5 kg CO_2/tonne and an upper limit of 58 kg CO_2/tonne. Samples M and N showed results close to the overall average CO_2 volume for Mexican slags, which was 21 kg CO_2/tonne.

Among the Mexican samples, L, O, and P showed the highest levels of CO_2 carbonation. Sample P had the highest quantified CO_2 among the eight samples from northern Mexico, with 51 kg CO_2/tonne of steel slag. Sample L showed an average of 25 kg CO_2/tonne, with a lower limit of 3.6 kg CO_2/tonne and an upper limit of 68 kg CO_2/tonne. For sample O, the average CO_2 content was 30 kg CO_2/tonne, with a lower limit of 3 kg CO_2/tonne and an upper limit of 74 kg CO_2/tonne within the error bars.

As referenced before, Scottish slags studied for this thesis showed the highest higher masses of passively captured CO_2, from which sample D carbonated 58 kgCO_2 per tonne of steel slag, with error bars of 13 kgCO_2/tonne $_{Steel\ Slag}$ and 114 kgCO_2/tonne $_{Steel\ Slag}$ for lower and higher level, respectively. Besides sample D, samples F and G were between the top three with higher mineralised CO_2 within the sixteen slag cubes tested. Sample F presented an average of 59 kgCO_2/tonne $_{Steel\ Slag}$ with a lower value of 17 kgCO_2/tonne $_{Steel\ Slag}$ and a higher value of 113 kgCO_2/tonne $_{Steel\ Slag}$ within the error bars. Measurement of mineralised carbon dioxide in sample G resulted in 55 kgCO_2/tonne $_{Steel\ Slag,}$ and the error bars were between 15 kgCO_2/tonne $_{Steel\ Slag}$ (*lower limit*) and 98 kgCO_2/tonne $_{Steel\ Slag}$ (*higher limit*).

Results presented in this section showed how slags that passively carbonated under open air conditions can have different mineralisation rates. The differing volumes of carbonated CO_2 calculated for the sixteen slag samples from Monclova, Mexico and Ravenscraig, Scotland, provided the means to consider local climate *(rainfall, seasonal temperature, atmospheric pressure*) as a potential influence over mineral carbonation occurring in slag heaps.

2.5 Discussion.

Parameters influencing mineral carbonation of slags have been studied over a lab-scale perspective, but there is limited research addressing external conditions (environment) implicated over mineral carbonation of slag heaps occurring with no human intervention. Therefore, it is worthwhile to explore the impact of environment over the sequestration of atmospheric CO_2 occurring in legacy steel slags, as this potentially explains the different volumes of CO_2 sequestrated within the deposited slags.

Legacy steel making slags from Mexico and Scotland were evaluated on their capacity to mineralise (*sequestrate*) atmospheric CO_2 in line with the chapter aim to better understand the implications of environmental conditions, among other parameters, influencing passive mineral carbonation of steel slags. The differences between quantified CO_2 carbonated in slags from Ravenscraig and Monclova supported the interest to explore why slags from northern Mexico and Scotland mineralise different amounts of CO_2.

2.5.1 Quantified CO_2 (Kg) per tonne of legacy steel slag: Mexico and Scotland.

Within the quantified volumes of mineralised CO_2 presented in section 2.4 of this chapter, Scottish samples showed a higher CO_2 uptake, with an average of 54 Kg of CO_2 per tonne of steel slag. This average volume is approximately double the amount of atmospheric CO_2 mineralised in Mexican slags, where the average volume quantified was 21 Kg of CO_2 per tonne. Summary of results from samples A to P is presented in Table 3, showing from highest to lowest the CO_2 capturing rates expressed in Kg of CO_2 per tonne of slag.

Table 3. Steel slags samples (A to P) classified from higher to lower in terms of CO_2 uptake.

+ to -	**E**	**F**	**D**	**G**	**A**	**H**	**C**	**P**	**B**	**O**	**L**	**N**	**M**	**K**	**I**	**J**
Kg CO_2/t	60	59	58	55	54	53	51	51	42	30	25	19	16	12	7	6

From the results, highlights were sample E from Scotland, with the highest quantified CO_2 volume (*60 KgCO_2/tonne $_{Steel\ Slag}$*); on the contrary, sample J from Mexico had the lowest volume of qualified CO_2 within the sixteen samples processed on this experimental work, with 6 Kg of CO_2/tonne $_{Steel\ Slag}$.

Sample B showed 42 KgCO_2/tonne $_{\text{Steel Slag}}$, the lowest value within the samples collected in Ravenscraig, Scotland. Sample P showed the highest CO_2 volume within Mexican samples, with 51 Kg of CO_2/tonne $_{\text{Steel Slag}}$, indicating similar capturing rates to samples C collected in Scotland. Overall, Mexican and Scottish legacy steel slags differed on their capacity to sequestrate atmospheric CO_2. Causes of this variability may be related to whether the slags passively carbonated or the different lengths of the mineral carbonation reaction.

2.5.1.1 Comparison of CO_2 Uptake in Mexican and Scottish Slags with Findings from Various Studies

When comparing the CO_2 sequestration potential of steel slags from this research to the findings of other studies, several key differences and similarities emerge. Scottish slag samples demonstrated a higher CO_2 uptake, with an average of 54 kg CO_2 per tonne of slag, compared to 21 kg CO_2 per tonne in Mexican samples. The most notable result was from Scottish sample E, which achieved the highest CO_2 capture at 60 kg CO_2 per tonne, while Mexican sample J recorded the lowest at 6 kg CO_2 per tonne.

This variability aligns with the broader range of sequestration capacities observed in the literature. For instance, Ukwattage et al. (2017) reported a CO_2 sequestration potential of 29.47 kg per tonne of slag, which is lower than the average Scottish samples in my study but higher than most Mexican samples. Similarly, Huijgen et al. (2005) and Huijgen & Comans (2006) estimated a theoretical CO_2 sequestration capacity of 250 kg CO_2 per tonne of steel slag, which significantly exceeds the capacities observed in my experiments, but their practical sequestration potential of 90 kg per tonne is more comparable to the upper range of my Scottish samples, particularly samples E and F.

The results from Bonenfant et al. (2008) also show a disparity in CO_2 capture based on slag type, with ladle furnace (LF) slag reaching up to 24.7 g CO_2 per 100 g slag (equivalent to 247 kg per tonne), which is much higher than the rates in both my Scottish and Mexican samples. However, the electric arc furnace (EAF) slag in their study captured only 1.74 g CO_2 per 100 g slag (17.4 kg per tonne), which aligns more closely with the lower end of my results, particularly for Mexican slags such as sample J.

Pullin et al. (2019) highlighted the role of slag mineralogy in determining sequestration potential, noting that mineralogy can limit carbonation, especially in slags with low-reactivity phases like melilites. This may explain why certain Mexican samples, such as sample J, showed much lower CO_2 capture rates than the Scottish slags. Additionally, Pullin et al. (2019)

observed that direct carbonation could capture up to 8.5–9.7 Mt of CO_2 in slag heaps, underscoring the long-term potential of slags as carbon sinks. The variability in the results presented in this thesis, particularly between the highest capturing Mexican sample P (51 kg CO_2 per tonne) and the lowest Scottish sample B (42 kg CO_2 per tonne), suggests that site-specific factors such as slag composition and exposure duration also play a critical role in determining sequestration efficiency, as noted in the study of Pullin et al. (2019), this to be address in further sections.

Moreover, in a study by Khudhur et al. (2023), CO_2 uptake values for steel slag samples were quantified using thermogravimetric analysis (TGA), with CO_2 contents ranging from 0.86% to 2.84% by weight. This corresponds to between 8.7 and 29.2 Kg CO_2 per tonne of slag on a CO_2-free basis, which falls within the range of our results for Mexican samples (6 to 51 Kg CO_2 per tonne) and partially overlaps with the lower range of Scottish samples. These values reflect typical CO_2 sequestration potential for legacy steel slags, highlighting their significant role as carbon sinks, although further optimization could enhance their carbonation efficiency.

2.5.2 Why does CO_2 mineralisation vary between slags from Mexico and Scotland?

The variation between volumes of CO_2 mineralised in slags from Mexico and Scotland might implicate the influence of diverse parameters over the carbonation reaction within the slags, for instance, properties of the slag (*physical, chemical*), the period of carbonation or the local environment characteristics such as: temperature, rainfall, atmospheric pressure, even soil pH or altitude conditions. Thus, having in mind the carbonation background of the slags and the differences between CO_2 quantified from both sets of studied samples, it is worthwhile to further discuss if context (*environment*) has an influence over mineral carbonation of steel slags.

2.5.2.1 Physical and chemical characteristics of steel slag and their role in CO_2 mineralisation.

The first parameter to discuss is the impact of physical and chemical properties of slags in the mineralisation of CO_2. This has been previously studied by Mattila et al. (2012), Klein et al. (2011) and Piatak et al. (2015a) using slags from elsewhere under laboratory-based experiments. The documented results showed that slag properties such as particle size, type and composition can influence the kinetics of the mineral carbonation reaction. Particle size, particularly, plays a significant role in determining the carbonation capacity of slags (Han et al., 2015).

As confirmed by Santos et al. (2012), CO_2 sequestration increases when the particle size of the slags decreases. In addition, if efficiency is considered in this context, carbonation rates related to smaller particle size of slags, were found to be higher than those observed in efficiency studies involving the role of Ca ion dissolution or the abundant content of MgO and CaO influencing CO_2 sequestration rates (Polettini et al., 2016).

For this research, although Mexican and Scottish samples theoretically have similar physical and chemical characteristics as both resulted from a Basic Oxygen Furnace (Kong et al., 2019), the volumes of mineralised CO_2 quantified showed a disparity in the results, where slags from Ravenscraig carbonated higher CO_2 amounts than slags from Monclova. This might be due to several factors involved in the mineral carbonation reaction, for example physical or chemical characteristics, like different particle size, as previously mentioned, or chemical properties of the slags, also determined by the method of production. As this can have an impact on the reactivity of the material, it increases or decreases the carbon sequestration potential of the slag (Baras et al., 2023).

Overall, physical and chemical characteristics between Mexican and Scottish slags were contrasting, e.g., Mexican slags presented larger dimensions than Scottish samples when collected, which might be one of the parameters influencing the lower CO_2 captured, as contact surface was limited. Other physical differences noticed at the beginning of the study were colour and superficial porosity. However, additional parameters that might have a bigger impact over the sequestration of CO_2 within the slags could be the time of carbonation, as slags from Scotland carbonated approximately 10 and 20 years more than Mexican Slags.

2.5.2.2 The relation between time of carbonation and passive CO_2 sequestration.

The length of time and the amount of CO_2 sequestered is still a major drawback for scaling up passive mineral carbonation as a wider carbon removal option. Bearing in mind that time is a controlled aspect during lab-based carbonation experiments, it would be valuable to better understand this factor from a carbonation perspective occurring in slag heaps with no human intervention, and where environment conditions directly influence the reaction.

Slags from Scotland and Mexico were assessed for CO_2 captured across decadal timescales to examine if time was a significant parameter in determining the different amounts of carbonated CO_2 between both locations, and/or if there were additional factors with a significant influence over the results obtained.

Time of passive carbonation for Scottish slags (*A to H*) was over ~30 years and for Mexican samples was ~ 20 (*I, J*) and ~10 (*K, L, M, N, O, P*) years respectively. This variance in carbonation periods was expected to correlate with older slags presented higher volumes of mineralised CO_2. This occurred partially, as Scottish slags were in fact the ones with higher volumes of CO_2 quantified; this followed the criteria provided by Wang et al. (2018) where extended periods of time are aligned to increased sequestration rates of atmospheric CO_2.

Within the Mexican slags, the samples with a longer period of carbonation (*I and J*) were the lowest in terms of CO_2 quantified. If time alone was a key factor in carbonation, then the older (*~20 years carbonation time*) Mexican slags (*samples I and J*) would be expected to have more mineralised CO_2 than the younger (*~10 years carbonation time*) Mexican slags (*samples K-P*); however, the XCT results showed this was not the case. Based on the accelerated carbonation laboratory studies of Chen et al. (2021) and Huijgen et al. (2005), mineralisation of CO_2 is rapid at the start of the reaction time and then slows. This might have been the case for the Mexican samples (*I and J*) discussed here, where early carbonation reached equilibrium.

Although samples I, J and K presented the lowest volumes of CO_2 mineralised, those values were consistent with a quantified range for passive carbonation documented by Riley et al. (2020) and Pullin et al. (2019) which was between 0.007 to 12.1 Kg of CO_2 per tonne of slag. If this criterion is used, Scottish samples (*A, B, C, D, E, F, G, H*) and the remaining Mexican samples (*L, M, N, O, P*) presented CO_2 calculated volumes above the referenced range. In response to the initial statement, time is clearly a factor influencing mineral carbonation, however results from analytical work carried out during this research indicate that additional factors might have influenced passive mineral carbonation of slag heaps in Monclova and Ravenscraig.

2.5.2.3 The influence of humidity in passive CO_2 mineralisation.

The influence of climate on the CO_2 uptake capacity of legacy steel slags is less documented, particularly when occurring with no human intervention. In this context, the work from Riley et al. (2020), Pullin et al. (2019) and Mayes et al. (2018a) have provided understanding on the CO_2 sequestration potential of slag heaps in the UK, also offering an insight into passive carbonation of slags. Derived from the same work, Mayes et al. (2018a), reported carbonate formation from drainage water within the slag heap, highlighting the significance of water as a facilitator for carbon sequestration through the mineral weathering of iron and steel slags.

The presence of water during mineral carbonation increases calcium ion dissolution and support CO_2 diffusion through the slag, therefore in an environment where water/moisture is a constant element, the formation of stable carbonates is higher and occurs throughout the slag particles and not just on their surfaces (Ko et al., 2015). Fernández Bertos et al. (2004) and Ko et al. (2015) determined from experimental work using BOF slags, that relative humidity of 60% in a mixture promotes carbonation without generating pore blockage in the slags. Moreover, if stirring is part of the process, the efficiency of carbonation increases, as documented in reactor-based studies from Huijgen et al. (2005), where a 40% conversion (*stable carbonate formation*) occurred within the first 30 minutes; during this experiment, conditions of temperature, pressure and humidity were monitored, also reporting a decrease of 13% in mineralisation of CO_2 after the first half an hour.

For the Scottish slags, besides a longer period of carbonation, there was another key parameter potentially influencing passive carbonation resulting in higher volume of CO_2 captured: the abundance of precipitation (*average of 1254 mm a year*) over Ravenscraig, the carbonation site. This longer exposure to moisture/water contact was not the case for Mexican samples, and might also cause the higher volume of carbonated CO_2 in slags from Ravenscraig, as humidity plays a key role during the precipitation of atmospheric CO_2 into stable carbonates, as documented by Georgakopoulos et al. (2016).

Therefore, if water plays a catalyst role during the mineralisation of CO_2, wetter climates, e.g. Scotland, might provide better conditions for an increased carbonation of atmospheric CO_2 than drier climates, such as at Monclova in Mexico. Enabling the conditions for higher CO_2 capture might potentially explain why steel slags from northern Mexico sequestrated less CO_2, considering the predominant semi-aridic climate characteristics from Monclova, where water/humidity only comes with an unpredictable rain season during the summer.

2.5.2.3.1 Differing precipitation conditions between Northern Mexico and Scotland.

Weather characteristics between Monclova and Ravenscraig differ in terms of rainfall (*moisture*) and seasonal temperature. This implies that the sampled slag heaps were subject to contrasting moisture amounts during carbonation time, which is a key parameter for optimal CO_2 capturing rates, either from the experience of studying passive carbonation as the work from Mayes et al. (2018a) reported or, as the documented work from laboratory experiments such as: Rahmanihanzaki et al. (2022), Ragipani et al. (2021) and Ko et al. (2015).

Within lab-based experiments, the findings indicated that humidity, temperature, pressure and time were factors determining the amount of CO_2 mineralised within slags. Therefore, if the approach is passive carbonation, where pressure, temperature and humidity are dependent on the local environment conditions, the mineralisation of atmospheric CO_2 would be influenced by the environment, particularly from the amount of rainfall or the pluvial sources present near slag heaps.

For this research, although the slags from Ravenscraig were not in direct contact with a pluvial source, as at the site studied by Mayes et al. (2018a), the average precipitation from the location provided a humid environment during the carbonation period (1990-2019) with 1254 mm a year, providing a moist environment for carbonate formation within the slag heaps.

This amount was three times higher than the average rainfall (425 mm) of Monclova, Mexico during the period of carbonation (*1999-2019*). Based on the humid characteristics at the former Ravenscraig Steel Works, it is considered that these conditions influenced the volumes of carbonated CO_2 measured, which were between 42 to 60 Kg of CO_2 per tonne of Scottish slag.

In the case of the Mexican samples, the volume of captured CO_2 was quantified between 6 and 51 Kg of CO_2 per tonne of slag, and there was no evidence of additional pluvial sources near the collection site. Thus, in passive mineral carbonation as in lab-based carbonation, the amount of water influences the kinetics of the reaction and the potential CO_2 mineralisation. However, if excessive amounts of water are present in the carbonation environment, this could represent a limiting factor on carbonation as excess amounts of water can block the slag porosity structure, making it unable for CO_2 to react (Baras et al., 2023). This adds to the discussion the role of liquid to solid ratio for efficient carbonation.

2.5.2.3.2 Liquid to solid ratio: assessment of humidity in mineral carbonation at lab-scale work.

The efficiency of CO_2 mineralisation within slags where water was a controlled parameter, was explored from a laboratory-scale perspective in Boone et al. (2014), Ukwattage et al. (2017) and Revathy et al. (2016), whose findings reported a corelation between water/humidity and increased carbonation rates of CO_2. Lab experiments by Huijgen et al. (2005) and Ghacham et al. (2016) reached carbonation measurements of ~250 Kg CO_2/tonne where L/S ratio was a controlled parameter influencing the carbonation of CO_2. From these perspectives, it is understood that water presence activates and increases carbonation.

Tested L/S ratios shown in Chang et al. (2012) found a L/S ratio of 20 mL/g mineralised 93.5% of CO_2 using BOF slags. Other studies such as Huijgen et al. (2005) documented 2 l/kg as L/S ratio for a 74% of conversion; in the same line Baciocchi et al. (2015) measured ~325 g of CO_2 carbonated per kilogram of BOF slag, using L/S ratios between 0.3 L/Kg to 5 L/Kg, through different accelerated carbonation routes and conditions. Thus, the optimal liquid to solid ratio related to achieving a high/maximum degree of carbonation is still unclear, but results from the literature are indicators of the significance of water/humidity for efficient mineralisation of CO_2. For the present study, there was not a precise L/S ratio measurement, therefore a comparison on this parameter is not possible.

The results of passive carbonation presented here, where slags from Ravenscraig (*high humidity*) achieved higher mineralisation of CO_2 than those from Monclova (limited humidity, semi-arid), are therefore in broad agreement with the literature on laboratory experiments with accelerated carbonation. The results showed that passive carbonation can occur in an environment where conditions of temperature, pressure, time or liquid to solid ratio are not controlled, and continue acting as a carbon removal method.

In an additional approach, the results from this research can guide an examination of the role of humidity in dry or aqueous carbonation of steel slags, contrasting it with its significance in passive carbonation occurring in slag heaps, where rainfall conditions vary. This comparison sheds light on the varying degrees of importance of humidity in different carbonation processes and could be approached in a future work, considering contrasting study sites such as Monclova and Ravenscraig**.**

2.5.2.4 The influence of temperature during CO_2 carbonation within steel slags.

Temperature, alongside humidity, has been identified as a key factor influencing mineral carbonation, particularly in the reaction speed and crystallization of carbonated products (Quaghebeur et al., 2015). During CO_2 carbonation in slags, higher temperatures accelerate the reaction, however exceeding 175°C negatively impacts CO_2 solubility within the slags (Baras et al., 2023; Huijgen et al., 2005). On the other hand, lower temperatures can limit carbonation to superficial slag pores, reducing its capturing potential (Nielsena et al., 2020). For the Mexican slags, temperature might have a more determining role influencing the reaction than humidity, as the temperature from Monclova is three times higher than the temperature of Ravenscraig(~40°C), on average throughout the year, and more consistent with the experimental conditions in Baras et al. (2023) and Huijgen et al. (2005), whose experiments have shown effective conversion of CO_2 into carbonates within a range of 25–50°C.

For Scottish slags, the primary parameter influencing higher capturing rates (when compared to Mexican slags) is interpreted to be the abundance of precipitation throughout the year.

As well as in the analysis of the liquid to solid ratio, there are different perspectives on the ideal temperature to achieve higher carbonation rates. Baras et al. (2023) considered 200°C as excessive during the carbonation of BOF slags, as the carbonate conversion started to decrease once this temperature was reached; however, Ko et al. (2015) found that 200°C promoted higher conversion of CO_2 in EAF slags.

These contrasting results might be related to additional factors such as slag type, pressure or water impact, but strengthen the importance of finding an ideal temperature range for the mineralisation of CO_2 to occur without compromising the length of the reaction, and in this way reinforce the use of steel slags as a carbon removal option. Other parameters such as pressure are easily assessed during lab-based carbonation, where the influence of this factor can be measured accurately. This is more difficult to assess in passive carbonation of slags.

2.5.2.5 Does pressure a have a determinative role in passive mineral carbonation?

Pressure has been shown to be an important parameter in the degree of carbonation of slag in laboratory experimental studies (Baras et al., 2023; Bonenfant et al., 2008; Nielsena et al., 2020). In passive carbonation, however, the role of this parameter becomes a tough and less explored field. In order to assess the role of this parameter during passive mineral carbonation, the atmospheric pressure over slag heaps, using altitude data, was used to enable a comparison. Carbonation sites in Mexico have an elevation of 622m above sea level and in Scotland, of 109m above sea level.

Following the methodology from Soares et al. (2015), this results in a ~ 500m differential, which means a change in pressure of ~ 5 kPa/0.7 psia/ 0.5 atm. This amount is likely too low to represent a major influence on the carbonation process. Therefore, this difference is unlikely to be as important as other environment conditions such as humidity or temperature in the volume of CO_2 mineralised in the studied samples from northern Mexico and Scotland.

2.5.2.6 pH.

pH is one of the less explored parameters influencing mineral carbonation. In the sense of assessing the impact of pH over slag heaps carbonating under environment conditions, it was

found that an alkaline pH derived from external sources might increase the solubility of calcium ions for carbonate formation as referenced by Bonenfant et al. (2008) and Mayes et al. (2018a). Although this parameter was not assessed during the study of slags from Monclova and Ravenscraig, it might be worth exploring further based on the cost-effective relevance this can have on scaling up of mineral sequestration using steel slags, as suggested by Baras et al. (2023).

2.5.3 Summary: Did environment influence the variation of CO_2 mineralisation between slags from Mexico and Scotland?

Differing conditions of time, temperature, humidity, pressure and pH from carbonation sites were assessed to determine the difference in captured CO_2 between Monclova, Mexico and Ravenscraig in Scotland. The parameter with the strongest influence over the capturing rates of the slag heaps was interpreted to be humidity. Additional parameters such as temperature, pressure or pH might influence the reaction occurring under natural environment, however compared to humidity they are less relevant.

In the case of Mexican slags, initially temperature was considered a potential differentiator parameter over the kinetics of the reaction, based on the documented data from Baras et al. (2023) and Huijgen et al. (2005) showing that temperatures between 25-50°C provide a feasible scenario for carbonate formation within the slags. However, despite the site temperatures *(~37.6°C*), the volumes of CO_2 mineralized in slags from Monclova were lower than those quantified in slags from Ravenscraig. This outcome contradicts the anticipated effect of warm environments on CO_2 sequestration, and might indicate that even small proportions of humidity resulting from minimal rainfall at the site, have greater influence in the degree of carbonation within the slag deposit, and potentially correlates limited precipitation with limited carbonation.

Overall, the observed results challenge the initial ideas on higher temperatures influencing higher conversion rates of CO_2 and suggest that warm temperatures did not lead to increased CO_2 sequestration, at least, during passive carbonation.

The abundance of humidity influencing the carbonation rates was documented by Rahmanihanzaki et al. (2022), Ragipani et al. (2021) and Ko et al. (2015), whose research implied that humidity might have a higher influence over the mineralisation reaction than temperature. This is consistent with the results obtained, where CO_2 volumes quantified in

Scottish slags were double the volume than in Mexican slags, strengthening the relevance of water above other parameters during carbonate formation.

The physical and chemical characteristics of the different slags were also considered when evaluating the potential parameters determining carbonation differences in the studied locations. In the case of physical and chemical conditions, as both slag sets derived from a Basic Oxygen Furnace method, literature indicates similar properties, but characteristics such as particle size could also be a potential factor influencing the differences between volumes of CO_2 captured, as Baras et al. (2023) considered it a key parameter increasing the reactivity of the carbonation reaction.

Although there was a difference in terms of carbonation time between both slag sets, this factor was deemed less relevant considering the results obtained; following the criteria of Wang et al. (2018), where the longer the time of carbonation, the higher the volumes of captured CO_2, this was partially corroborated by the results as slags from Ravenscraig carbonated for 29 years and resulted with higher CO_2 mineralised. However, within Mexican slags, the samples had two carbonation periods, 10 and 20 years respectively, and the slags with the lower carbonation time ended up having higher CO_2 mineralised, which suggests that environmental conditions from the site had a higher influence than time.

Thus, in passive carbonation, humidity seems to be the primary factor influencing the reaction, as evidenced by evaluating carbonated slags from Scotland and Mexico. The volume of CO_2 sequestered in slags from Ravenscraig indicates that high humidity levels facilitate mineral carbonation. In the same line, the analysis of slags from Monclova showed the need of humidity to enhance CO_2 sequestration within legacy slag heaps. Therefore, humidity is a determinative parameter during passive mineral carbonation, increasing or restricting the mineralisation of atmospheric CO_2.

2.6 Conclusion.

2.6.1 Conclusion.

The further understanding of environmental factors determining mineral carbonation occurring on steel slags is of significance, not only to improve this carbon removal technology aimed at reducing atmospheric CO_2 concentrations, but it will also be beneficial to provide a wider overview on behaviour of solid alkaline geomaterials to conduct effective waste management solutions. With this objective in mind, the aim of this chapter was to study whether external factors (*environment*) influenced the mineralisation of atmospheric carbon dioxide in slag heaps located in northern Mexico and in Scotland.

The study involved the use of x-ray tomography for scanning the slag samples collected in Ravenscraig, Scotland and in Monclova Mexico. Further to XCT, a quantification of the CO_2 precipitated as calcite within the slags was completed; this action involved using Avizo software to segment the digitised slag cubes to measure the volume fraction of the components (*Slag, Calcite, Pores*), where calcite was the component of interest as it contained the amount of CO_2 carbonated within the samples. The findings from this part of the research are described below:

- The initial findings from the CO_2 quantification indicated contrasting volumes of CO_2 between both slag sets. The volume of mineralised CO_2 in the legacy slags from Ravenscraig was double the amount of the carbonated CO_2 in Mexican slags, where the average amount of CO_2 measured in Scottish slags was 54 Kg of CO_2 per tonne of steel slag, while for Mexican slags the average results were about 21 Kg of CO_2 per tonne of steel slag.

- While four out of the eight Scottish samples presented above average volumes of CO_2, within Mexican slags 3 out of 8 samples presented above average volumes of CO_2 and none of the Mexican slags presented values above the Scottish average measurement. Within the 16 samples studied from both collection sites, a value of 60 $KgCO_2$/tonne $_{Steel\ Slag}$ from Ravenscraig was the highest value measured; the lowest volume quantified was 6 Kg of CO_2/tonne $_{Steel\ Slag}$ and was from Monclova, Mexico. Overall, CO_2 sequestration between slags from Monclova and Ravenscraig was contrasting, showing lower carbonation rates from Mexican slags.

Further to the quantification of CO_2, an assessment on the contextual (*environment*) background was completed for both sites, as a potential explanation for the different amounts of CO_2 measured; this involved comparing parameters such as: the period of carbonation, physical and chemical properties, humidity (*rainfall*), temperature, atmospheric pressure related to altitude, pH of the area. Findings from this assessment are summarized below:

- The role of humidity was considered the most important parameter influencing CO_2 mineralization in both locations studied within this research. The abundance of humidity as rainfall in Ravenscraig, Scotland potentially explains the higher CO_2 uptake quantified and the low humidity (*rainfall*) from Monclova, Mexico correlates to the lower CO_2 mineralised within the slags.

- The analysis of temperature determining higher volumes of CO_2 carbonated was based on literature from Baras et al. (2023) and Huijgen et al. (2005), where it is reported that higher temperatures lead to higher CO_2 conversion within the mineral carbonation reaction occurring in steel slags. However, the outcomes from this research indicated the opposite of this, as the amount of CO_2 measured in slags from Monclova was on average half the amount of the volumes obtained in slags from Ravenscraig. This is despite the fact that northern Mexico provides a more optimal temperature (*~37.6°C*) for carbonation, within the ranges documented in literature. As a result, humidity was deemed a more determinative influence in the conversion of CO_2 into stable carbonates occurring with no human intervention.

- Pressure has been demonstrated as a key parameter when mineral carbonation is evaluated under lab-based experiments. In the case of passive carbonation, however, pressure given by the altitude of the sites did not seem to have a determinative influence during the carbonation reactions.

- Time is a significant parameter in mineral carbonation, whether conducted in a laboratory setting or occurring passively under open-air conditions. It influences the amount of CO_2 mineralized within the slags by providing a timeframe for the reaction to occur and continue sequestering CO_2 over decadal periods. However, this parameter is exceeded by the influence of other factors such as humidity, or is not always a factor at all, demonstrated by the fact that younger slags from Monclova contained more mineralised CO_2 than older ones from the same site.

- In the case of pH it would be worth conducting further research in the role this parameter has within passive carbonation, as pH has been demonstrated to increase solubility of the calcium ions during the mineralisation of CO_2 in slags (Bonenfant et al., 2008; Mayes et al., 2018b).

- Physical and chemical properties of slags were not assessed in this research, however it is of significance to mention that characteristics such as particle size, slag type or chemical properties of the material have an influence on the capacity of the slags to carbonate CO_2, for instance, CO_2 mineralization increases when particle size decreases (Han et al., 2015; Polettini et al., 2016; Santos et al., 2012).

Therefore, for passive mineral carbonation, humidity has a key role influencing the reaction, as shown from the results within the examination of carbonated slags from Scotland and Mexico. In addition, the analysis of slags from Monclova highlights the role of humidity from a perspective where rainfall was a limited resource during the reaction, resulting in lower CO_2 carbonation within the legacy slag heaps. The amount of CO_2 sequestered in slags from Ravenscraig confirm the significant role of high humidity levels in promoting mineral carbonation. Other parameters reviewed such as physical and chemical properties, temperature or time might have an impact in the carbonation of CO_2 in steel slags, but humidity remains the main parameter facilitating the reaction in an efficient way.

2.6.2 Future work.

Given the findings presented in this study, future research projects can explore certain initiatives that can provide deep understanding of passive carbonation occurring in slag heaps. The first of these ideas could be to further explore or consider other parameters that might be key when analysing the environmental influence over passive carbonation of steel slags; is unclear that environment might shape the sequestration potential that the slag heap would develop, and amount of rainfall (*moisture*), the variation of temperature, altitude related to atmospheric pressure and pH of the area could determine the volumes of atmospheric CO_2 to be carbonated (Ghacham et al., 2016; Pullin et al., 2019).

Considering further use of iron and steel slags either for carbon sequestration or for utilisation on a suitable field, such as construction, agribusiness, or environmental remediation (Baras et al., 2023), it would be worth investigating the long-term stability or durability characteristics of the carbonated slags within those applications, to better understand how slags that

carbonated passively behave across time and under different environments. Moreover, considering further utilisation of carbonated slag, future research can explore the socio-economic implications of the slag, where the benefits and challenges within a community can be assessed. Where, it would be valuable to first understand the perspective of the community around the slag heaps. Following this, exploring the economic feasibility of repurposing the material through a cost-benefit analysis would help clarify the impact of potential reutilization projects within these communities. These steps would provide insight into the potential for project development, job creation, and benefits for nearby households. The project should also include environmental and health impact assessments, alongside the development of policies and regulations to create a framework that promotes sustainable slag utilization.

Additional parameters to consider in the further utilisation of mineralised/carbonated slags might also rely on considering geographical location of slag heaps, as a variable for scaling up a mineral carbonation facility in-situ, as the proximity of the slags to the steel making site (legacy and recently produced) would reduce production and transportation costs, facilitating in situ passive mineral carbonation (Ukwattage et al., 2017). This is the case from the collection site in Mexico, as AHMSA steel works is currently operating and uses nearby land to dispose steel slag generated from BOF, EAF and ladle furnaces. In the case of Scottish legacy slag, the disposal site is close to the former Ravenscraig Steel Works and considerations on the feasibility of performing in-situ or ex-situ mineral carbonation would need to be considered in the context of logistics costs, properties of the material and geographic characteristics of the location (Mo, 2018; Piatak et al., 2015a; Thonemann et al., 2022).

References.

AHMSA. (2020). *Reporte_Anual_AHMSA_2020*.

Baciocchi, R., Costa, G., Di Gianfilippo, M., Polettini, A., Pomi, R., & Stramazzo, A. (2015). Thin-film versus slurry-phase carbonation of steel slag: CO2 uptake and effects on mineralogy. *Journal of Hazardous Materials*, *283*, 302–313. https://doi.org/10.1016/j.jhazmat.2014.09.016

Baras, A., Li, J., Ni, W., Hussain, Z., & Hitch, M. (2023). Evaluation of Potential Factors Affecting Steel Slag Carbonation. *Processes*, *11*(9), 2590. https://doi.org/10.3390/pr11092590

Bonenfant, D., Kharoune, L., Sauvé, S., Hausler, R., Niquette, P., Mimeault, M., & Kharoune, M. (2008). CO2 sequestration potential of steel slags at ambient pressure and temperature. *Industrial and Engineering Chemistry Research*, *47*(20), 7610–7616. https://doi.org/10.1021/ie701721j

Boone, M. A., Nielsen, P., De Kock, T., Boone, M. N., Quaghebeur, M., & Cnudde, V. (2014). Monitoring of stainless-steel slag carbonation using X-ray computed microtomography. *Environmental Science and Technology*, *48*(1), 674–680. https://doi.org/10.1021/es402767q

Castrejón, D., Zavala, A. M., Flores, J. A., Flores, M. P., & Barrón, D. (2018). Analysis of the contribution of CCS to achieve the objectives of Mexico to reduce GHG emissions. *International Journal of Greenhouse Gas Control*, *71*, 184–193. https://doi.org/10.1016/j.ijggc.2018.02.019

Chang, E. E., Pan, S. Y., Chen, Y. H., Tan, C. S., & Chiang, P. C. (2012). Accelerated carbonation of steelmaking slags in a high-gravity rotating packed bed. *Journal of Hazardous Materials*, *227–228*, 97–106. https://doi.org/10.1016/j.jhazmat.2012.05.021

Chen, Z., Cang, Z., Yang, F., Zhang, J., & Zhang, L. (2021). Carbonation of steelmaking slag presents an opportunity for carbon neutral: A review. In *Journal of CO2 Utilization* (Vol. 54). Elsevier Ltd. https://doi.org/10.1016/j.jcou.2021.101738

Chukwuma, J. S., Pullin, H., & Renforth, P. (2021). Assessing the carbon capture capacity of South Wales' legacy iron and steel slag. *Minerals Engineering*, *173*. https://doi.org/10.1016/j.mineng.2021.107232

Costa, G., Baciocchi, R., Polettini, A., Pomi, R., Hills, C. D., & Carey, P. J. (2007). Current status and perspectives of accelerated carbonation processes on municipal waste combustion residues. In *Environmental Monitoring and Assessment* (Vol. 135, Issues 1–3, pp. 55–75). https://doi.org/10.1007/s10661-007-9704-4

Cruz-Navarro, D. S., Mugica-Álvarez, V., Gutiérrez-Arzaluz, M., & Torres-Rodríguez, M. (2020). CO2 capture by alkaline carbonation as an alternative to a circular economy. *Applied Sciences (Switzerland)*, *10*(3). https://doi.org/10.3390/app10030863

Fernández Bertos, M., Simons, S. J. R., Hills, C. D., & Carey, P. J. (2004). A review of accelerated carbonation technology in the treatment of cement-based materials and sequestration of CO2. In *Journal of Hazardous Materials* (Vol. 112, Issue 3, pp. 193–205). Elsevier. https://doi.org/10.1016/j.jhazmat.2004.04.019

Ferreiraa, T. R., Piresb, L. F., Wildenschildc, D., Heckd, R. J., & Antoninoe, A. C. D. (2018). X-ray microtomography analysis of lime application effects on soil porous system. *Geoderma*, *324*(324), 119–130.

Georgakopoulos, E., Santos, R. M., Chiang, Y. W., & Manovic, V. (2016). Influence of process parameters on carbonation rate and conversion of steelmaking slags – Introduction of the 'carbonation weathering rate.' In *Greenhouse Gases: Science and Technology* (Vol. 6, Issue 4, pp. 470–491). https://doi.org/10.1002/ghg.1608

Ghacham, A. Ben, Pasquier, L. C., Cecchi, E., Blais, J. F., & Mercier, G. (2016). CO2 sequestration by mineral carbonation of steel slags under ambient temperature: parameters influence, and optimization. *Environmental Science and Pollution Research*, *23*(17), 17635–17646. https://doi.org/10.1007/s11356-016-6926-4

Han, D. R., Namkung, H., Lee, H. M., Huh, D. G., & Kim, H. T. (2015). CO2 sequestration by aqueous mineral carbonation of limestone in a supercritical reactor. *Journal of Industrial and Engineering Chemistry*, *21*, 792–796. https://doi.org/10.1016/j.jiec.2014.04.014

Huijgen, W. J. J., Witkamp, G. J., & Comans, R. N. J. (2005). Mineral CO2 sequestration by steel slag carbonation. *Environmental Science and Technology*, *39*(24), 9676–9682. https://doi.org/10.1021/es050795f

Hume, J. (2007, August 7). *Motherwell, Ravenscraig Steelworks*. National Record of the Historic Environment.

Klein, F., & Garrido, C. J. (2011). Thermodynamic constraints on mineral carbonation of serpentinized peridotite. *Lithos*, *126*(3–4), 147–160. https://doi.org/10.1016/j.lithos.2011.07.020

Ko, M. S., Chen, Y. L., & Jiang, J. H. (2015). Accelerated carbonation of basic oxygen furnace slag and the effects on its mechanical properties. *Construction and Building Materials*, *98*, 286–293. https://doi.org/10.1016/j.conbuildmat.2015.08.051

Kong, D., Wu, S., Chen, M., Zhao, M., & Shu, B. (2019). Characteristics of Different Types of Basic Oxygen Furnace Slag Filler and its Influence on Properties of Asphalt Mastic. *Materials*, *12*(24), 4034. https://doi.org/10.3390/ma12244034

Liu, W., Teng, L., Rohani, S., Qin, Z., Zhao, B., Xu, C. C., Ren, S., Liu, Q., & Liang, B. (2021). CO2 mineral carbonation using industrial solid wastes: A review of recent developments. In *Chemical Engineering Journal* (Vol. 416). Elsevier B.V. https://doi.org/10.1016/j.cej.2021.129093

Luo, Y., & He, D. (2021). Research status and future challenge for CO2 sequestration by mineral carbonation strategy using iron and steel slag. In *Environmental Science and Pollution Research* (Vol. 28, Issue 36, pp. 49383–49409). Springer Science and Business Media Deutschland GmbH. https://doi.org/10.1007/s11356-021-15254-x

Macente, A., Vanorio, T., Miller, K. J., Fusseis, F., & Butler, I. B. (2019). Dynamic Evolution of Permeability in Response to Chemo-Mechanical Compaction. *Journal of Geophysical Research: Solid Earth*, *124*(11), 11204–11217. https://doi.org/10.1029/2019JB017750

Mattila, H. P., Grigaliu-naite, I., & Zevenhoven, R. (2012). Chemical kinetics modeling and process parameter sensitivity for precipitated calcium carbonate production from steelmaking slags. *Chemical Engineering Journal*, *192*, 77–89. https://doi.org/10.1016/j.cej.2012.03.068

Mayes, W. M., Riley, A. L., Gomes, H. I., Brabham, P., Hamlyn, J., Pullin, H., & Renforth, P. (2018b). Atmospheric CO2 Sequestration in Iron and Steel Slag: Consett, County Durham, United Kingdom. *Environmental Science and Technology*, *52*(14), 7892–7900. https://doi.org/10.1021/acs.est.8b01883

Mercado Fernandez, R., & Baker, E. (2022). The sustainability of decarbonizing the grid: A multi-model decision analysis applied to Mexico. *Renewable and Sustainable Energy Transition*, *2*, 100020. https://doi.org/10.1016/j.rset.2022.100020

Met Office UK. (2023). *UK climate: climate summaries*. Weather and Climate Records for the UK.

Mo, L. (2018). Carbon dioxide sequestration on steel slag. In *Carbon Dioxide Sequestration in Cementitious Construction Materials* (pp. 175–197). Elsevier. https://doi.org/10.1016/B978-0-08-102444-7.00008-3

Mota-Nieto, J., Fernández-Reyes, J. A., & García-Meneses, P. M. (2023). The Mexican Carbon Capture and Storage Platform: Construction of a boundary object for bridging the gaps between contexts, actors, and disciplines. *International Journal of Greenhouse Gas Control*, *129*. https://doi.org/10.1016/j.ijggc.2023.103965

Nielsena, P., Booneb, M. A., Horckmansa, L., Snellingsa, R., & Quaghebeura, M. (2020). Accelerated carbonation of steel slag monoliths at low CO2 pressure – microstructure and strength development. *Journal of CO2 Utilization*, *36*(36), 124–134.

Olajire, A. A. (2013). A review of mineral carbonation technology in sequestration of CO2. In *Journal of Petroleum Science and Engineering* (Vol. 109, pp. 364–392). Elsevier B.V. https://doi.org/10.1016/j.petrol.2013.03.013

Pan, S. Y., Chiang, P. C., Chen, Y. H., Tan, C. S., & Chang, E. E. (2013). Ex Situ CO2 capture by carbonation of steelmaking slag coupled with metalworking wastewater in a rotating packed bed. *Environmental Science and Technology*, *47*(7), 3308–3315. https://doi.org/10.1021/es304975y

Piatak, N. M., Parsons, M. B., & Seal, R. R. (2015a). Characteristics and environmental aspects of slag: A review. In *Applied Geochemistry* (Vol. 57, pp. 236–266). Elsevier Ltd. https://doi.org/10.1016/j.apgeochem.2014.04.009

Piatak, N. M., Parsons, M. B., & Seal, R. R. (2015b). Characteristics and environmental aspects of slag: A review. In *Applied Geochemistry* (Vol. 57, pp. 236–266). Elsevier Ltd. https://doi.org/10.1016/j.apgeochem.2014.04.009

Polettini, A., Pomi, R., & Stramazzo, A. (2016). Carbon sequestration through accelerated carbonation of BOF slag: Influence of particle size characteristics. *Chemical Engineering Journal*, *298*, 26–35. https://doi.org/10.1016/j.cej.2016.04.015

Pullin, H., Bray, A. W., Burke, I. T., Muir, D. D., Sapsford, D. J., Mayes, W. M., & Renforth, P. (2019). Atmospheric Carbon Capture Performance of Legacy Iron and Steel Waste. *Environmental Science and Technology*, *53*(16), 9502–9511. https://doi.org/10.1021/acs.est.9b01265

Quaghebeur, M., Nielsen, P., Horckmans, L., & Van Mechelen, D. (2015). Accelerated carbonation of steel slag compacts: Development of high-strength construction materials. *Frontiers in Energy Research*, *3*(DEC). https://doi.org/10.3389/fenrg.2015.00052

Ragipani, R., Bhattacharya, S., & Suresh, A. K. (2021). A review on steel slag valorisation: Via mineral carbonation. In *Reaction Chemistry and Engineering* (Vol. 6, Issue 7, pp. 1152–1178). Royal Society of Chemistry. https://doi.org/10.1039/d1re00035g

Rahmanihanzaki, M., & Hemmati, A. (2022). A review of mineral carbonation by alkaline solidwaste. In *International Journal of Greenhouse Gas Control* (Vol. 121). Elsevier Ltd. https://doi.org/10.1016/j.ijggc.2022.103798

Riley, A. L., MacDonald, J. M., Burke, I. T., Renforth, P., Jarvis, A. P., Hudson-Edwards, K. A., McKie, J., & Mayes, W. M. (2020). Legacy iron and steel wastes in the UK: Extent, resource potential, and management futures. *Journal of Geochemical Exploration*, *219*. https://doi.org/10.1016/j.gexplo.2020.106630

Romanov, V., Soong, Y., Carney, C., Rush, G. E., Nielsen, B., & O'Connor, W. (2015). Mineralization of Carbon Dioxide: A Literature Review. In *ChemBioEng Reviews* (Vol. 2, Issue 4, pp. 231–256). Wiley-Blackwell. https://doi.org/10.1002/cben.201500002

Roy, S., Rautela, R., & Kumar, S. (2023). Towards a sustainable future: Nexus between the sustainable development goals and waste management in the built environment. In *Journal of Cleaner Production* (Vol. 415). Elsevier Ltd. https://doi.org/10.1016/j.jclepro.2023.137865

Rushendra Revathy, T. D., Palanivelu, K., & Ramachandran, A. (2016). Direct mineral carbonation of steelmaking slag for CO2 sequestration at room temperature. *Environmental Science and Pollution Research*, *23*(8), 7349–7359. https://doi.org/10.1007/s11356-015-5893-5

Santos, R. M., Ling, D., Sarvaramini, A., Guo, M., Elsen, J., Larachi, F., Beaudoin, G., Blanpain, B., & Van Gerven, T. (2012). Stabilization of basic oxygen furnace slag by hot-stage carbonation treatment. *Chemical Engineering Journal*, *203*, 239–250. https://doi.org/10.1016/j.cej.2012.06.155

Santos, R. M., Van Bouwel, J., Vandevelde, E., Mertens, G., Elsen, J., & Van Gerven, T. (2013). Accelerated mineral carbonation of stainless steel slags for CO2 storage and waste valorization: Effect of process parameters on geochemical properties. *International Journal of Greenhouse Gas Control*, *17*, 32–45. https://doi.org/10.1016/j.ijggc.2013.04.004

Servicio Meteorológico Nacional. (2023). *Coahuila de Zaragoza*. Normales Climatológicas Por Estado.

Shi, C. (2004). *Steel Slag-Its Production, Processing, Characteristics, and Cementitious Properties*. https://doi.org/10.1061/ASCE0899-1561200416:3230

Soares, C. (2015). *Basic Design Theory Contents*.

Sorrentino, G. P., Guimarães, R., Valentim, B., & Bontempi, E. (2023). The Influence of Liquid/Solid Ratio and Pressure on the Natural and Accelerated Carbonation of Alkaline Wastes. *Minerals*, *13*(8). https://doi.org/10.3390/min13081060

Stewart, D. I., Bray, A. W., Udoma, G., Hobson, A. J., Mayes, W. M., Rogerson, M., & Burke, I. T. (2018). Hydration of dicalcium silicate and diffusion through neo-formed calcium-silicate-hydrates at weathered surfaces control the long-term leaching behaviour of basic oxygen furnace (BOF) steelmaking slag. *Environmental Science and Pollution Research*, *25*(10), 9861–9872. https://doi.org/10.1007/s11356-018-1260-7

Stokreef, S., Sadri, F., Stokreef, A., & Ghahreman, A. (2022). Mineral carbonation of ultramafic tailings: A review of reaction mechanisms and kinetics, industry case studies, and modelling. In *Cleaner Engineering and Technology* (Vol. 8). Elsevier Ltd. https://doi.org/10.1016/j.clet.2022.100491

Teir, S., Eloneva, S., Fogelholm, C. J., & Zevenhoven, R. (2007). Dissolution of steelmaking slags in acetic acid for precipitated calcium carbonate production. *Energy*, *32*(4), 528–539. https://doi.org/10.1016/j.energy.2006.06.023

Thermo Fisher Scientific. (2019). *User's Guide Avizo Software 2019* (pp. 236–242).

Thomas, C., Rosales, J., Polanco, J. A., & Agrela, F. (2018). Steel slags. In *New Trends in Eco-efficient and Recycled Concrete* (pp. 169–190). Elsevier. https://doi.org/10.1016/B978-0-08-102480-5.00007-5

Thonemann, N., Zacharopoulos, L., Fromme, F., & Nühlen, J. (2022). Environmental impacts of carbon capture and utilization by mineral carbonation: A systematic literature review and meta life cycle assessment. In *Journal of Cleaner Production* (Vol. 332). Elsevier Ltd. https://doi.org/10.1016/j.jclepro.2021.130067

Ukwattage, N. L., Ranjith, P. G., & Li, X. (2017). Steel-making slag for mineral sequestration of carbon dioxide by accelerated carbonation. *Measurement: Journal of the International Measurement Confederation*, *97*, 15–22. https://doi.org/10.1016/j.measurement.2016.10.057

Vega-Ortiz, C., Avendaño-Petronilo, F., Richards, B., Sorkhabi, R., Torres-Barragán, L., Martínez-Romero, N., & McLennan, J. (2021). Assessment of carbon geological storage at Tula de Allende as a potential solution for reducing greenhouse gas emissions in central Mexico. *International Journal of Greenhouse Gas Control*, *109*. https://doi.org/10.1016/j.ijggc.2021.103362

Wang, C. Y., Bao, W. J., Guo, Z. C., & Li, H. Q. (2018). Carbon Dioxide Sequestration via Steelmaking Slag Carbonation in Alkali Solutions: Experimental Investigation and Process Evaluation. *Acta Metallurgica Sinica (English Letters)*, *31*(7), 771–784. https://doi.org/10.1007/s40195-017-0694-0

Yadav, S., & Mehra, A. (2017). Experimental study of dissolution of minerals and CO2 sequestration in steel slag. *Waste Management*, *64*, 348–357. https://doi.org/10.1016/j.wasman.2017.03.032

Yildirim, I. Z., & Prezzi, M. (2011). Chemical, mineralogical, and morphological properties of steel slag. *Advances in Civil Engineering*, *2011*. https://doi.org/10.1155/2011/463638

Chapter III. Geospatial evaluation of legacy iron and steel slag sites in Mexico for CO_2 sequestration.

3.1 Introduction.

The geospatial evaluation of legacy steel slags deposits in Mexico represents a promising option to mitigate atmospheric CO_2 emissions, while providing better waste management solutions for the steel manufacturing industry of the country. Data on the volume of legacy stockpiled slag has not been yet recorded in Mexico, although the production of steel and related industries are in the top three of key drivers in terms of national income since its boom in 1900 (Hasanbeigi et al., 2016). Steel manufacturing is one of the largest contributors of GHG in Mexico and has grown 56% in carbon emissions since 1990 (Martin & De Melo, 2023). With CO_2 emissions exceeding 819 Mton in 2023, representing 1.52% of global emissions (Crippa et al., 2023). Therefore, by assessing the amount of stockpiled slag in Mexico, the utilisation of steel slags can emerge as a potential alternative for CO_2 sequestration or sustainable concrete production, respectively explored in chapters II and IV of this thesis.

This chapter detail a geospatial analysis of 16 slag deposits across 11 Mexican regions, where approximately 273,000 tonnes of slag are deposited, primarily from Basic Oxygen Furnaces (BOF) and Electric Arc Furnaces (EAF). Digital Elevation Models (DEMs) were used to quantify the volume of slag heaps, enhancing the accuracy of the volume estimation process. The findings show that the region of Coahuila, particularly the site operated by Altos Hornos de Mexico, contains the largest slag deposits, followed by the ArcelorMittal site in Michoacán. The absence of conservation designations at these sites further supports their potential for industrial reuse, though any initiatives must align with the interests of steel manufacturers and local authorities.

The chapter also explores the CO_2 capture potential of Mexican slag deposits. Through both theoretical models and practical estimates, it is projected that between 80.9 and 159.7 Kt of CO_2 could be sequestered through direct or enhanced carbonation methods. Repurposing these slags could lead to significant economic and environmental benefits, particularly by reducing greenhouse gas emissions and mitigating the impacts of waste disposal. Additionally, the development of slag-based industries offers opportunities for job creation and economic growth, especially in resource-abundant regions like Coahuila and Michoacán.

In summary, this chapter not only presents a detailed geospatial evaluation of legacy steel slag deposits in Mexico but also highlights their potential as valuable resources for carbon sequestration and sustainable concrete production. By continuing to explore and quantify these deposits, Mexico can better position itself to develop efficient waste management strategies, promote recycling projects, and stimulate economic growth through the sustainable use of industrial by-products.

3.2 Literature Review.

3.2.1 Iron and steel industry in Mexico, historical evolution.

The industry of iron and steel production in Mexico has evolved across time, with a central place in the economic development of the country and is considered a marker of industrial progress within the last 150 years (López-Díaz et al., 2018). The early beginning of the steel manufacturing in Mexico dates back to the late 19th century, where the first steel mills were established in certain areas of the country with abundant iron ore and coal (González-Chavez, 2008). Since the beginning, the iron and steel sector has been important in the industrial environment of the country and experienced a main growth during the 20th century (Plumb, 1948; Rojas-Sandoval & Rodríguez, 1985).

Development of the steel production started to be formalized and scaled up in 1900 with the foundation of Fundidora de Fierro y Acero de Monterrey, also known under the acronym FUMOSA (Rojas-Sandoval & Rodríguez, 1985); the formalization of this company in the city of Monterrey was fundamental to increase the industry experience and a continuous growth also supported by national and international demand in the fields of construction, railway network, car manufacturing and other industrial sectors. Figure 15 shows the former Basic Oxygen Furnace that used to operate in the site, which was closed in 1986 and further transformed into the museum of steel.

Figure 15 *Overview of Fundidora Park (former Fundidora de Fierro y Acero de Monterrey, also known under the acro-nym - FUMOSA). The first steel production site in Mexico. Basic Oxygen Furnace of Fundidora Park, operat-ed from 1900 to 1986 (Google Earth Pro, 2024)*

Based on the growing demand for iron and steel products in the mid 1900's, the Mexican government supported the steel industry for an expansion, which derived in the origin of the major steel producers and the enlarged use of blast and basic oxygen furnaces (Plumb, 1948; Rojas-Sandoval & Rodríguez, 1985; Sanchéz-Díaz, 2009). In the late 20th century, the steel industry was nationalized and state-owned companies were integrated, such as Altos Hornos de México (*AHMSA*) and Nacional Siderúrgica (*Nasim*). However, this did not last long, as financial policies created in the 90's allowed the entry of international investment, which re-shaped the structure of the steel industry (Chabrand, 2023; López-Díaz et al., 2018).

In recent times, the production of steel in Mexico has been adapted to the global market trends and the need for sustainable manufacturing methods (González-Chavez, 2008; Hasanbeigi et al., 2016). In this regard, although the country has emerged as one of the main producers in Latin America, the increasing GHG emissions related to the production of steel resulted in exploration of further ways to decrease the environmental impact of the sector while continuing its extension (Sellitto & Kazuhiro, 2020). In this sense, the re-use of steel slags in a circular economy approach has gained popularity around the world, and has been considered in various sectors in Mexico. Although there is some experience using iron and steel slags as construction aggregates (López-Díaz et al., 2018), road building or railway ballast, there is much to explore in the utilisation of steel slags for capturing atmospheric CO_2.

Overall, steel manufacturing in Mexico has evolved since its early beginnings in the late 19th century and continuous to be a dynamic sector by mixing technological progress, and an historical identity, while representing a strong income for the Mexican economy (Chabrand, 2023); the methods for steel production have also evolved, changing from blast and basic oxygen furnaces to mostly produce steel using electric arc methods in most of the sites located in most of the regions of the country (INEGI Mexico, 2013).

3.2.2 Geographical distribution of iron and steel industry in Mexico.

Considering the large territory of Mexico, steel manufacturing sites were (*and continue to be*) strategically distributed nationwide, mostly concentrated in the northern, centre and western regions of the country. The allocation of the steel industry site is directly linked to the proximity of iron ore mines located along the country (Mesta et al., 2019). Figure 16 shows an overview of the geographic distribution of iron ore mines in Mexico and their proximity to main iron and steel industrial sites.

This geographical organization, where production sites were designed to be close to the raw materials remains mostly unchanged since these sites were opened during the 20th century, relying mainly on their proximity to raw materials, efficient transportation and convenient logistics for product distribution. The companies leading the sites have evolved in their branding or maybe have integrated new boards of executives, however they continue to operate from these same locations, based on the benefits derived from the geography (Chabrand, 2023).

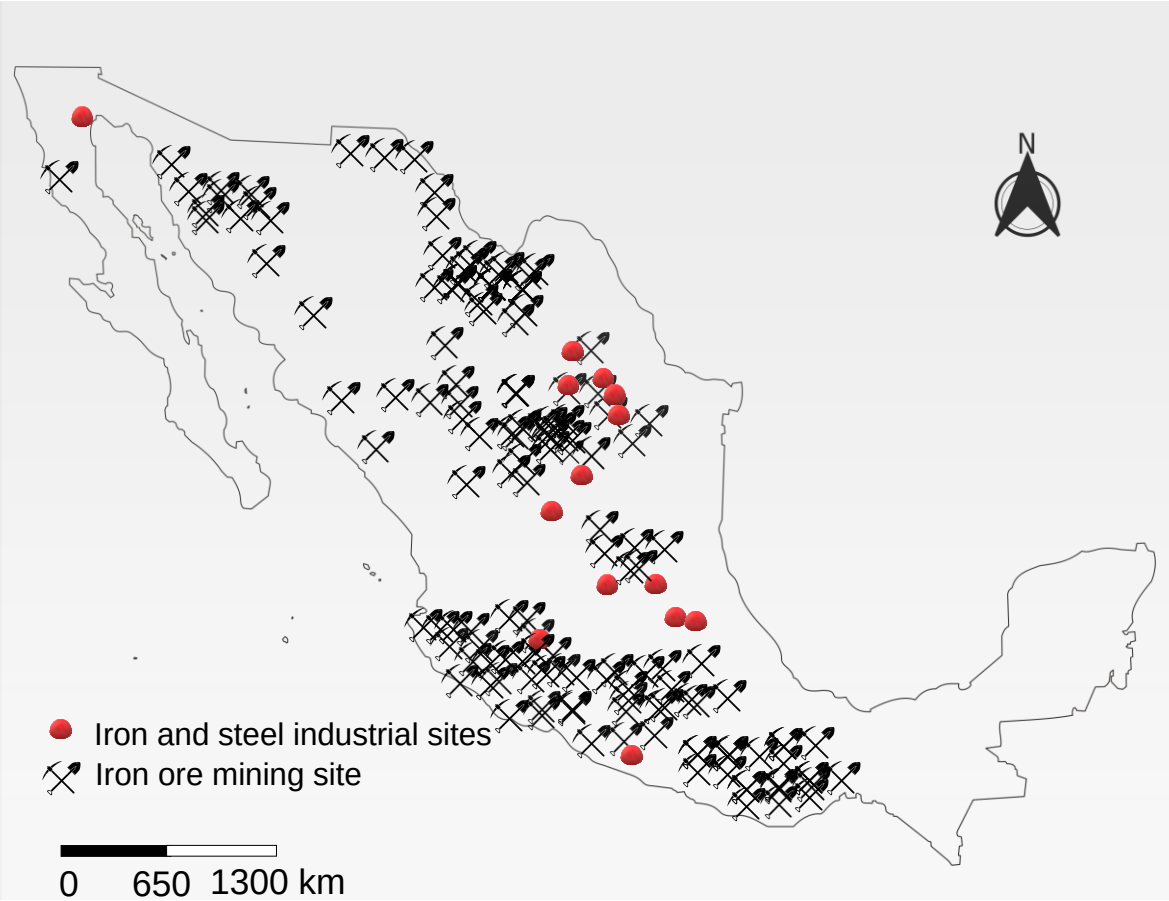

Figure 16. Iron ore mining sites in Mexico, image sourced from Servicio Geológico Mexicano (2024).

As mentioned, the main factors contributing to positioning steel production sites in the country and for the companies to develop their industrial sites, involved finding locations with a good railway network and easy access for transportation, e.g. Mexico City (*region*), Guadalajara or San Luis Potosi. In spite of their inland position in the country, companies such as Grupo SIMEC and Grupo Acerero are able to manage raw materials supply and products delivery without the need to be close to mining sites or shipping facilities (INEGI Mexico, 2013). In the north of Mexico, companies such as Altos Hornos de Mexico or Ternium (*former HYLSA*), based in Mexicali, Monclova and Monterrey have grown exponentially as a result of their close relationships with US clients since they started operations in mid-20th century and their advantageous location closer to the US border (Rojas-Sandoval & Rodríguez, 1985).

An example of a strategically located steel making site is ArcelorMittal (*formerly Las Truchas*) in Lázaro Cárdenas, Michoacán, which benefits from its ideal location on the Pacific coast of Mexico, with access to major shipping routes from the local port and a strong supply of iron ore and coal from the *"Las Truchas"* mine, just 27 km away from the production site (INEGI Mexico, 2016). As referenced before, there is a wide list of steel making sites in the country, however the regions in the south remain with no evidence of former or future investment for steel industry; this is based on limited material supply and lack of logistic infrastructure (Sanchéz-Díaz, 2009).

Location of the production typically involved some allocated areas for secondary activities such as raw material storage or waste materials deposition (González-Chavez, 2008). In this sense, it is common to find extensive areas where, for instance, steel slags remain stockpiled under local environment conditions. In Mexico, there is currently no comprehensive record of the amount of steel slag deposits, nor is there a controlled procedure for slag reutilization or permanent disposal.

3.2.3 Iron and steel slag in Mexico.

Steel slag production was about 20 million tonnes in 2022 as documented by National Council of Steel Industries (*CANACERO*) (2023). The methods used to produce steel have changed through time in Mexico. In the beginning, blast furnace technology was primarily used for the production of iron (CANACERO, 2019; Plumb, 1948; Sanchéz-Díaz, 2009). Where Iron ore was smelting into the furnaces fed by coke or coal, this procedure involved a refinement and alloyed stage to produce grades of steel based on the client's demand (Pauliuk et al., 2013).

As time passed and new methods arrived into the Mexican industrial sector, Basic Oxygen Furnaces were adopted in the production sites, remaining as a production route for several decades (Sanchéz-Díaz, 2009). Then at the end of the 20th century, Electric Arc Furnaces were adopted as a secondary procedure for steel making and gradually substituted BOF technology (González-Ortega et al., 2014). At the moment, only two out of twenty-three sites maintain BOF technology, the rest following the EAF procedure due to lower energy consumption, decreased GHG emissions and the capacity for scrap metal recycling. Figure 17 shows the slag heaps around Altos Hornos de Mexico (*AHMSA*) site, located in Monclova, Coahuila, one of the largest steel producing sites in the country that remain operating. The three images, from 2006, 2014 and 2023 show how the slag heaps changed through time.

Figure 16 *View of slag heap Monclova, Mexico across time: (a) 2006, (b) 2014, (c) 2023; images from Google Earth Pro (2024).*

The production of steel slags is considered a growing challenge in Mexico, based on the amount of material produced and the limited management opportunities to avoid long-term/permanent stockpiling (Chabrand, 2023; Ozie Méndez Guerrero et al., 2011). In Mexico, as in any other locations, slag from steel manufacturing is commonly accumulated in the surroundings of the industrial sites throughout the country (Mercado-Borrayo et al., 2018; Mesta et al., 2019). Whereas there is an extended potential for the utilisation of stockpiled slags, there is a lack of data and researched procedures to increase the use of this material.

There are few regulations determining the slag management such as the *"Ley General para la Prevención y Gestión Integral de los Residuos*" (2023), which broadly regulates the administration of this mineral resource but does not provide specifications of the potential utilisation of the material once their post-processing (*cooling*) is completed. It is important to mention that in Mexico there are no historical records of quantified volumes of steel slags produced since the industrialization of the steel making started. Studies such as Riley et al. (2020) could be taken as a reference to develop an extended database organising waste materials and all available resources derived/related to the steel industry. It is also desirable to better shape the regulatory system and ensure an optimized utilisation of iron and steel slag, instead of just representing a potential environmental or land use concern.

3.2.4 Iron and steel slag utilisation in Mexico.

The wider utilisation of steel slags in Mexico is growing in recognition in various industrial sectors of the country (Chabrand, 2023; Sellitto & Kazuhiro, 2020). Research conducted with iron and steel slags (*BF, BOF, EAF GGBFS*) in other countries have demonstrated suitable properties of the slags to be used not only in various applications within the construction industry, but also considered for environmental remediation based on their capacity to sequestrate atmospheric CO_2 through mineral carbonation (Ukwattage et al., 2017; Yildirim et al., 2023). In the past, Mexican steel slags derived from BOF and EAF routes have shown the adequate chemical and physical properties to be used as a base in road building to increase pavement performance or as a filler material for landfill remediation/closure (CANACERO, 2019; Mesta et al., 2019; Sanchéz-Díaz, 2009); slags have also been also used in agribusiness as a nutrient booster, with feasible results in farming productivity (Chabrand, 2023; Ozie Méndez Guerrero et al., 2011).

A wider implementation for steel slags has been investigated during the last decade, where slags could be used for construction purposes as a supplementary cementitious material (Snellings et al., 2023; Suraneni et al., 2019).

Resulting experience from the conducted studies, indicated that the use of steel slags in concrete not only increases the sustainability of the product, it also has an impact in the general costs of the operation, without compromising the performance of the material (Snellings & Scrivener, 2016; Suraneni & Weiss, 2017).

3.2.5 The geospatial distribution of steel slag in Mexico.

The utilisation of Mexican steel slags in their capacity to capture atmospheric CO_2 and their properties to be used as a supplementary cementitious material are further explored in chapters 2 and 4 of this thesis. For both study cases, the need of a geospatial evaluation on the distribution of steel slag in Mexico will provide a more accurate overview of the existent volumes of the material and the accessibility conditions for any potential utilisation. This gap in the literature is explored in this chapter, by identifying steel slag sites and quantifying the amount of the material to have an idea of how much CO_2 could be potentially captured or has been potentially captured and the volume of slag that could be available for construction matters as a SCM or to be further explored in their capacity to be useful in agribusiness, another key sector of the Mexican economy.

The geospatial evaluation of the steel slag volume in Mexico is conducted using QGIS software, which will enable better understanding on the amount of stockpiled slag in the country, in addition to visual resources to better understand other parameters influencing the potential utilisation of the material. Within QGIS, an initial mapping of the potential study sites will be completed; preliminary data about the location of the sites will be derived from archival research of historical records related to steel industry. The analysis of the sites using geospatial tools allowed the clear identification, extent and distribution along the Mexican geography. This will facilitate the spatial analysis of the slag deposits and whether those sites have any relevant environmental or social factors determining their future utilisation.

Understanding the geospatial distribution of steel slag in Mexico when compared to other studies such as Riley et al. (2020), would provide a contextual knowledge of what to expect during this analysis. Moreover, the previous studies conducted in the United Kingdom, for instance, Mayes et al. (2018), Pullin et al. (2019) would serve as a guidance for comparing geospatial patterns or land utilisation. In summary, the knowledge gained through the research will increase the potential utilisation of this material, whether for mitigating carbon dioxide emissions or to be used as a sustainable aggregate in concrete production, or maybe as a source of nutrient supply for agribusiness. Additionally, better waste management practices could be developed and used as a reference for other studies with a similar scope.

3.3 Methodology.

The methods used in this chapter for the volume estimation of deposited iron and steel slags in Mexico is further described. Initially, historical records were analysed for site identification; also, the assessment of these archival resources provided an overview of the steel industry evolution across time, outlining the current land use around the slag heaps. Geospatial tools were key for the volume estimation of iron and steel slags in the identified deposits, enabling a fuller picture of the current status of the slags to consider their potential reutilisation.

3.3.1 Identification of legacy and current iron and steel slag sites.

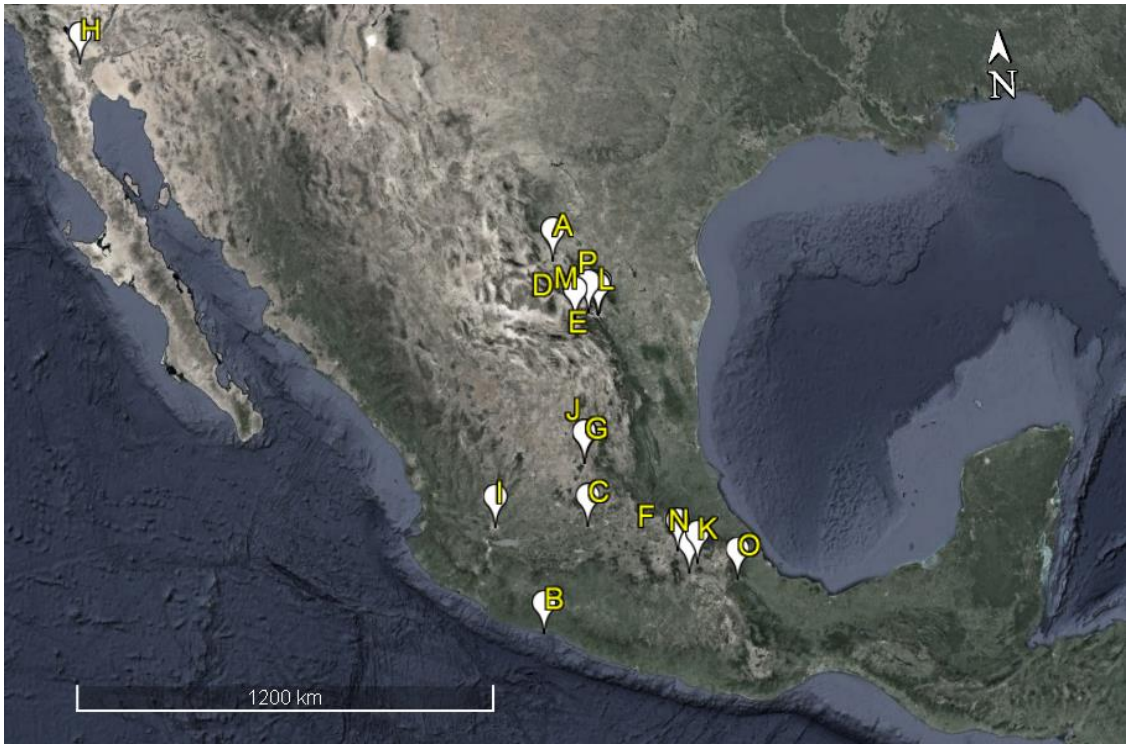

Figure 17 *Location of 16 slag deposits studied, image from Google Earth Pro (2024).*

The first approach in identifying former and current steel making sites involved the assessment of historical records from the National Council of Steel Industries (*CANACERO*) (2024) and from the Museo Horno 3 (*Museum of Mexican Steel Industry*) (2024), looking for traces of information related to the industrialisation of Mexico since early 20th century, as Sanchéz-Diaz (2009) documented that 1900 was the year where steel manufacturing had a significant growth.

The crosscheck from both sources enabled an initial list of twenty-three former and current steel manufacturing sites to be identified, where iron and steel slag heaps remained in the immediate surroundings. The information was corroborated using the documented records from the Mexican Geologic Service (*Servicio Geológico Mexicano*) (2024); this search also provided data on production methods, operation periods, and management changes, among other contextual information.

Following this, a preliminary screening of the data was conducted through a spatial inspection of the twenty-three sites located from archival research; this was done through Google Maps (Google Maps, 2024), which facilitated an aerial view of the terrain, enhancing a digital observation of the sites with a close up between 5 to 20 m. The *'street view'* of the tool facilitated an initial confirmation of stockpiled slag in 16 of the 23 sites; 7 sites were dismissed from the study, as there were no indicators of slag presence within a 2 km^2 perimeter around the location, either from an aerial or street view perspective from the use of the geospatial tools.

Thus, the presence of stockpiled slags was identified in 16 out of 23 of the documented locations and corroborated by doing a 3D terrain exploration of the sites using the high-resolution imagery from Google Earth Pro (Google Earth Pro, 2024) and QGIS (QGIS, 2024). Google Earth Pro was also used to record latitude, longitude and altitude data from the 16 confirmed locations, which were labelled from A to P, as shown in Figure 17.

3.3.2 Quantification of Mexican iron and steel slag deposits.

The estimation of the volume of iron and steel slags in Mexico started with an initial measurement of the area (m^2) where each of the confirmed locations were stockpiled. The measurement was completed using QGIS software, an open-source Geographic Information System (*GIS*), with a wide range of tools for geospatial exploration.

The interface between QGIS and Google Earth Pro enabled geolocation of the sixteen sites previously identified (*section 3.3.1*). Then by using the 'area' tool from the software (*QGIS*), the dimension in squared meters for the sixteen sites was estimated. The area occupied by the slag deposits was also measured using Google Earth Pro to have a corroborative perspective of the procedure. See Figure 18 for a visual description of the methods.

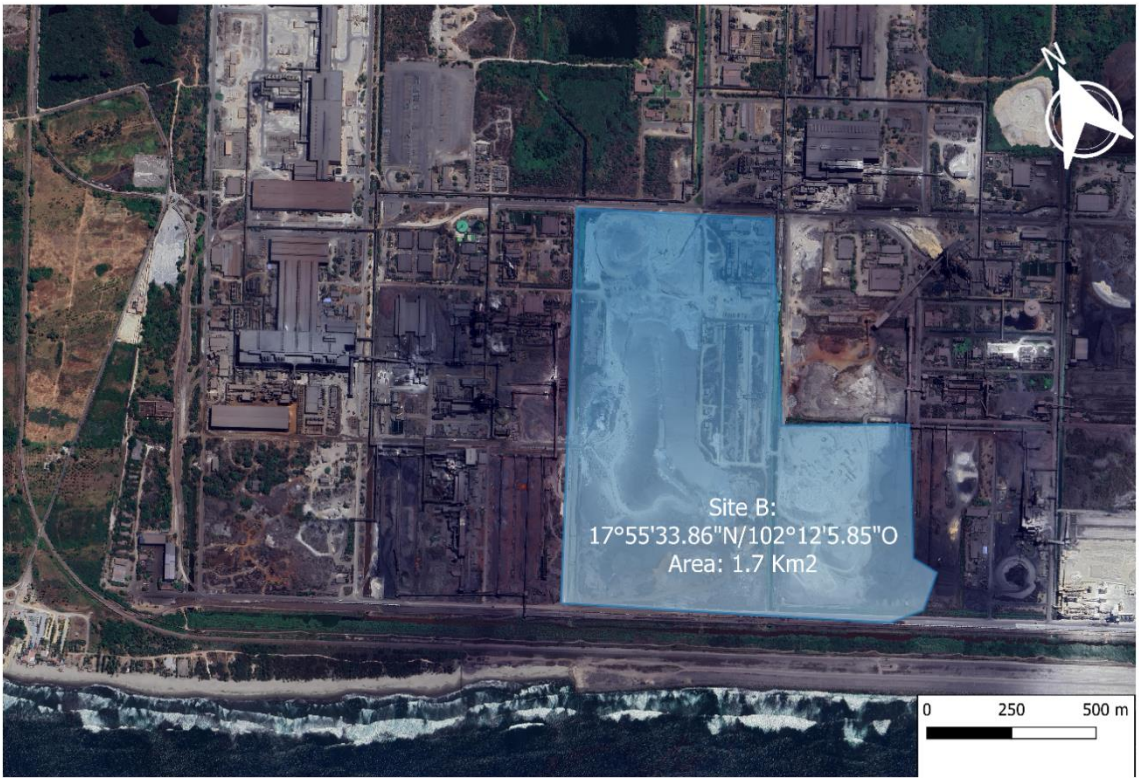

Figure 18 *Site B (17°55'33.86"N / 102°12'5.85"O) used to illustrate the area measurement process using QGIS (2024).*

3.3.2.1 Slag heap volume calculation.

The volume estimation of iron and steel slag deposits in Mexico was also completed through QGIS software and utilised Digital Elevation Models (*DEM*) with a 1.5 to 5 m resolution, and were obtained from the repository of the Mexican Institute of Geography (INEGI Mexico, 2016) and covered the sixteen sites studied. It is important to note that the DEM resolution of 1.5 to 5 m may introduce some limitations in accurately representing smaller-scale topographic variations of the slag heaps, especially in regions with complex terrain, such as Coahuila, Nuevo Leon and San Luis Potosi. Additionally, variations in DEM quality across different sites could affect the precision of volume estimates, potentially leading to under or overestimations in areas with lower resolution. To account for this, calculations, result analysis, and quantification were performed in a conservative manner, considering that variations in the DEM data might influence the final results.

First step in the process volume estimation was to create a polygon layer file (*.SHP*) for each of the sixteen sites of study, delimiting the area occupied by the slag heaps, this was completed using satellite images from Google Earth Pro as a baseline.

The creation of a shapefile, was necessary for a subsequent raster extraction of the Digital Elevation Model (*DEM*) to ensure that the volume estimation was completed just for the identified slag piles. Figure 19 shows the polygon layer definition using the imagery from Google Earth Pro as a baseline.

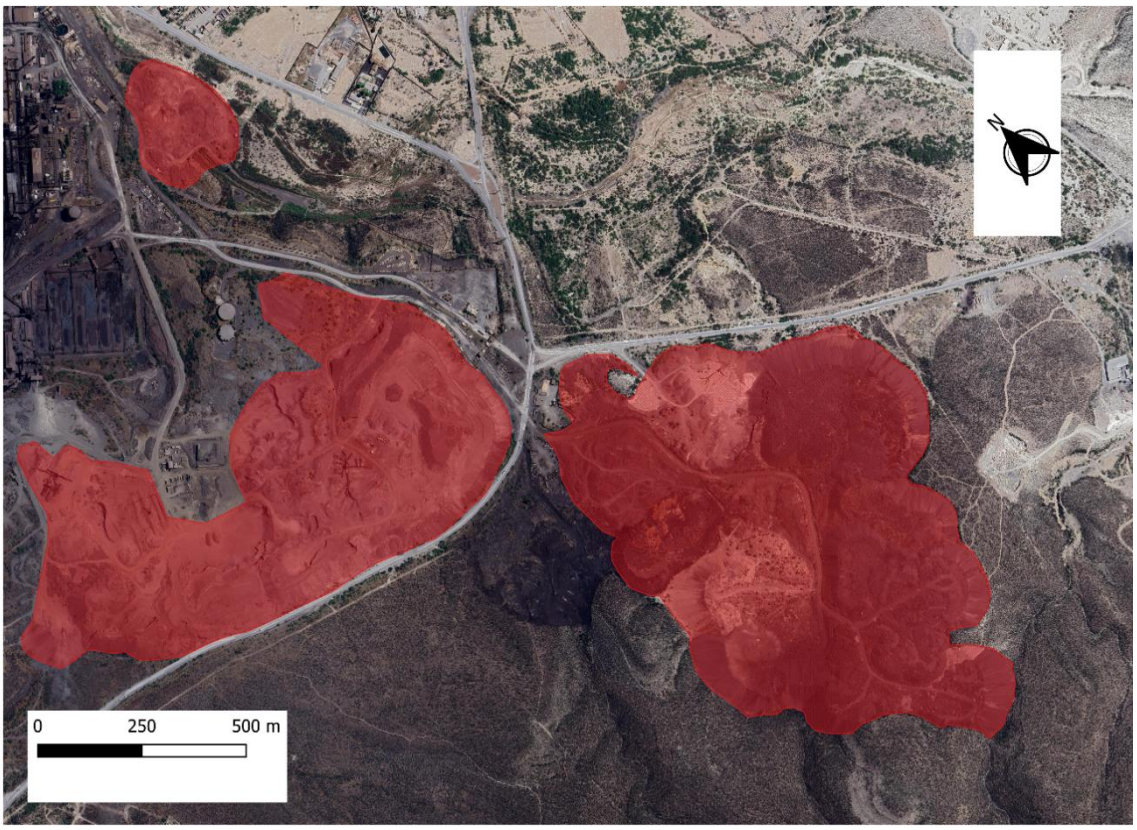

Figure 19 *Site A (26°52'8.81"N 101°24'35.78"O) used to illustrate the polygon layer definition in QGIS (2024).*

The following step was undertaken to complete a raster extraction from the Digital Elevation Model (*DEM*) of the location in QGIS: *Raster* > *Extraction* > *Clip Raster by Mask Layer*, where the input layer was the Digital Elevation Model (*DEM*) of the site and the mask layer was the *polygon (.SHP),* used to define the area of interest (*slag heaps*). The outcome of the operation was a clipped DEM layer of the slag pile, where the area of interest was clearly established as shown in Figure 20. Once the area of interest was defined, the elevation of the terrain was confirmed by using the raster tool package from QGIS*,* and the resulting layer contained the contour lines of each site, with defined base level values to be used during the volume quantification of the slag heaps. The route performed in the software for this step was: *Raster* > *Extraction* > *Contour*. The volume estimation for each of the sites involved the processing of the data through the *'Raster Surface Volume'* tool from the *'Raster Analysis'* package in QGIS.

The raster resolution used to estimate the volume of the slag heaps was of 50x50 m. In each case, the input layer was the clipped DEM produced for the sixteen sites. The base level value used was the lowest elevation point resulting from the contour lines evaluation, and the selected method for characterising only the slag heaps, without any other trace of land, was *Count Only Above Base Level*. When the processing was done, a report with calculated area in m^2 and volume in m^3 was provided for each location and saved as a file.

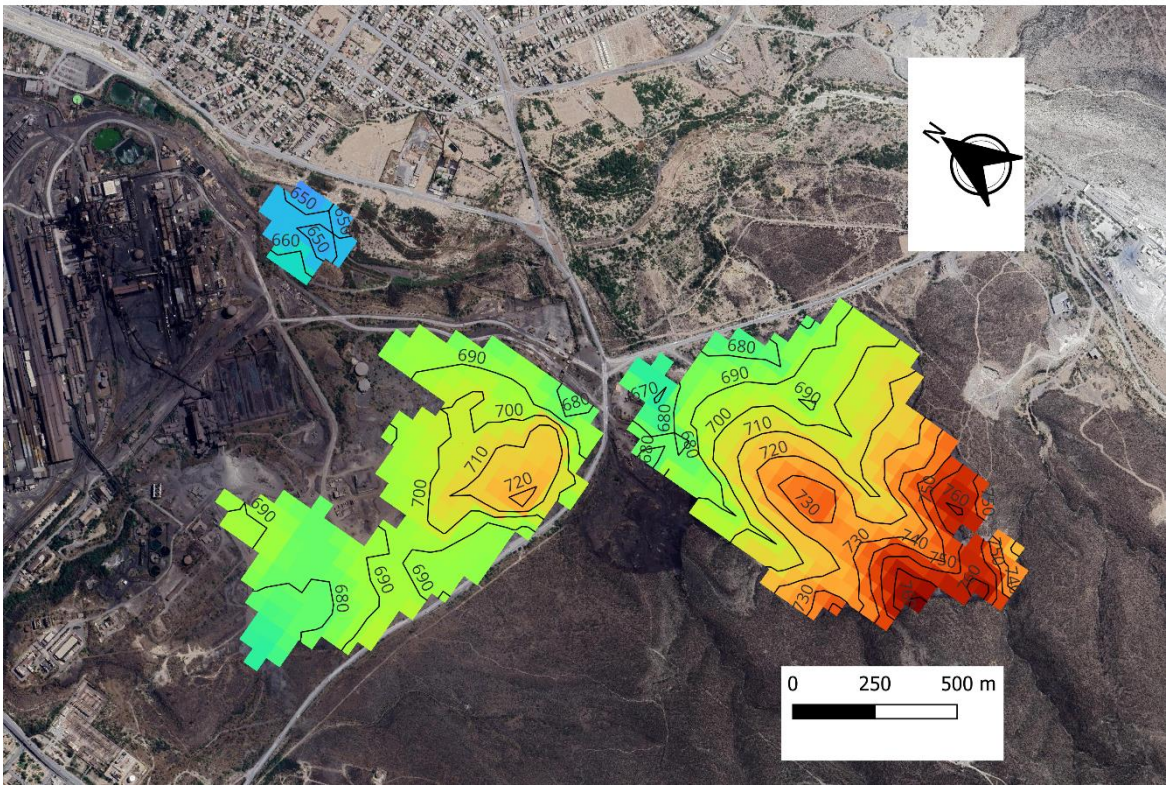

Figure 20 *Site A (26°52'8.81"N 101°24'35.78"O) used to illustrate the Digital Elevation Model (DEM) extraction of the slag heap to further perform a surface volume estimation in QGIS (2024).*

The volume estimation for the study sites was given in cubic meters (m^3) from the QGIS report and the results were converted into mass units (tonnes) by using *Equation 4* below. Density used was $\rho_{steel\ slag} = 1.4\ \frac{Kg}{m^3}$, resulting from the calculated average from the density values (1.1 to 1.7 kg/m^3) documented in the work of Riley et al. (2020), Pullin et al. (2019), Reddy et al. (2019) and Mayes et al. (2018). Density values of 1.1 to 1.7 kg/m^3 were later used as error bars to plot the results.

Equation 4.

$$Mass_{Slags} = \left(QGIS\ Volume\ in\ m^3 * \rho_{steel\ slags} = 1.1 - 1.7\ \frac{Kg}{m^3} * 0.001 \frac{Tonnes}{Kg}\right) =$$

Where:

- Mass $_{Slags}$= the mass of the slag heaps processed in QGIS (Tonnes).
- QGIS Volume= volume of the slag heaps calculated in QGIS (m^3).
- $\rho_{steel\ slags}$= Range of densities of steel slags (Kg/m^3) (Mayes et al., 2018; Pullin et al., 2019; Reddy et al., 2019; Riley et al., 2020).
- Conversion factor from Kg to Tonnes= 0.001 Tonnes/Kg.

3.4 Results.

3.4.1 Geographical location of the steel slag sites.

The geospatial evaluation of steel slag resources in Mexico started by analysing historical records to generate a picture of the slag deposits throughout the country. During this step, initially a selection of 23 sites was done. Google Maps and Google Earth Pro were then used to locate the sites and determine the presence of slag heaps, both legacy heaps and those recently created. The presence of slag could not be confirmed at seven sites, as the Google imagery did not show any landforms within a buffer area of 2 km^2 around the initial research location. A total of 16 sites presented slag heaps that remained in the immediate surroundings of the steel manufacturing sites. Figure 21 shows the 16 sites, labelled A to P.

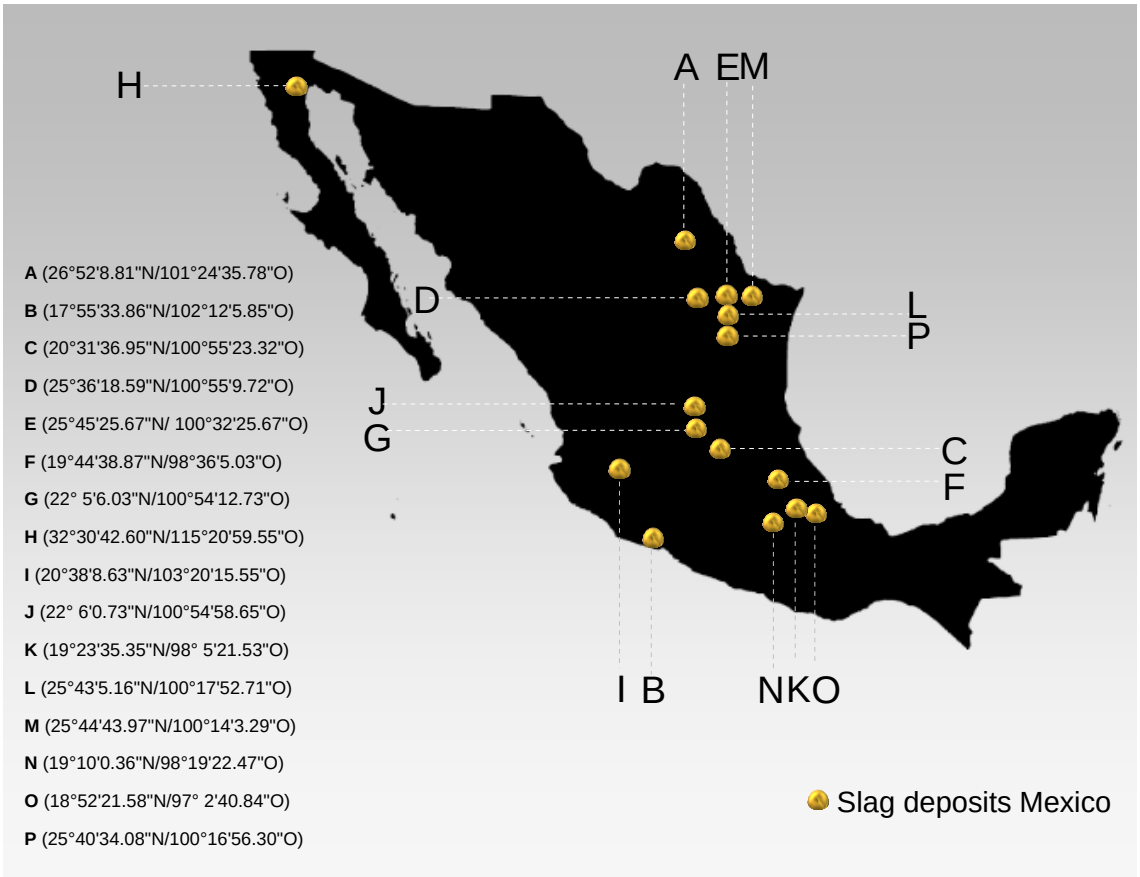

Figure 21 *Distribution of the 16 slag deposits studied and their geographic coordinates.*

3.4.2 Operational context.

A summary of the information after a data screening is presented in Table 4 below, giving a recap of the background of each of the 16 sites identified. Steel slag deposits were found in 11 out of 32 regions of Mexico, distributed along 16 cities/towns from the north, centre and west (*Pacific coast*) of the country.

Table 4. Summary of operative context of the 16 slag deposits studied.

Site	Region in Mexico	Latitude	Longitude	Method used	Raw materials	Operating since	Company
A	Coahuila	26°52'8.81"N	101°24'35.78"O	BOF	Iron ore	1941	*Altos Hornos de Mexico AHMSA*
B	Michoacan	17°55'33.86"N	102°12'5.85"O	BOF/EAF	Iron ore	1976	*ArcelorMittal Mexico*
C	Guanajuato	20°31'36.95"N	100°55'23.32"O	EAF	Steel recycling	1998	*DeAcero*
D	Coahuila	25°36'18.59"N	100°55'9.72"O	EAF	Steel recycling	2013	*DeAcero*
E	Nuevo Leon	25°45'25.67"N	100°32'25.67"O	EAF	Steel recycling	2016	*Frisa Forjados*
F	Hidalgo	19°44'38.87"N	98°36'5.03"O	EAF	Steel recycling	2015	*Gerdau Corsa*
G	San Luis Potosi	22° 5'6.03"N	100°54'12.73"O	EAF	Steel recycling	2008	*Grupo Acerero*
H	Baja California Norte	32°30'42.60"N	115°20'59.55"O	EAF	Steel recycling	2001	*Grupo Simec*
I	Jalisco	20°38'8.63"N	103°20'15.55"O	EAF	Steel recycling	2001	*Grupo Simec*
J	San Luis Potosi	22° 6'0.73"N	100°54'58.65"O	EAF	Steel recycling	2008	*Grupo Simec*
K	Tlaxcala	19°23'35.35"N	98° 5'21.53"O	EAF	Steel recycling	2004	*Grupo Simec*
L	Nuevo Leon	25°43'5.16"N	100°17'52.71"O	EAF	Iron ore	1942	*Ternium Mexico*
M	Nuevo Leon	25°44'43.97"N	100°14'3.29"O	EAF	Iron ore	1942	*Ternium Mexico*
N	Puebla	19°10'0.36"N	98°19'22.47"O	EAF	Iron ore	1963	*Ternium Mexico*
O	Veracruz	18°52'21.58"N	97° 2'40.84"O	EAF	Steel recycling	1985	*Tyasa*
P	Nuevo Leon	25°40'34.08"N	100°16'56.30"O	BOF	Iron ore	1900-1986	*Fundidra Park*

A key element found was that ironstone mines were in the proximity of the 16 sites studied and was a significant element determining the location of the sites. Iron ore mining sites are proximal to site A (*Monclova*) and B (*Lazaro Cardenas*), providing the raw materials for their production. In the case of sites L, M, N, raw materials are supplied from mining sites located in the regions of Colima, Jalisco and Michoacan. Steel production of sites: C to K and O used recycled steel as their raw materials, in the EAF process. The largest mining sites in the country are: *"Las Truchas"* operated by ArcellorMittal (*site B*), which also manages the mining site

"San José" and have a shared agreement with Ternium Mexico for mineral extraction in *"Peña Colorada"* mine. Ternium also use iron ore from the *"Encinas"* mining site located near the Pacific coast of the country. Altos Hornos de Mexico (*A*) conducts mining operations in the iron stone mines*: "Cerro de Mercado", "El Bazán" and "Mineral del Norte".*

15 out of the 16 sites studied maintain operative steel processes. The methods used involve electric arc furnaces in 13 of the sites (*C to O*); 1 site (*B*) uses, BOF and EAF, while site A in Monclova uses Basic Oxygen Furnaces. Site P is a former steelwork that produced steel using BOF methods when it was in operation between 1900 to 1986; the site was converted into a museum and recreation area in the last decade of the 20th century. The sixteen sites are operated by national and multinational corporations, from which Grupo SIMEC runs four sites (*H, I, J and K*), Ternium operates sites L, M and N and DeAcero have two active sites (*C and D*). Sites A, B, E, F, G and O are single operation with an integrated system to develop a wide range of steel-base finished products.

3.4.3 Land use context.

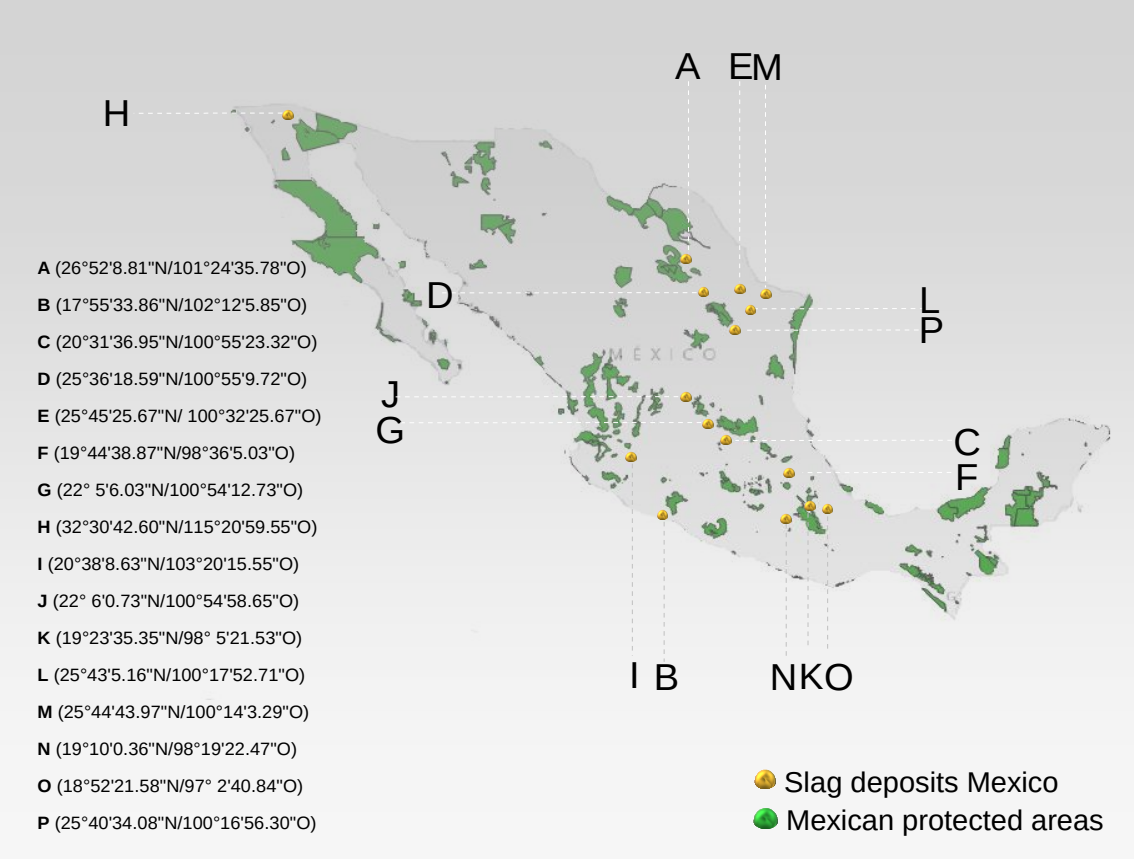

Figure 22 *Map of Mexican protected areas and their interaction with slag deposits studied.*

Further to assessing the volume of iron and steel slag deposits in Mexico, a background exploration was done in the identified sites; the focus was to better understand their context in a perspective of land use and potential constraints on the future utilisation of the slags. Findings from the assessment indicate that the 16 sites are still in use, receiving a constant feed of EAF and BOF slag from the companies in charge (CANACERO, 2024). Figure 22 shows the locations of the 16 study sites and their interaction with the natural protected areas of Mexico, coloured in green. An analysis of the boundaries of the protected areas and their proximity to the study cases was completed for the 16 sites; none of them remains in a considered protected area. However, 15 of the sites are located on private property owned/controlled by the companies (*Table 4*) running steel production. Within these 15 sites, the slag is stockpiled besides the production sites and/or in areas nearby, also considered private property based on their enclosed conditions.

3.4.4 Volume estimation.

The identified sites, categorized from A to P were processed in QGIS software to calculate the mass of slag deposited in each location. The total amount of steel slags present in Mexico was 273, 612.5 tonnes. Figure 23 below shows BOF and EAF mass distribution.

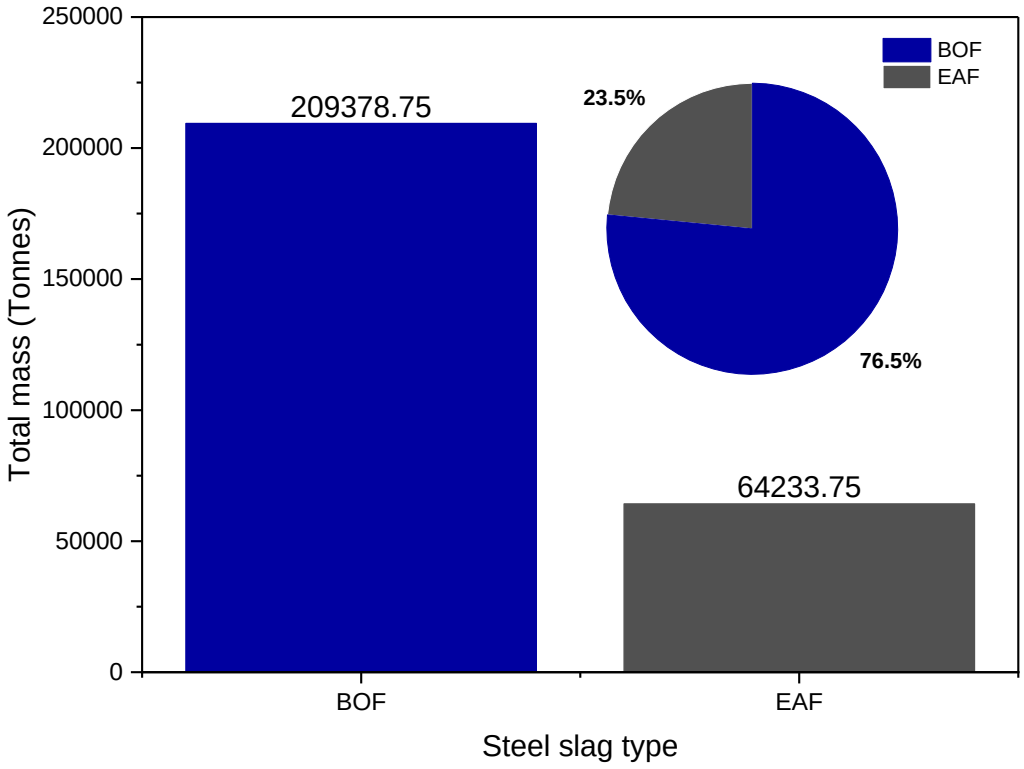

Figure 23 *Total mass of steel slags quantified in Mexico.*

Based on the furnace type in each of the operating sites, 1 site (*A*) in Monclova produces steel using the Basic Oxygen Furnace method, while site B (*Lazaro Cardenas, Michoacán*) has a dual approach with BOF and EAF operations; sites C to O, produce steel by using Electric Arc Furnaces. Therefore, from a theoretical point of view based on the production methos: 76 % (*~209378.75 tonnes*) corresponded to Basic Oxygen Furnace slag and the 23 % (*~64233.75 tonnes*) to Electric Arc Furnace slag. Figure 24 below illustrates the quantified slag for each of the 16 sites studied and provides a visual guide to their location in the Mexican territory.

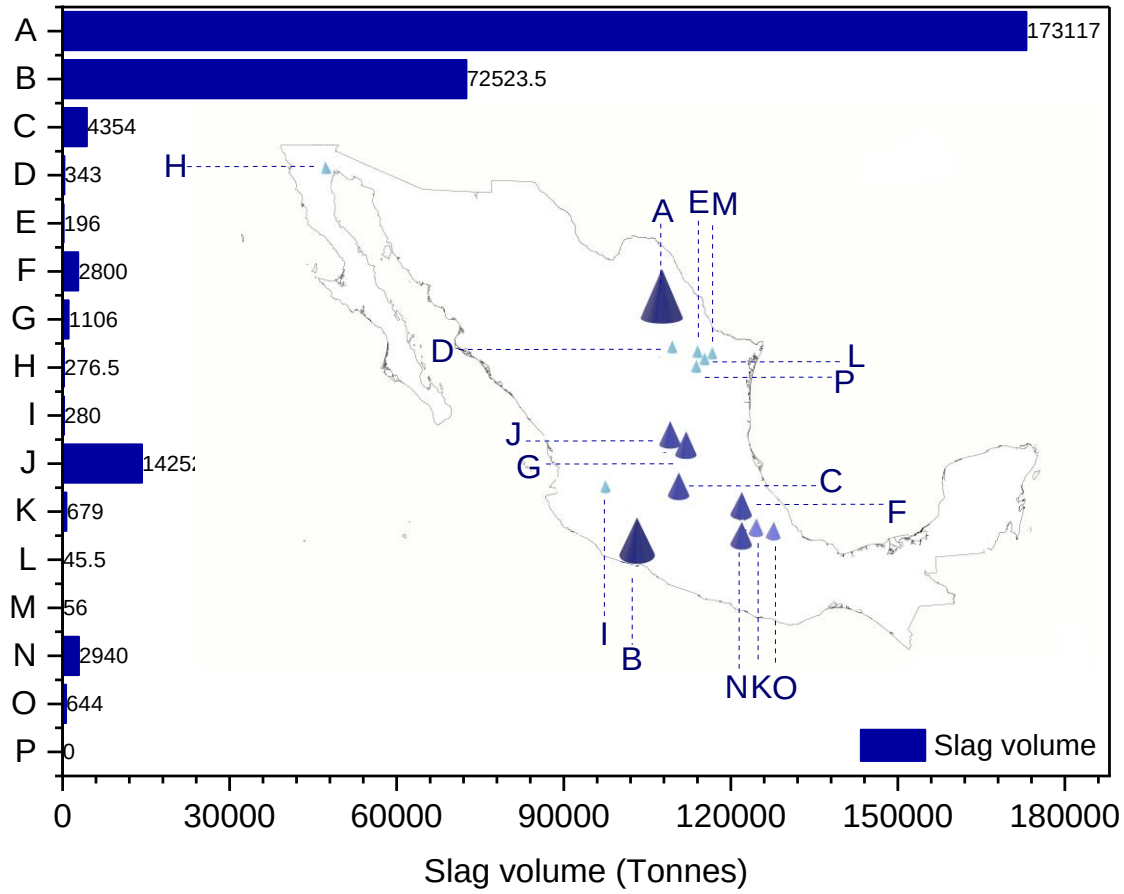

Figure 24 *Volume of steel slags quantified, organised by site location.*

Most of the BOF slag was quantified in site A, a steel production site opened in 1941 near the city of Monclova, in the north of Mexico. The total slag measured there was ~173117 tonnes, 63% of the total mass quantified in the 16 sites studied. BOF slag was also found in site B, near the city of Lazaro Cardenas in the pacific coast of Mexico; within site B steel is produced through EAF and BOF methods and the quantified slag is around 72523.5 tonnes; there is no particular data confirming the exact amount or proportion corresponding to each slag type, therefore for this study it is assumed half of it is BOF and half is EAF.

Medium size sites classified were San Luis Potosi (*J and G*), Guanajuato (*C*), Puebla (*N*) and Hidalgo (*F*), if compared to sites A and B which were considered the largest studied in this thesis; slag from those sites was produced under Electric Arc Furnaces and the quantified mass in tonnes was as follows: J (*14252*); C (*4354*); N (*2940*); F (*2800*); G (*1106*). The lowest amount of slag was quantified in sites: Coahuila (*D*); Jalisco (*I*); Baja California Norte (*H*); Nuevo León (*E*); Nuevo León (*M*); Nuevo León (*L*); Nuevo Leon (*P*), where the measured slag, from higher to lower, was: 343 tonnes (*D*); 280 tonnes (*I*); 276 tonnes (*H*); 196 tonnes (*E*); 56 tonnes (*M*); 45 tonnes (*L*) respectively; there was no slag in site P, as it was removed to build a park and museum under the steel industry theme.

Data of quantified slag was also organised in terms of total steel slag (*tonnes*) per region of Mexico, where steel production was confirmed. In regions such as San Luis Potosi or Coahuila two sites were identified in each; in Nuevo Leon 4 sites were confirmed, although the volume of slag deposited there was classified within the lowest range in this study. Figure 25 shows total mass of deposited slag grouped per region of Mexico.

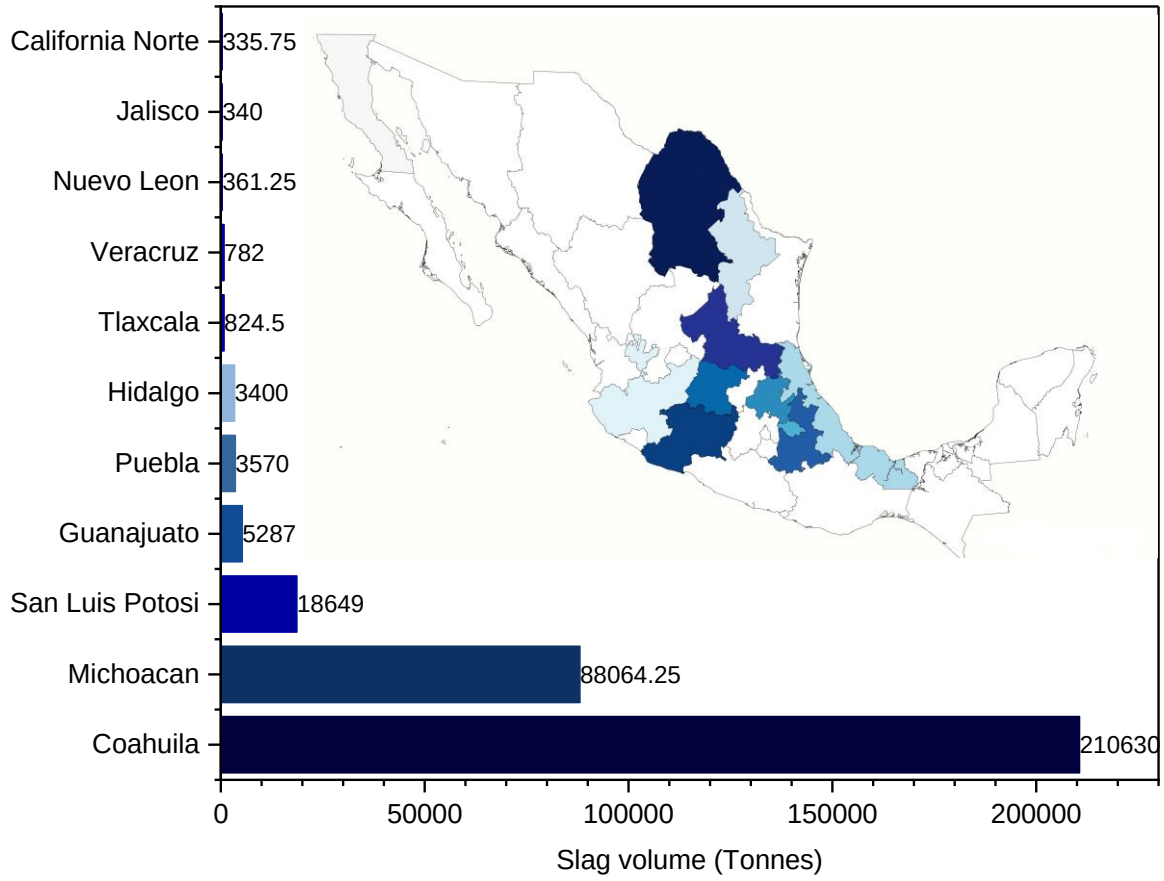

Figure 25 *Volume of steel slags quantified, organised by region.*

3.5 Discussion.

The study of the potential reutilisation of iron and steel slags in Mexico remains underexplored. The first stage in assessing reutilisation approaches is to compile background information and geospatial data on current and legacy slag deposits to develop plans for further utilisation. This chapter is motivated to contribute to this aim by identifying and quantifying iron and steel slag deposits in Mexico, where an estimation of the slag mass (*tonnes*) is provided and proposals for an approach for practical application is made.

3.5.1 Trends in iron and steel slag heap distribution in Mexico.

A key element influencing the location of a steel production site is the close proximity to raw materials. In the case of Mexico, the iron and steel industry started its growth in the 20th century (Plumb, 1948), based on available iron ore mines and enough coal reserves to keep production for extended periods as referenced in Abbott (2019). This influenced the geographical distribution of the steelworks opened in Mexico since 1900, and is consistent with the findings of this chapter, as the archival researched showed that ironstone mines were located or well-connected to the 16 sites examined, playing a crucial role in determining their locations. For instance, sites A (*Monclova*) and B (*Lázaro Cárdenas*) benefit from proximity to iron ore mining sites, ensuring a readily available supply of raw materials for steel production; this is the reason why those sites remain as primarily producers of steel in the country. Sites L, M, and N rely on mining sites in regions like Colima, Jalisco, and Michoacan, thus the railway network is key to maintain the raw material supply. In another approach, based on the environmental need to transform the steel manufacturing industry into a more sustainable field, sites C to K and O utilize recycled steel in the Electric Arc Furnace (*EAF*) process.

As mentioned, the importance of feasible logistics for raw material supply influenced the location of production sites. In this matter, an example of the strategic mining partnerships for securing iron ore in Mexico was shown by the management operations within the major mining sites *“Las Truchas"* and *"San José"*, currently managed by ArcelorMittal (*site B*), which have a shared operative agreement with Ternium Mexico for mineral extraction in *"Peña Colorada"* mine. Furthermore, Altos Hornos de Mexico (*site A*) operates significant ironstone mines like *"Cerro de Mercado," "El Bazán,"* and *"Mineral del Norte",* further emphasizing the correlation between iron ore deposits and steelwork’s locations. The proximity to iron ore mines and coal fields, as well as strategic collaborations, optimizes logistical efficiency and influences the siting and progress of steelworks.

From understanding the factors behind the allocation of the operational sites, it is logical to think that slag deposits would remain in the nearby areas. As documented in Pullin et al. (2019), slags from iron and steel sites continue to be simply dumped into adjacent available land close to the production sites; this practice seems to continue to be replicated in many parts of the world through time, including Mexico. This slag was typically stockpiled with little environmental consideration due to a lack of regulations governing disposal methods in the country and minimal or not available opportunities for the potential utilization of slag in other fields. Waste disposal in Mexico is regulated by the *"Ley General para la Prevención y Gestión Integral de los Residuos* (2023)" (*Law for Waste Management*), where the disposal and further use of iron and steel slags remains unclear, as detailed procedures or advice is not provided. This leaves the management and utilisation of the slags under the steel companies' discretion, or any further buyers. There is not a specific methodology in law for further utilization of the material in suitable sectors; the use of the slags relies on the interest from other industries, primarily construction, which have demonstrated some interest in having a low-cost access to the materials, however this is variable. From a steel producers' perspective, generally, slags do not generate a constant income, therefore, limited or no attention is given to its management or logistics.

3.5.2 Land use designations.

Slag deposits, as studied in this research could hold potential for repurposing into carbon removal resources, raw materials sources, or redevelopment projects. However, their rehabilitation requires careful consideration of environmental impacts and community needs to ensure sustainable practices within these areas. As documented in Riley et al. (2020), stockpiled slags (*legacy slag deposits*) could be protected due to their ecological function, as they might represent a habitat for some fauna or local vegetation. In the cited study, most of the sites remained within land designation parameters, which limit their further utilisation based on conservation purposes.

Within this research, as part of the archival research completed for site identification, land use within slag deposits A to P was also considered. The background exploration was conducted to understand their context in terms of land use and potential constraints for future utilization. Results presented in Figure 9 showed that none of the 16 slag sites have overlaps or remain close to natural conservation areas in the country. Therefore, further utilisation of the slags is not constrained by conservation protections for protected species.

However, land use should be assessed, as the 16 Mexican sites are situated on private property administrated by the steel manufacturers or governmental agencies. In addition, the sites (*A to P*) are located within urban areas, which might represent links to the communities nearby. 15 out of the 16 sites under study remain active, meaning they are continuously receiving slag from steel companies, where the stockpiling occurs either adjacent to production sites or in nearby areas, all within the confines of companies' space. Therefore, the utilisation of the slags would be in agreement with the companies managing the waste materials. In this aspect, the National Council of Steel Industries (*CANACERO*) (2024) might work as an instrument of mediation for any attempt related to the use of the slags.

Overall, this work underlines a difference between the constraints on the reutilization of slag in Mexico compared to the United Kingdom. While in the United Kingdom, where the work from Riley et al. (2020) took place, there were constraints based on the cultural and environmental importance of the sites, Mexican slag heaps lack any such conditions, as the regulatory frameworks governing slag reutilization in Mexico are not as specific as in the UK. Despite the absence of conservation designations, the presence of local species on the slag heaps in Mexico suggests potential ecological significance. Thus, this aspect should be analysed, as the further utilisation of the slag deposits might represent an impact for local biodiversity or urban development. For instance, for the slag heaps located in Monclova, Mexico (*site A*), which started operations since mid-20th century and now cover a ~170 hectares site, it is possible that local animal species might have found suitable conditions to form their habitats in the heaps. While the biodiversity should be further studied, the lack of conservation designations means there is the opportunity to potentially reutilise the slag heaps for CO_2 sequestration, or as a source of material for sustainable production of concrete.

3.5.3 CO_2 sequestration potential.

3.5.3.1 Estimation on CO_2 sequestrated in Mexican slags.

The findings from Pullin et al. (2019) involved atmospheric CO_2 quantification in legacy slag heaps, where carbonation occurred with no human intervention. The collection site in Consett, England, is a former steelworks site with similar environment conditions to the Ravenscraig collection site in Scotland, also studied in this thesis (*Chapter II*). In the case of Mexico, it is hard to compare CO_2 carbonation measurements, as there is limited (*null*) references documenting mineral carbonation or the quantification of average volumes of CO_2 sequestrated within legacy slag heaps in the country.

However, in chapter II of this thesis the average amount of CO_2 mineralised by Mexican slags from Monclova, Coahuila was calculated to be 21 kg of CO_2 per tonne of steel slag, with minimum and maximum amounts of 6 kg and 51 kg of CO_2 per tonne of slag, respectively. This provides a realistic overview of the capacity of Mexican slags to passively carbonate atmospheric CO_2, and given the similar climatic conditions between the 16 slag heaps studied in this chapter, it is feasible to assume these data from Monclova are representative of all Mexican slags and can therefore be used to obtain an estimation of the atmospheric CO_2 carbonated within the slag deposits.

By using the below *Equation 5*, where total mass of slag heaps is given in tonnes and the calculated carbonated CO_2 is given in Kg per tonne of steel slag, an upscaled mass (*in Kg of CO_2 per tonne of steel slag*) of CO_2 likely to be sequestered in Mexican slag heaps can be calculated.

Equation 5.

$$Carbonated\ CO_2 = (Total\ mass\ of\ the\ slag\ heaps) * (Calculated\ CO_2\ carbonated\ in\ Mexican\ slags)$$

Where:

- Carbonated CO_2= estimated mass of CO_2 carbonated in Mexican slag deposits (Kg of CO_2).
- *Total mass of the slag heap (cumulative of the 16 slag deposits studied in Mexico) = 273, 612.5 tonnes (273 K tonnes)*
- ***Calculated CO_2 carbonated in Mexican slags:***
  - *Average CO_2 carbonated in Mexican slag heaps is= 21 kg of CO_2 per tonne of steel slag.*
  - *Minimum CO_2 carbonated in Mexican slag heaps is= 6 kg of CO_2 per tonne of steel slag.*
  - *Maximum CO_2 carbonated in Mexican slag heaps is= 51 kg of CO_2 per tonne of steel slag.*

Table 5. Summary of calculated CO_2 carbonated within Mexican slag heaps studied; giving average, as well as maximum and minimum values for error bars.

	Total Average	**Total Minimum**	**Total Maximum**
CO_2 carbonated in Mexican slag heaps *(Kg of CO_2)*	5,745,862.5	1,641,675	13,954,237.5
CO_2 carbonated in Mexican slag heaps *(Tonnes of CO_2)*	5,745.9	1,641.7	13,954.24
CO_2 carbonated in Mexican slag heaps *(Kt of CO_2)*	5.7	1.64	13.9

Table 5. shows the calculated cumulative CO_2 carbonated within the 16 Mexican slag deposits studied in this chapter; results are expressed in Kg/Tonnes/K tonnes of CO_2, and are organised as Total Average measurement (*5.7 Kt of CO_2*) indicating the estimated mass of CO_2 carbonated per tonne of slag within the slag deposits; Total Maximum (*13.9 Kt of CO_2*) and Total Minimum (*1.64 Kt of CO_2*) data, provide, respectively, the higher and lower values for estimated error within the estimation.

3.5.3.2 Estimate on CO_2 sequestration potential of Mexican slags.

Conducting a realistic assessment of the carbonated CO_2 contained within Mexican slag deposits, is key for gaining an insight into their potential for carbon sequestration. This was done in chapter II of this thesis and the results were applied in the previous section (*3.5.3.1*) to estimate the volume of CO_2 carbonated in the 16 slag deposits assessed in this chapter. However, having a comprehensive overview of these slag heaps as carbon removal resources requires us to fully understand their sequestration potential.

Therefore, a projection of carbonation potential of slag deposits can be used as an instrument to further explore the utilisation of the by-products. In this line, the work from Pullin et al. (2019) provided a calculated projection of the carbonation potential of a slag deposit located in Consett, England by using a modified version of the Steinour Equation. This was further applied in the research of Riley et al. (2020), where the carbonation rate and cumulative CO_2 uptake potential of a legacy slag deposit was evaluated considering different processes: Direct Carbonation, Enhanced Weathering and Passive Carbonation. The projection on carbonation potential from Riley et al. (2020) is summarized in Table 6 below.

Table 6. Carbonation potential for slag deposits under three carbonation regimes from Riley et al. (2020).

Projected carbonation potential of quantified slag deposits under three carbonation regimes (rates of CO_2 sequestration from Pullin et al. (2019)).

Carbonation method	*Carbonation rate (kg CO_2/t slag)*	*Cumulative CO_2 uptake potential (Kt /Mt)*
Direct carbonation	*296-337*	*56.6-79.4 Mt*
Enhanced weathering	*422-584*	*80.7-137.6 Mt*
Passive carbonation	*0.007-12.1*	*1.3 Kt-2.9 Mt*

Key differences between the carbonation routes detailed in Table 6 are for instance that direct carbonation involves reacting CO_2 with minerals or industrial by-products in a controlled environment to form stable carbonates (Miao et al., 2023; Rushendra Revathy et al., 2016). Enhanced weathering implicates arranging reactive minerals to accelerate the natural weathering process for CO_2 sequestration (Ukwattage et al., 2017). Passive carbonation, as studied in Chapter II of this thesis, refers to the gradual reaction of atmospheric CO_2 when exposed to minerals without human intervention, as studied in chapter II of this thesis (Khudhur et al., 2022).

The approach from Riley et al. (2020) and Pullin et al. (2019) was taken as a guidance in the projection of the cumulative carbonation potential of the 16 slag deposits identified in Mexico (*Equation 6*), using the total mass of slag deposits (*273 K tonnes*), through the three regimes (*Direct carbonation, Enhanced Weathering and Passive Carbonation*) using the below methods.

Equation 6.

$$Total\ cumulative\ CO_2\ uptake_{\ X} = Slag\ deposits\ total\ mass * CO_2\ uptake\ potential_X$$

Where:

- *Total cumulative CO_2 uptake potential = (kg CO_2/t slag)*
- *Slag deposits total mass = 273, 612.5 tonnes (273 K tonnes)*
- *X= CO_2 uptake regime in in Kg CO_2/t slag* (Riley et al., 2020)
- ***Carbonatation rates for CO_2 uptake potential calculation; regimes ranges*** (Riley et al., 2020)*:*
    - *Direct carbonation = 296-337 Kg CO_2/t slag*
    - *Enhanced carbonation= 422-584 Kg CO_2/t slag*
    - *Passive carbonation = 0.007-12.1 Kg CO_2/t slag*

Table 7 shows the projected carbonation rates (Riley et al., 2020) and the cumulative CO_2 uptake potential results calculated for the Mexican slag deposits through the three carbonation regimes.

Table 7. Calculated CO_2 capture potential within Mexican slag deposits, based in the estimations of Riley et al. (2020).

Carbonation method	*Total Carbonation rate (kg CO_2/t slag)*	*Total Cumulative CO_2 uptake potential (kg of CO_2)*	*Total Cumulative CO_2 uptake potential (tonnes /K tonnes of CO_2)*
Direct Carbonation	*296-337*	*80989300 – 92207412*	*80.9 – 92.2 Kt*
Enhanced Weathering	*422-584*	*115464475 – 159789700*	*115.4 – 159.7 Kt*
Passive Carbonation	*0.007-12.1*	*1915 – 3310711*	*1.9 t - 3.3 Kt*

3.5.3.3 CO_2 capture potential within Mexican slag deposits.

The potential of CO_2 capture within Mexican slag deposits was explored in section 3.5.3.1 through an empirical approach using the findings from Chapter II of this thesis and the total mass of slags found within this chapter, through QGIS processing. The volumes of CO_2 quantified in Chapter II of this research were taken as the general rate of sequestration for the 16 sites evaluated; in addition, the maximum (*51 kg of CO_2 per tonne of steel slag*) and minimum (*6 kg of CO_2 per tonne of steel slag*) values were also obtained, giving higher and lower values for error bar estimation (*error bars*).

The total mass (*273 K tonnes*) quantified within the 16 slag deposits in Mexico was multiplied by the average (*21 kg of CO_2 per tonne of steel slag*) measurement of carbonated CO_2 from steel slags from Monclova. Therefore, it was estimated that approximately 5.7 Kt of CO_2 mineralised within the 16 sites, where the minimum measurement would be 1.6 Kt of CO_2 and the maximum was 13.9 Kt of CO_2. This first approach provides a realistic overview of the CO_2 sequestrated within Mexican slags through passive carbonation.

A second approach, where passive carbonation was also assessed using the capturing rates ranges from the work of Riley et al. (2020) and Pullin et al. (2019) aimed to have a more speculative view of the CO_2 sequestration potential of Mexican slags, while examining direct and enhanced carbonation as well as passive carbonation as in section 3.5.3.1. This was detailed over section 3.5.3.2, where the estimation for direct carbonation using the total mass of stockpiled slags within Mexico and the ranges presented in literature, resulted in a potential cumulative CO_2 uptake between 80.9 – 92.2 Kt of CO_2. In the case of enhanced carbonation, the potential amount that can be captured through this regime was between 115.4 – 159.7 Kt of CO_2; the differences between these two mineral carbonation approaches were considerable, however from a passive carbonation perspective the projected outcome became less effective if compared to the engineered procedures, with a sequestration potential going from 1.9 t to 3.3 Kt of CO_2. These projected results remained below the estimated CO_2 sequestration through empirical measurements in section 3.5.3.1, where CO_2 mineralization above 5.7 Kt was the cumulative total from the 16 sites. The difference between both approaches, might be related to external parameters influencing the carbonation reaction within the slag heaps, as explored in Chapter II. In any case, both measurements are within the error bars calculated for the empirical route: 1.6 Kt of CO_2 (*minimum*) and 13.9 Kt of CO_2 (*maximum*); therefore, the underestimate from section 3.5.3.2 remains useful to project conservative scenarios for passive carbonation within slag heaps.

Overall, the assessment of the Mexican slag deposits through different mineral sequestration routes provided an understanding of the possibilities that legacy slag can represent for the mitigation of CO_2 emissions.

Whereas the empirical approach presented in section 3.5.3.1 showed a feasible and realistic outcome to capture CO_2 in a passive way, the projections of enhanced and direct carbonation (*section 3.5.3.2*) show it would be more effective in reducing atmospheric CO_2. Thus, in a scenario where mineral carbonation is aimed to be developed in Mexico, the most effective route to take would involve enhanced or direct mineralisation of CO_2. However, as this carbon removal option is still in a very early stage for the country, passive carbonation would continue to be the main method to sequestrate CO_2 within the existent slag deposits.

There would also need to be a consideration of the energy and therefore likely CO_2 expended in conducting direct and/or enhanced carbonation. Overall, the potential utilisation of legacy slags as a mitigation strategy to reduce CO_2 emissions, seems to be in need of further research to gain wider acceptance within the environmental context of Mexico.

3.5.4 Resource utilisation potential.

The utilisation of legacy iron and steel slags offers significant economic and environmental benefits for Mexico. For instance, the use of slags can be promoted for repurposing industrial waste into valuable materials; as explored in Chapter IV of this thesis, where the use of iron and steel slags was assessed in their potential to be used as supplementary cementitious materials, from which one of the Mexican samples tested resulted in potential pozzolanic characteristics if implemented in concrete blends. This was an indicator to wider investigate the properties of Mexican slags and their capacity to be used in the construction field.

Based on the significance of concrete production and its extended operations along the Mexican territory, the use of carbonated slags in this field, either for sustainable products production or for remediation actions, might help in reducing greenhouse emissions associated with traditional manufacturing processes and mitigate the environmental impact of waste disposal. Furthermore, the development of slag-based industries can create new job opportunities and stimulate economic growth in regions with abundant slag resources, such as the sites located in the regions of Monclova (*site A*) or Lázaro Cárdenas (*site B*).

The initial step of knowing the available amount of legacy slag within the country was explored in this research; this is important to develop waste management strategies, and to further develop utilisation mechanisms to analyse and guide the initiatives where this slag can be potentially used; this is helpful to create plans for the future where environmental impact can be reduced through reutilisation of legacy slags.

In addition, by following the global trend to produce steel by electric arc furnace methods, there is a research gap in Mexico to promote repurposing projects for EAF slags to be produced in the future.

3.6 Conclusion.

The geographic distribution of steel production sites in Mexico has historically been influenced by proximity to raw material sources, particularly iron ore mines. This correlation was shown as a result from the archival research completed, which highlighted the strategic location of steelworks near iron ore mining sites or the existence of efficient transportation to ensure a continuous supply of raw materials. Additionally, partnerships between steel companies and mining operations further optimize logistical efficiency and resource accessibility. However, the disposal and utilization of iron and steel slags represent a challenge for the country, based on disposal practices and limited regulatory frameworks. Thus, within this context, this chapter used geospatial tools and different data sources to compile a data repository on the amounts of iron and steel slags distributed throughout the country. This was done to understand their background, their role as carbon sequestration instruments and to propose further utilisation ideas based on key industrial fields of Mexico. The geospatial data of the 16 slag deposits studied in this chapter, along with other supplementary material, can be found in the appendix section. To access the *OneDrive* folder containing these materials, please refer to the link provided in thesis *appendix A.*

The findings from the research conducted over this chapter are listed below:

- 16 slag deposits were identified along Mexican territory, located in 11 out the 32 regions of the country. The cumulative mass of the 16 sites where mainly BOF and EAF slags are deposited is about 273 K tonnes. The region with the most slag deposits in Mexico is Coahuila, particularly the site operated by Altos Hornos de Mexico in the city of Coahuila, followed by Lazaro Cardenas site from ArcelorMittal in the region of Michoacan.

- The absence of conservation designations presents opportunities for the potential reutilization of slag heaps, such as for CO_2 sequestration or sustainable production of concrete, underscoring the importance of balancing ecological considerations with resource utilization goals. However, the sixteen sites studied are situated on private property within urban areas, and so any utilization plans must align with the interests of the steel manufacturers or governmental agencies operating the sites.

- As presented, the capturing potential of slag deposits could be approached from distinct views. By using the findings from Chapter II of this research, a realistic estimate

of the CO_2 captured in Mexican slags was completed, where the calculated CO_2 mineralised within Mexican slag heaps following this route was 5.7 Kt of CO_2. In a more theoretical approach based on the work from Riley et al. (2020) and Pullin et al. (2019), between 80.9 to 92.2 Kt of CO_2 could be sequestered through direct carbonation, while the projection of CO_2 captured using enhanced carbonation estimates that 115.4 – 159.7 Kt of CO_2 could be captured by these two routes if further developed in the country.

- The utilization of legacy iron and steel slags in Mexico could represent economic and environmental benefits. Through repurposing industrial waste into valuable materials, such as supplementary cementitious materials, there is a promising potential for reducing greenhouse emissions and mitigating the environmental impact of waste disposal, particularly in the concrete production sector. Moreover, the development of slag-based industries not only offers opportunities for job creation but also stimulates economic growth, especially in regions abundant in slag resources, such as Coahuila or Michoacan.

This study showed the significance of quantifying legacy slag deposits in Mexico for the formulation of efficient waste management plans and utilization methods. As an idea for future work, by continuing studying the properties and potential benefits of Mexican slags, particularly those made by electric arc furnaces, Mexico can promote recycling projects to make key industries more sustainable. This shows how important it is to keep exploring industrial waste and finding new ways to use slag to support the environment and economic growth.

References.

Abbott, M. (2019). Organizational structure, public policy, and technological change: the origins of the dominion steel industries. *Management and Organizational History*, *14*(3), 245–265. https://doi.org/10.1080/17449359.2019.1683039

CANACERO. (2019). *proceso_de_fabricacion_de_productos_siderurgicos_2019*.

CANACERO. (2024). *CANACERO*.

Chabrand, A. (2023). Industria siderúrgica en México, con potencial de crecimiento. *Mexico Industry*.

Congreso de la Unión México. (2023). *LEY GENERAL PARA LA PREVENCIÓN Y GESTIÓN INTEGRAL DE LOS RESIDUOS*.

González-Chavez, G. (2008). *El Estado y la globalización en la industria siderúrgica mexicana*.

González-Ortega, M. A., Segura, I., Cavalaro, S. H. P., Toralles-Carbonari, B., Aguado, A., & Andrello, A. C. (2014). Radiological protection and mechanical properties of concretes with EAF steel slags. *Construction and Building Materials*, *51*, 432–438. https://doi.org/10.1016/j.conbuildmat.2013.10.067

Google Earth Pro. (2024). *Google Earth Pro*.

Google Maps. (2024). *Google Maps*.

Hasanbeigi, A., Arens, M., Cardenas, J. C. R., Price, L., & Triolo, R. (2016). Comparison of carbon dioxide emissions intensity of steel production in China, Germany, Mexico, and the United States. *Resources, Conservation and Recycling*, *113*, 127–139. https://doi.org/10.1016/j.resconrec.2016.06.008

INEGI Mexico. (2013). *DR © 2013, Instituto Nacional de Estadística y Geografía*. www.inegi.org.mx

INEGI Mexico. (2016). *Perfil de la industria del hierro y del acero en México*. www.inegi.org.mx

López-Díaz, A., Ochoa-Díaz, R., & Grimaldo-León, G. (2018). Vista de Uso de escoria BOF y polvo de alto horno en concretos asfálticos_ una alternativa para la construcción de pavimentos _ DYNA. *DYNA*.

Martin, R., & De Melo, B. (2023). *GHG EMISSIONS OF ALL WORLD COUNTRIES JRC SCIENCE FOR POLICY REPORT*. https://doi.org/10.2760/235266

Mayes, W. M., Riley, A. L., Gomes, H. I., Brabham, P., Hamlyn, J., Pullin, H., & Renforth, P. (2018). Atmospheric CO2 Sequestration in Iron and Steel Slag: Consett, County Durham, United Kingdom. *Environmental Science and Technology*, *52*(14), 7892–7900. https://doi.org/10.1021/acs.est.8b01883

Mercado-Borrayo, B. M., González-Chávez, J. L., Ramírez-Zamora, R. M., & Schouwenaars, R. (2018). Valorization of Metallurgical Slag for the Treatment of Water Pollution: An Emerging Technology for Resource Conservation and Re-utilization. In *Journal of Sustainable Metallurgy* (Vol. 4, Issue 1, pp. 50–67). Springer Science and Business Media Deutschland GmbH. https://doi.org/10.1007/s40831-018-0158-4

Mesta, C., Kahhat, R., & Santa-Cruz, S. (2019). Geospatial Characterization of Material Stock in the Residential Sector of a Latin-American City. *Journal of Industrial Ecology*, *23*(1), 280–291. https://doi.org/10.1111/jiec.12723

Ozie Méndez Guerrero, D., Alicia Vázquez Méndez, B., & Álvarez Méndez, A. (2011). Obtención de un material vitrocerámico a partir de una escoria de acería mezclada con vidrio de desecho. *Boletin de La Sociedad Espanola de Ceramica y Vidrio*, *50*(3), 143–150. https://doi.org/10.3989/cyv.192011

Patronato Museo del Acero, A. C. (2024). *Museo Horno 3*.

Pauliuk, S., Milford, R. L., Müller, D. B., & Allwood, J. M. (2013). The steel scrap age. *Environmental Science and Technology*, *47*(7), 3448–3454. https://doi.org/10.1021/es303149z

Plumb, C. E. (1948). *Mexico's Steel Industry*.

Pullin, H., Bray, A. W., Burke, I. T., Muir, D. D., Sapsford, D. J., Mayes, W. M., & Renforth, P. (2019). Atmospheric Carbon Capture Performance of Legacy Iron and Steel Waste. *Environmental Science and Technology*, *53*(16), 9502–9511. https://doi.org/10.1021/acs.est.9b01265

QGIS. (2024). *QGIS*.

Reddy, K. R., Gopakumar, A., & Chetri, J. K. (2019). Critical review of applications of iron and steel slags for carbon sequestration and environmental remediation. In *Reviews in Environmental Science and Biotechnology* (Vol. 18, Issue 1, pp. 127–152). Springer Netherlands. https://doi.org/10.1007/s11157-018-09490-w

Riley, A. L., MacDonald, J. M., Burke, I. T., Renforth, P., Jarvis, A. P., Hudson-Edwards, K. A., McKie, J., & Mayes, W. M. (2020). Legacy iron and steel wastes in the UK: Extent, resource potential, and management futures. *Journal of Geochemical Exploration*, *219*. https://doi.org/10.1016/j.gexplo.2020.106630

Rojas-Sandoval, J., & Rodríguez, M. (1985). *HYLSA history*.

Sanchéz-Díaz, G. (2009). *Los orígenes de la industria siderúrgica mexicana_ Continuidades y cambios tecnológicos en el siglo XIX*.

Sellitto, M., & Kazuhiro, F. (2020). View of Destination of the waste generated by a steelmaking plant_ a case study in Latin America _ Aestimum. *AESTIMUM*.

Servicio Geológico Mexicano. (2024). *Servicio Geológico Mexicano*.

Snellings, R., & Scrivener, K. L. (2016). Rapid screening tests for supplementary cementitious materials: past and future. *Materials and Structures/Materiaux et Constructions*, *49*(8), 3265–3279. https://doi.org/10.1617/s11527-015-0718-z

Snellings, R., Suraneni, P., & Skibsted, J. (2023). Future and emerging supplementary cementitious materials. *Cement and Concrete Research*, *171*. https://doi.org/10.1016/j.cemconres.2023.107199

Suraneni, P., Hajibabaee, A., Ramanathan, S., Wang, Y., & Weiss, J. (2019). New insights from reactivity testing of supplementary cementitious materials. *Cement and Concrete Composites*, *103*, 331–338. https://doi.org/10.1016/j.cemconcomp.2019.05.017

Suraneni, P., & Weiss, J. (2017). Examining the pozzolanicity of supplementary cementitious materials using isothermal calorimetry and thermogravimetric analysis. *Cement and Concrete Composites*, *83*, 273–278. https://doi.org/10.1016/j.cemconcomp.2017.07.009

Ukwattage, N. L., Ranjith, P. G., & Li, X. (2017). Steel-making slag for mineral sequestration of carbon dioxide by accelerated carbonation. *Measurement: Journal of the International Measurement Confederation*, *97*, 15–22. https://doi.org/10.1016/j.measurement.2016.10.057

Yildirim, I. Z., Balunaini, U., & Prezzi, M. (2023). Strength-Gain Characteristics and Swelling Response of Steel Slag and Steel Slag–Fly Ash Mixtures. *Journal of Materials in Civil Engineering*, *35*(8). https://doi.org/10.1061/jmcee7.mteng-14823

Chapter IV. Utilisation of legacy iron and steel slag as sustainable construction materials.

4.1 Introduction.

The utilisation of iron and steel manufacturing slag in cementitious blends has increased in popularity in recent years. The acceptance of this material as an admixture for concrete is based on its hydraulic and pozzolanic reaction when $Ca(OH)_2$ is present in cement hydration. In addition, the abundance of iron and steel slag around the globe increases the feasibility of the material to be used as a supplementary component in cementitious blends. According to the World Steel Association's 2021 report, 200 to 400 kg of slag is produced per tonne of steel manufactured (World Steel Association, 2023). The utilisation of steel slag as Supplementary Cementitious Materials (SCM) will reduce the environmental impact of the concrete industry by promoting better management of steel manufacturing residues and improve Ordinary Portland Cement production (Snellings et al., 2023).

Ground granulated blast furnace slag (*GGBFS*) is regarded as a suitable material to incorporate into cementitious blends, as high performance of the mixtures is recorded in terms of durability, high strength over longer periods and denser microstructure (Moranville-Regourd et al., 2019). However, studies of other iron and steel slag variants such as Basic Oxygen Furnace (*BOF*), Blast furnace (*BF*), Electric Arc Furnace (*EAF*) slags showed a lower performance when included in construction blends, these relying on the material properties (Wang & Suraneni, 2019). It would be valuable to better understand the challenges of using BOF, BF and EAF as supplementary cementitious material (*SCM*) and to clearly identify the composition or characteristics that made them less suitable compared to GGBFS. In this way the structural limitations identified, such as: chemical composition imbalance or crystalline/amorphous nature, could be compensated with suitable additives and alkaline activators to equilibrate their performance as a cementitious option. Avoiding lower reactivity, hydraulic retardation or strength reduction and could benefit from the ~400 Kg of iron and steel slag generated per tonne of steel globally every year (World Steel Association, 2023).

In this chapter, the cementitious characteristics of various legacy iron and steel slag materials is assessed and involved the evaluation of reactivity and hydraulic behaviour through x-ray diffraction, calorimetry and thermogravimetric analysis. These methods are used to simulate and understand the kinetics of a concrete blend when slag is used as a SCM in a controlled environment.

The underpinning knowledge produced on the cementitious properties analysis of legacy BOF, BF and EAF slag will enable the identification of the characteristics to compensate in the implementation of passively carbonated iron and steel slag as a supplementary cementitious material (*SCM*) in sustainable concrete blends.

4.2 Literature Review.

4.2.1 Concrete fundamentals.

The widespread use of concrete as a building material relies on the adaptability this mixture showed during construction industry evolution and the understanding of the structural chemistry of the constituents within the composite blend (Z. Li et al., 2023). The most basic formula of concrete involves aggregates, binding materials, water and admixtures, all bound together resulting in a cementitious mixture, where the most common binder element is cement and the most used aggregates are crushed minerals, gravel, rocks or sand (Kurdowski, 2014).

Concrete is categorized according to the type of building or civil structure where it is implemented and the compressive strength required by each, for instance ultra-light and lightweight (*low compressive strength needed*) concrete is used for low grade constructions, and normal and heavy weight are used for reinforced structures (Kurdowski, 2014; Liska et al., 2019; Sims et al., 2019). Additional concrete classification involves specific functionalities resulting from the construction needs or the methods to be utilised (Liska et al., 2019), for example hydraulic or nor-hydraulic concrete classification derived from the type of cement (*binder*) used; in this case non-hydraulic concrete is the most common formula implemented since ancient times, while hydraulic concrete is a *"recent"* variation of the blend as the cement used gained strength when in contact with water (Wang, 2016a).

4.2.2 Ordinary Portland Cement.

While there are various types of concrete for different construction applications, the key part of all of them is the cementitious binder. The most used cement is Ordinary Portland Cement, formulated as in the 19th century, and since that moment its application haven been widespread worldwide, based on the enhanced mechanical properties and long-term stability shown under complex environments (Del Strother, 2019). The functionality of the Ordinary Portland Cement formula also gained acceptance as the most used as binder material in the construction industry, because of the adaptability shown when implemented over challenging infrastructure developments like buildings, bridges, roads, nuclear plants or dams (Del Strother, 2019; Herfort & Macphee, 2019; Kurdowski, 2014; Trout, 2019).

Composition of Portland cement mainly involves alumina, silica, calcium and sulfate, expressed theoretically as oxides, but this does not occur during the mixing reaction (Herfort & Macphee, 2019).

In the presence of water, those compounds chemically activate hydration reactions which directly impact on the strength capacity of cement and influence durability of the blend when hardened, also enabling shrinking and drying properties (Beaudoin & Odler, 2019).

4.2.3 Hydration reactions in concrete and cement.

The understanding of hydration reactions occurring on a concrete blend is still incomplete, because of the complex reactivity around tricalcium silicate (*3CaOSiO₂*) one of the main components of OPC, with a significant influence in the hydration dynamics of the blend and with a direct impact in the microstructural behaviour of the cementitious material (Liska et al., 2019). The hydration process is represented in *Reaction 5*, where the reactants, OPC mixed with water, react at ambient temperature to produce amorphous C-S-H (*calcium silicate hydrate*) and calcium hydroxide (Beaudoin & Odler, 2019).

Reaction 5.

$$3CaO \cdot SiO_2 + (3 + m - n)H_2O = nCaO \cdot SiO_2 \cdot mH_2O + (3 - n)Ca(OH)_2$$

Hydration reactions are fundamental to the understanding of cement and how this impacts concrete properties (Beaudoin & Odler, 2019; Kurdowski, 2014). The impact of properties such as the ratio between water and binding material, mixing techniques, properties of admixtures and aggregates like size, microstructural conditions or hardened capacity, are significant on concrete applications (Beaudoin & Odler, 2019).

Moreover, as construction science developed, aggregates and admixtures evolved accordingly, improving the mechanical properties of the concrete used in the modern era. For instance, knowledge of new supplementary cementitious materials such as globally abundant waste by-products like iron and steel slag, fly ash, limestone or silica fume contributes to building durability and positively impact the sustainability of concrete as the amount of Ordinary Portland Cement used is decreased (Sims et al., 2019; Snellings & Scrivener, 2016; Wang, 2016b).

4.2.4 Sustainability of concrete.

The construction industry has a significant impact on the environment, as the resource consumption required globally to fulfil the global demand for concrete continues growing (Snellings et al., 2023). Major issues identified in concrete production are energy intake, high volume of water use in the manufacturing process, greenhouse gas emissions (*mainly CO_2 released to the atmosphere*), and raw materials consumption for construction materials manufacture (*aggregates, admixtures, additives, etc*.).

To minimise virgin raw materials consumption and CO_2 emissions from Ordinary Portland Cement manufacture, feasible options on supplementary cementitious materials have been identified, which may allow continued development of the construction materials industry without compromising natural resources and the environment (Li et al., 2022). An example of cementitious material replacement in concrete formulation is the use of slag from iron and steel manufacturing, where ground granulated blast furnace slag (*GGBFS*) demonstrated good binding performance and durability properties, when mixed for concrete paste as part of a cement blend, based on high the alumina content of the SCM (Barabanshchikov et al., 2020; Moranville-Regourd et al., 2019).

4.2.5 Use of iron and steel slag in construction materials.

Iron and steel slag reutilisation throughout different sectors has increased in recent times. The interest in reutilising slag is because it is not only convenient as a waste management solution supporting reutilisation of metallurgical co-products, but it also contributes as an optimisation strategy to reduce mining and raw material consumption for infrastructural aims (Jiang et al., 2018; Thomas et al., 2018; Wang, 2016a, 2016b). Initial application of slag was mainly for construction purposes, but the constant increasing amounts of the stockpiled coproduct, and good performance recorded over concrete utilisation supported research ideas to increase core knowledge on the material and better regulate its utilisation (Brand & Fanijo, 2020). A key element of iron and steel slag utilisation relies on the composition of each slag type, as there are common properties all slag types have, regardless of the iron or steel manufacturing route that produce them. There are some distinctive variations each type has, related to production mechanisms and contrasting cooling conditions, determining the importance to conduct verification testing or individually design initial analysis for each slag type (Jiang et al., 2018; Wang, 2016a, 2016b; Wang & Suraneni, 2019).

Research on cementitious characteristics of iron and steel slag for construction applications are mostly centred on GGBFS, based on the good performance when implemented on cement batches, as findings indicated mechanical affinity over microstructural reactions strictly linked to strength gain and long-term durability related to high silicate and aluminosilicates composition (Wang, 2016a; Wang & Suraneni, 2019; Xu et al., 2023).

Knowledge gained over cementitious tests using GGBFS indicate a need to extend those analyses for cementitious properties of other iron and steel slag types widely, as the compressive strength and tensile characteristics of cement when using GGBFS and other variations of iron and steel slag are still uncertain based on the variable composition each slag type can provide (Donatello et al., 2010; McCarthy & Dyer, 2019).

This gap in the literature requires evaluation of the hydraulic response of slags from different iron and steel manufacturing backgrounds as SCMs to better understand how parameters like age, reactivity, fineness and inherent chemical composition of the material react at different concrete hardening stages. This enables an open perspective about the long-term properties of iron and steel by-products when implemented in concrete blends under normal environmental conditions and using common mixing techniques.

4.2.6 Testing supplementary cementitious properties of legacy iron and steel slag.

The study of iron and steel slag from different production and cooling contexts, requires the measurement of hydraulic and pozzolanic properties against existent evidence and methodologies on cementitious reactivity from similar compounds. Pozzolanic properties refer to the ability of a material, such as iron and steel slag, to react with calcium hydroxide in the presence of water, forming compounds with cement-like behaviour that contribute to stronger and more durable formulations (Donatello et al., 2010; Snellings & Scrivener, 2016; Tironi et al., 2013). In this regard, tests such as: Chappelle or Frattini, commonly used to assess pozzolanic activity on potential cementitious materials, are not considered feasible, as there is not enough experience evaluating calcium hydroxide consumption and hydraulic behaviour using these testing routes over iron and steel slag (Wang & Suraneni, 2019).

However, evaluation of the hydraulic behaviour and pozzolanic characteristics of GGBFS through the pozzolanic test enabled the utilisation of this testing route to evaluate feasibility on less studied iron and steel slag types and its further implementation as a SCM (Suraneni et al., 2019; Suraneni & Weiss, 2017; Wang & Suraneni, 2019).

The suggested pozzolanic test involves assessing the thermal capacity, pozzolanic behaviour, calcium hydroxide consumption, and mineral phase composition of iron and steel slag. This is done by creating model systems with cementitious characteristics and performing tests such as isothermal calorimetry and thermogravimetry to evaluate their reactivity and hydraulic response. These tests allow for the quantification of the heat released and the calcium hydroxide consumed, providing essential insights into the reaction kinetics of iron and steel slags. This helps establish a deeper understanding of how slags from different production contexts behave when mixed into cementitious pastes (Suraneni et al., 2019; Suraneni & Weiss, 2017; Wang & Suraneni, 2019).

Complementary qualitative x-ray diffraction testing is also suggested for phase identification and comparative composition analysis against steel slag data reported on literature (Snellings, 2016; Tironi et al., 2013).

The expected outcomes of the study are:

- to increase understanding of the properties of iron and steel slag samples with differing manufacturing and cooling circumstances.

- to contribute to the understanding and utilisation of pozzolanic model systems to evaluate cementitious characteristics on alkaline compounds and different types of iron and steel slag.

- to differentiate cementitious properties, suitable for cement utilisation, and limitations of iron and steel slag, suggesting feasible approaches to improve those deficiencies.

4.3 Methodology.

4.3.1 Materials and experimental methods.

The experimental methods for analysis on the feasibility of potential SCMs followed in this chapter were developed based on published the literature of Suraneni et al. (2017) and Wang et al. (2019). The approach followed involved the evaluation of the pozzolanic properties of the legacy BOF, BF and EAF iron and steel slag by conducting calorimetry and a thermogravimetric analysis on ten slag samples labelled from A to J. This provided a wide range of data to better understand how legacy slag from contrasting environments behaves as a SCM. Heat release (*J/g of SCM*) from the calorimetry test and calcium hydroxide consumption, reported as grams per 100 grams of supplementary cementitious material, resulted from thermogravimetric analysis are plotted to classify the pozzolanic and hydraulic characteristics of the tested legacy steel manufacturing slag used on the cementitious pastes, as per the method of Wang et al. (2019).

The analysis was performed using ten iron and steel slag samples from England, Mexico and Scotland. Context on the iron and steel slag origin was varied, as the ten samples derived from three production methods: Basic Oxygen Furnace (*BOF*), Blast Furnace (*BF*) and Electric Arc Furnace (*EAF*), providing a contrasting background on the sample's properties, suitable for the aims of the study. Confirmation on the iron and steel slag background (*type, age, location*) was supported by the analysis of historical records from the collection/original sites summarized in Table 8.

Table 8. Context of legacy iron and steel slag analysed for supplementary cementitious material potential in this study.

	Collection site	Iron and steel slag age	Iron and steel slag type
A	Ravenscraig, Scotland	1964-1990	Basic Oxygen Furnace (BOF)
B	Ravenscraig, Scotland	1964-1990	Basic Oxygen Furnace (BOF)
C	Monclova, Mexico	1999	Basic Oxygen Furnace (BOF)
D	Monclova, Mexico	2009	Basic Oxygen Furnace (BOF)
E	Barrow, England	1860-1983	Blast Furnace (BF)
F	Clydesdale, Scotland	1975-1991	Open-hearth/ Electric Arc Furnace (EAF)
G	Consett, England	1864-1980	Blast Furnace (BF)
H	Glengarnock, Scotland	1841-1985	Blast Furnace (BF)
I	Hodbarrow, England	1867-1968	Blast Furnace (BF)
J	Warton, England	1846-1929	Blast Furnace (BF)

Samples A and B were collected in November 2019 by selecting slag pieces from the surface layer of the slag deposit, chosen based on visible mineralization of atmospheric CO_2 on the external pores of the rock. Due to COVID-19 restrictions, no additional samples from Mexico were considered beyond samples C and D.

To ensure variety and meet the experimental objectives, samples E to J from England and Scotland were selected for their legacy characteristics and exposure to outdoor conditions in slag deposits. These samples were obtained from the repository of iron and steel slag collected by Dr John MacDonald, the primary supervisor of the research project. This approach ensured that all samples were representative of legacy mineral carbonation occurring naturally, without human intervention.

4.3.2 Historical context on legacy iron and steel slag studied.

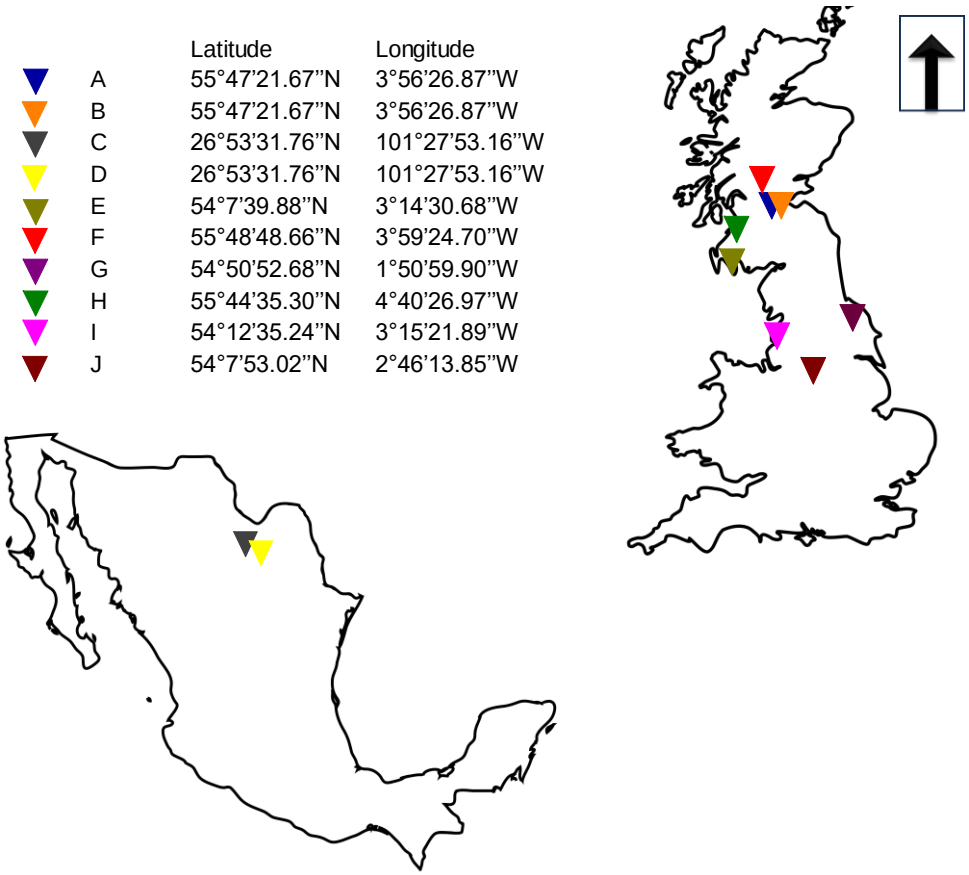

Figure 26 *Geographic context of legacy iron and steel slag collection sites in Mexico and the United Kingdom.*

Figure 26 provides illustrative context regarding the geographic locations of legacy iron and steel slag collection sites in Mexico and the United Kingdom. For instance, sample A and B were sourced between 1964-1990 at Ravenscraig Steel Works (Colvilles Ltd), a steel making company located in the Lanarkshire council near Motherwell, Scotland.

Ravenscraig Steel works installed Basic Oxygen Furnaces in 1964, as previously to 1964 they operated using the Open-Hearth steel making process; the site was closed in 1990 and demolished around 1996 (Hume, 2007; North Lanarkshire Council, 2023b, 2023a).

Mexican steel slag (*samples C and D*) was a donation from Altos Hornos de Mexico a steel manufacturing company located in the city of Monclova in the northern region of Coahuila, this company is the major producer of steel in Mexico since 1941. Sample C (*disposed of in 1999*) and sample D (*disposed of in 2009*) were produced using Basic Oxygen Furnace (Vélez et al., 2002). Samples E, G, H, I and J were produced in separate locations of Scotland and England using Blast Furnaces. Sample E (*1860-1983*) was collected from the slag banks of the Barrow Hematite Steel Company, situated in the city of Barrow in-Furness (*Cumbria*); one of the biggest steel making sites in the UK, closed in 1983 (Cumbria Archive and Local Studies Centre, 2018).

Sample G was collected in the former site of Consett Steel Works (*Derwent Iron Company*), established in 1864 at Consett, county of Durham in the north of England (Durham County Council, 2020); in this site blast furnaces were operated for over 140 years until the company's closure in 1980, although slag with variable pre-1980 age is still found in adjacent areas of the former steel making site (Mayes et al., 2018).

Pre-1985 BF iron slag gathered for sample H came from Glengarnock Steel Works, an iron and steel making company located in North Ayrshire, on the perimeter of Kilbirnie, Scotland; operations in the site started in 1841 and provided employment and development for the area until its closure in 1985 (Reade, 2013). Sample I was generated between 1867 and 1968 from the Hodbarrow Steel Works production, a prosperous site strategically located close to the Hodbarrow iron mine near Millom, England (Baker, 2023). BF slag stockpiled between 1846 and 1929 on the boundaries of the Warton Crag Local Nature Reserve derived on sample J, the former site of Carnforth Ironworks Company located in Carnforth (*Lancashire County in England*) is now a recreation area with views of the Morecambe Bay (Yates, 2022).

Electric Arc Furnace slag for sample F was collected on the former site of Clydesdale Steel Works in Coatbridge, Scotland; the slag was derived from steel manufacturing between 1975 and 1991, when electric arc furnaces were operated. The company established in the 19th century using open-hearth steel manufacture was known as Stewart and Lloyd's Clydesdale Works, which later evolved to the Clydesdale Iron and Steel Works and remained as Clydesdale Steel Works until its closing date in 1991 (Historic Environment Scotland, 2018).

4.3.3 Preparation of model system.

The ten representative legacy iron and steel manufacturing slag pieces were crushed to a particle size of under ~ 105 µm, and ~50 g of each sample labelled (*A-J*) was set aside for analysis. Water was removed by placing the samples in a hotbox oven (*Gallenkamp, hotbox oven temperature range: 0-200°C*) at ~60°C for 24 hours in advance of the pozzolanic test.

A fundamental step of the procedure involved the preparation of a model system (*Table 9*) emulating the natural reaction happening when a potential cementitious material is mixed with concrete. The model system composition should contain 3 parts of solid calcium hydroxide (*reagent grade*) and 1 part of supplementary cementitious material (*legacy BOF/BF/EAF ~105 µm*) to complete a 3 to 1 ratio solid mixture to be blended with liquid potassium hydroxide (*0.5M*) with a liquid to solid ratio of 0.9 (Suraneni et al., 2019; Suraneni & Weiss, 2017; Wang & Suraneni, 2019).

Table 9. Model system composition for pozzolanic analysis.

Chemical name of the component	Chemical formula of the component	Amount required per unit of paste mixture	Total, amount of component:
Calcium hydroxide	$Ca(OH)_2$	30 g	300 g
Potassium hydroxide	KOH	36 g	360 g
Supplementary cementitious material	Steel slag	10 g	100 g

**Balance used: Avery Weight-Tronix (MH-214)*

4.3.4 Isothermal calorimetry.

Preparation measures to complete in advance of calorimetry measurement involved setting the isothermal temperature on the calorimetry instrument 24 h before the experiment commenced. The temperature set for the experiment was 50 °C (Suraneni & Weiss, 2017). This action is done using the operative system (*Cal Commander v.2.20*) of the calorimeter (*I Cal 4000H*). In addition, preparation of the reference masses on the equipment is necessary, for the I Cal 4000H instrument this step is an automated action, but normally is related to the total weight of the sample paste to be analysed.

The model system paste was prepared using uniform conditions, instruments and material quantities for the ten cementitious pastes (*A-J*) involving the mixture of 30 g of Calcium Hydroxide (*Ca (OH)$_2$) + 10 g of legacy iron/steel slag (BOF/BF/EAF*). The solids were weighted on the precision balance first (*Avery Weight-Tronix (MH-214*) and then mixed manually on a plastic vial using a spatula, with both components presenting uniform consistency after 4 minutes of constant mixing. 36 g of Potassium Hydroxide (*KOH*) 0.5 M were added to the solid blend (*Ca (OH)$_2$ + legacy iron/steel slag*).

The KOH was set inside the calorimeter 2 hours in advance of the experiment to reach isothermal temperature of 50°C. The mixture of KOH + Ca $(OH)_2$ + legacy iron/steel slag (*BOF/BF/EAF*) was done manually for 4 minutes using a spatula; this step can be done using a vortex or ultrasonic mixer depending on the amount of model system to be prepared. Once the cementitious paste was well mixed, it was introduced into the calorimeter to run the 168-hour analysis.

The initial period (*minute: 45 to 60*) of the calorimetry test should not be recorded, as temperature inside the instrument should stabilize first. Initial data and cumulative heat released of the ten cementitious pastes mixed with legacy iron/steel slag were collected over 168h on the operative software (*Cal Commander v.2.20*) of I Cal 4000H, to assure trackability and enabling the analysis of the reactivity and potential legacy steel can be used as supplementary material on sustainable concrete.

4.3.5 Thermogravimetric analysis (TGA).

Once the calorimetry analysis was completed, between 20-50 mg of the model system pastes prepared for cementitious characterisation were taken for thermogravimetric analysis using TGA 8000 Perkin Elmer Thermogravimetric analyser within a thermometric interval of 23-600 °C in nitrogen purge atmosphere (Wang & Suraneni, 2019). TGA analysis generated the data to evaluate the hydration activity of each of the ten model systems as calcium hydroxide presence is detected between 350-550°C (Lothenbach et al., 2016; Scrivener et al., 2016)

TGA operative software (*Pyris V.13.4.0*) was used to quantify the weight loss differential indicating the presence of calcium hydroxide at a 350-550°C (*Reaction 6*) using the tangential method. During this procedure the 1st derivative plotting data from the ten model systems was also collected to calculate calcium hydroxide consumption using *Equations 7 to 9.*

Reaction 6.

$$Ca(OH)_2 \xrightarrow{\Delta} CaO + H_2O \text{ @ 350-550 °C}$$

Equation 7.

$$\text{Measured } Ca(OH)_2 = WL_{Ca(OH)_2} . \frac{m_{Ca(OH)_2}}{m_{H_2O}}$$

Where:

- Measured portlandite amount [(Ca $(OH)_2$]: is the measured calcium hydroxide @350-500 °C lost, based on literature at this temperature range (Suraneni et al., 2019; Suraneni & Weiss, 2017; Wang & Suraneni, 2019).
- WL Ca $(OH)_2$: is the weight loss of calcium hydroxide calculated by the tangential method on the plots.
- M Ca $(OH)_2$: is the molecular mass of calcium hydroxide.
- M H_2O: is the molecular mass of water.

Equation 8.

$$Ca(OH)_2 \text{consumption} = \text{MS mass } [\text{Initial } Ca(OH)_2 - \text{ Measured } Ca(OH)_2]$$

Where:

- [(Ca $(OH)_2$]: consumption is the amount of calcium hydroxide consumed from the model system mass.
- Model system mass: mass of the supplementary cementitious material model system, in this case 76g.
- Initial [(Ca $(OH)_2$]: calcium hydroxide initial mass from the model system total mass.
- Measured [(Ca $(OH)_2$]: calcium hydroxide measured mass @350-550°C.

Normalization for SCM units (g/100g SCM):

Equation 9.

$$\frac{Ca(OH)_2 \text{consumption}}{\text{mass of SCM}} = \frac{X}{100 \text{ g SCM}}$$

Where:

- [(Ca $(OH)_2$] consumption is the amount of calcium hydroxide consumed from the model system mass.
- mass of SCM is the mas of potential supplementary cementitious material used on the model system, in this case 10 g of legacy steel slag.
- X is the normalized amount of calcium hydroxide consumption per 100 g of supplementary cementitious material.
- 100g of SCM is the standard expression for potential supplementary cementitious materials (Suraneni et al., 2019; Suraneni & Weiss, 2017; Wang & Suraneni, 2019).

4.3.6 Qualitative x-ray diffraction analysis (XRD).

The study of crystallinity and amorphous characteristics on diffraction patterns from the legacy slag are key indicators of the supplementary cementitious properties the material can have when mixed with concrete. As a corroborative test for supplementary cementitious characteristics of the legacy BOF/BF/EAF, the ten pieces of iron/steel slag were ground and sieved to a size of <105 µm to perform qualitative x-ray diffraction (*XRD*) (*Malvern Panalytical Empyrean; Cu Kα radiation; reflection geometry 5-80°2Θ; step size 0.0131°*). Qualitative processing of diffraction patterns obtained from XRD was completed evaluating cementitious properties, commonly associated with amorphous humps along the diffraction patterns. In this case XRD data of legacy iron/steel slag presented crystallinity peaks indicating a limitation of the slag to be used in high quality concrete blends. Consistent with this first approach, a subsequent identification of mineral phases was completed, where certain peaks were selected for crystallographic analysis using High Score Plus software (*Malvern Panalytical B.V. version 5.1a (5.1.1.30138)*).

The crystallographic processing of x-ray diffraction patterns from legacy steel involved the following steps:

4.3.6.1 Determine background curve.

When XRD data is loaded on the software, the initial step is to determine a background curve. In this case the software will correct any noise automatically and will provide a guidance line to process the diffraction patterns and conduct phase identification. Background curve determination is dependent on bending and granularity factors, as these influence inflection points of the background curve; these were kept on default values suggested by the software to secure accurate results (*bending factor: 7; granularity: 20*).

4.3.6.2 Search peaks.

The following step is to localize the crystalline peaks over the diffraction pattern; this requires selection of the *search peaks* option and adjustment of parameters for this action to run (*Minimum significance: 1; minimum tip width gonio:01; maximum tip width gonio: 2; peal base width gonio:5; method: minimum 2nd derivative*). An optional action is to manually review each of the peaks of interest selected to assure quality control of the identified phases and avoid noise interference over the pattern.

This can be done by graphically zooming in on the peaks and adding or deleting when noise is mistaken by the software for crystalline peaks. The process is complete when a diffraction pattern curve fits into the background curve determined. There are automatic options provided by the software to increase the fit of both curves, and it is recommended to run this step to avoid error on the phase identification.

4.3.6.3 Phase identification.

The core step of the crystallographic analysis is based on the identification of the mineral phases associated with the peaks of interest previously selected. For this action to provide accurate results, a restriction set was implemented. The software facilitates different filters (*chemistry, quality, crystallography, strings, minerals, etc.*) to refine the peak matching. Diffraction patterns from the studied legacy iron/steel slag were analysed using chemical composition as a filter to complete phase identification. The elements provided to the software as guidance were Al, O, Ca, Fe, K, Mg, Na, S, Si, Ti, As, Ba, Cd, Co, Cr, Cu, Ni, Pb, Zn; these elements are constituents of minerals found in iron- and steel-making slags (Piatak et al., 2015). After this refinement is set, the matching between the peaks of interest selected and the mineral phase is complete, with the predominant phases identified and organised based on their matching score.

4.4 Results.

Cementitious properties of legacy iron and steel slag were evaluated through the experimental methods documented in Suraneni et al. (2019), Suraneni & Weiss (2017) and Wang & Suraneni (2019); in this literature, procedures testing the suitability of the material were described, as well as future research to be completed to better understand the utilisation of slagging compounds in concrete blends. The protocols followed in this research, took the above cited literature to test pozzolanic characteristics of the steel manufacturing slag, examining the performance of ten cementitious samples with a composition of 14% legacy iron/steel slag, 39% calcium hydroxide and 47% potassium hydroxide through calorimetry and thermogravimetric processes (Suraneni & Weiss, 2017).

Initial results showed limited hardening conditions of the mixture, compromising strength properties as a cementitious material. This indicated a need to conduct further experimental work to explore the chemistry of the cementitious blend, to then identify microstructural limitations related to crystalline nature and finally to compensate for those. This work aims to emulate amorphous characteristics and utilise legacy iron/steel slag as an aggregate for cementitious materials.

4.4.1 Qualitative x-ray diffraction analysis (XRD) results.

The main phases identified from x-ray diffraction data are summarized in Table 10. Calcite ($CaCO_3$) was identified on all ten-legacy iron and steel slag samples, followed by Akermanite ($Ca_2MgSi2O_7$), which was found in 9 out of 10 of the iron and steel manufacturing slag samples tested.

Table 10. Mineral phases identified by x-ray diffraction over legacy steel slag.

Mineral Phase	A	B	C	D	E	F	G	H	I	J
Akermanite ($Ca_2MgSi2O_7$)	x	x	x	x	-	x	x	-	x	x
Calcite ($CaCO_3$)	x	x	x	x	x	x	x	x	x	x
Gehlenite ($Ca_2Al_2SiO_7$)	-	-	-	-	x	-	-	-	-	-
Graphite (C)	-	-	x	-	-	-	-	x	-	-
Thaumasite ($Ca_3Si\ (OH)_6(SO_4)\ (CO_3)12H_2O$)	-	-	-	-	x	x	-	-	-	x
Quartz (SiO_2)	-	-	-	-	x	-	-	-	x	-
Periclase (MgO)	-	-	-	-	-	-	-	x	-	-

Figure 27 shows the characteristic peaks identified for calcite and akermanite between the 28-32 range on the scanning angle [2Θ (°)].

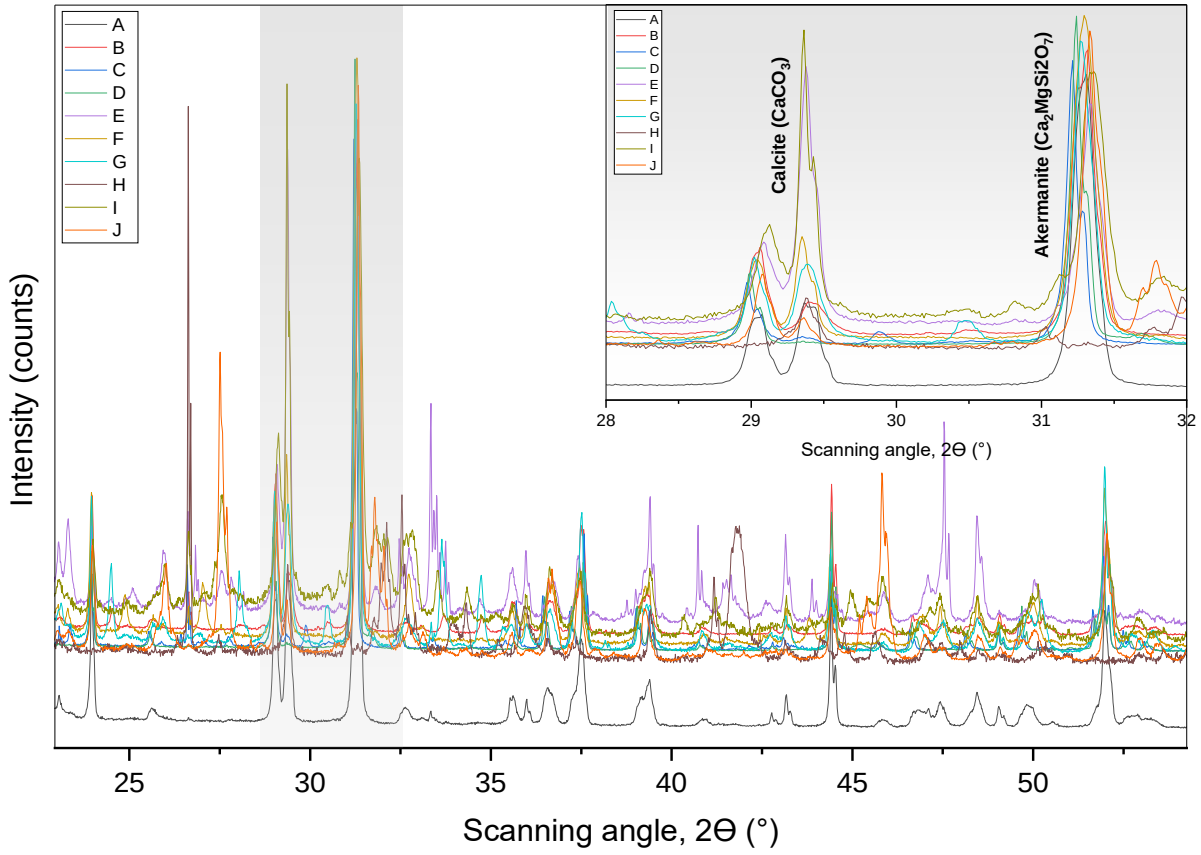

Figure 27 *Characteristic peaks of Calcite and Akermanite within diffraction patterns from XRD for samples A to J.*

Sample E presented Gehlenite ($Ca_2Al_2SiO_7$) instead, which is related to Akermanite as both are endmembers of the Melilite solid solution (Zadehnajar et al., 2021). Thaumasite ($Ca_3Si(OH)_6(SO_4)(CO_3)12H_2O$) was present in samples E, F and J. Less common mineral phases from the XRD analysis were Graphite (C), Quartz (SiO_2) and Periclase (MgO), although these three mineral phases are known in steel manufacturing by-products (Piatak et al., 2015). The ten-legacy iron and steel slags presented major crystalline peaks over the diffraction patterns, a clear signal of limited amorphous behaviour, which may reduce the cementitious properties of the tested material when mixed for construction aims (Snellings et al., 2023).

Figure 28 shows the diffraction patterns from the ten samples, with peaks annotated of the phases identified. In general, the samples showed a crystalline nature in the XRD results, with little in the way of 'humps' (*as opposed to peaks*) in the diffraction pattern (*Figure 28*). Characteristic peaks corresponding to Calcite ($CaCO_3$) were identified in the ten samples, and the calcite identified in the samples was derived from decadal carbonation (*slag weathering*) under natural environment conditions. A distinctive Akermanite ($Ca_2MgSi_2O_7$) peak was found in samples A, B, C, D, F, G, I, J over the 31-32 range on the scanning angle [2Θ (°)].

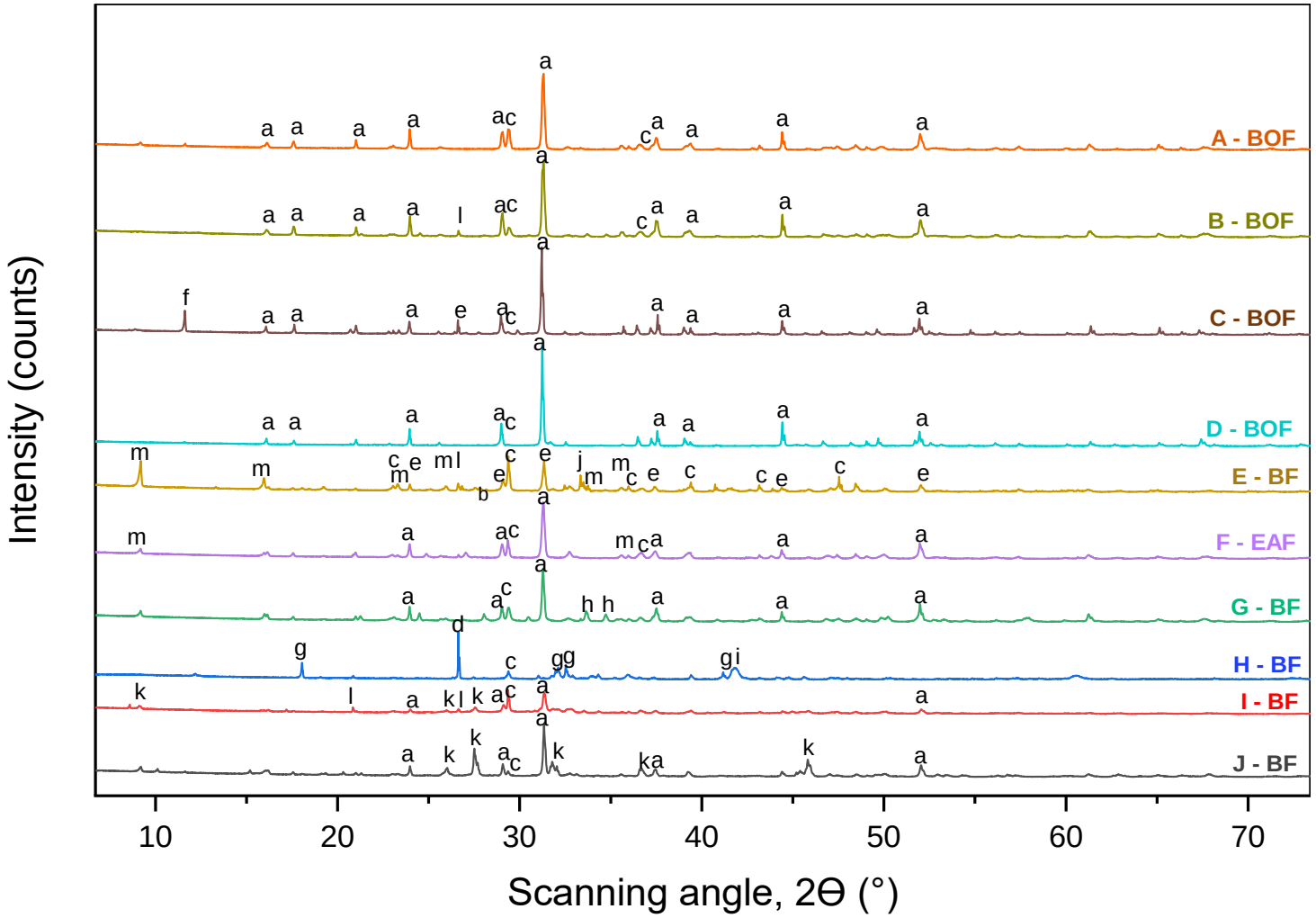

Diffraction patterns from samples A to J and identified phases:

a. Akermanite ($Ca_2MgSi_2O_7$)

b. Bornite (Cu_5FeS_4)

c. Calcite ($CaCO_3$)

d. Graphite (C)

e. Gehlenite ($Ca_2Al_2SiO_7$)

f. Gypsum ($CaSO_4$)

g. Larnite (β-Ca_2SiO_4)

h. Monticellite ($CaMgSiO_4$)

i. Periclase (MgO)

j. Perovskite ($CaTiO_3$)

k. Pseudo-wollastonite (Ca-$OSiO_2$)

l. Quartz (SiO_2)

m. Thaumasite ($Ca_3Si(OH)6(SO_4)(CO_3)12(H_2O)$

Figure 28 *Qualitative x-ray diffraction analysis (XRD) for BOF, EAF, BF.*

Samples E and H did not show traces of Akermanite, instead sample E showed the presence of Gehlenite ($Ca_2Al_2SiO_7$) and sample H showed Larnite (β-$Ca2SiO_4$).

Basic Oxygen Furnace slag samples (*labelled A to D*) have similar diffraction patterns, with Akermanite and Calcite present, as well as minor crystalline peaks corresponding to Quartz (SiO_2), Graphite (C) and Gypsum ($CaSO_4$) identified on samples B and C.

In sample F (*Electric Arc Furnace Slag*) crystalline peaks associated with Calcite were minor, Akermanite was the main phase identified over the selected peaks of interest, as well as Thaumasite ($Ca_3Si\ (OH)_6(SO_4)\ (CO_3)12H_2O$) which was also identified in sample E (*BF*).

Blast Furnace Slag (*samples labelled E, G, H, I, J*) showed greater diversity of mineral phases over the XRD crystalline peaks. The diffraction pattern of sample E showed a crystalline behaviour, from which Thaumasite ($Ca_3Si\ (OH)_6(SO_4)\ (CO_3)12H_2O$), Calcite ($CaCO_3$), Gehlenite ($Ca_2Al_2SiO_7$), Quartz ($SiO_2$), Bornite ($Cu_5FeS_4$) and Perovskite ($CaTiO_3$) peaks were also identified. Peaks associated with Akermanite and Calcite were identified in samples G, I and J but not in sample H. Sample G presented distinctive Monticellite ($CaMgSiO_4$) peaks. Sample H recorded Larnite (β-$Ca2SiO_4$), in addition to Graphite and Periclase (MgO). Samples I and J contained Akermanite, Pseudo-wollastonite ($CaOSiO_2$) and Calcite ($CaCO_3$) as well as Quartz.

4.4.2 Isothermal calorimetry results.

Heat flow of the ten legacy slag samples (*A-J*) are shown in Figure 29. The main hydration peaks for samples collected in England and Scotland were recorded within the first 3 hours of the 168h isothermal calorimetry test in a 50°C environment. A distinct hydration peak from samples C and D (*originated in Mexico*) was identified between 29-31 hours, exceeding previous values recorded and setting the highest peak over the heat flow measurement of the ten-legacy iron & steel slag samples. These higher hydration peaks measured in the Mexican samples (*C & D*) might be derived from a sulfate imbalance, normally occurring after 28h of the test beginning (Wang & Suraneni, 2019) and caused by a large amount of $C_{12}A_7$ release, which delayed the dissolution of silicate compounds. An additional explanation might be composition differences originated during BOF production or based on the cooling process followed after.

Although samples A and B come from the same production method as samples C and D, samples A and B did not show retardation in hydration peaks, whereas samples C and D did. This suggests that local conditions may have influenced the chemistry of the slag.

The highest to lowest hydration peaks measured are: D > C > I > F > H > E > J > A > B > G.

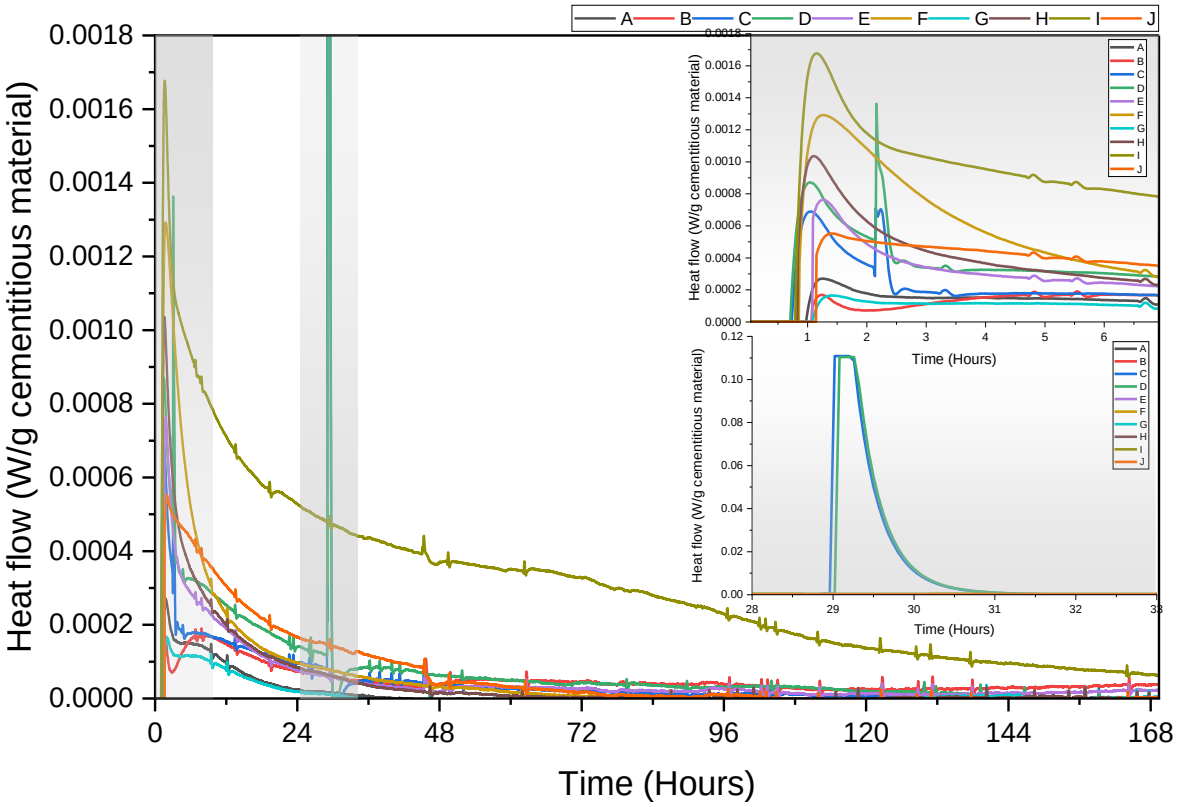

Figure 29 Heat flow of model systems using legacy iron and steel slag on isothermal calorimetry at 0-168h; 2-3h; 27-31h at 50°C.

The measurement of cumulative heat release in potential supplementary cementitious materials reflects the reactivity of the material within a cementitious blend (Suraneni et al., 2019). A higher cumulative heat release indicates greater reactivity, which contributes to a more effective hydration process (Pang et al., 2022; Xu et al., 2023).

The measurement of this parameter in mortars using legacy slags is an indicator of the suitability of blend to replace Portland cement, and its potential to enhance mechanical strength and durability in concrete applications (Wang & Suraneni, 2019). According to the classification of Wang et al. (2019) cumulative heat release also reflects the pozzolanic activity of the material, parameter used to assess the suitability of legacy slags for concrete applications.

Figure 30 shows cumulative heat release between the ten-legacy iron and steel slag samples analysed under isothermal calorimetry, where sample I (*Hodbarrow, England, between 1867-1968*) showed the highest heat released during the isothermal calorimetry test, while sample G (*Consett, England, 1864-1980*) showed the lowest heat released value of 6 J/g of SCM.

Samples C and D from Monclova, Mexico, deposited in 1999 and 2009 respectively, showed an above average exothermic behaviour (*with 88.27 and 103 J/g of SCM respectively*) if compared to other BOF such as sample A and B, which were classified as the lowest exothermic samples of this analysis as their measurement was between 8 to 15 J/g of SCM. Samples F (*EAF*) and J, H, E (*BF*) presented heat release between 20 to 38 J/g SCM. Overall, heat released from the ten-legacy iron and steel slag can be summarized from highest to lowest as: I > D > C > J > F > H > E > B > A > G.

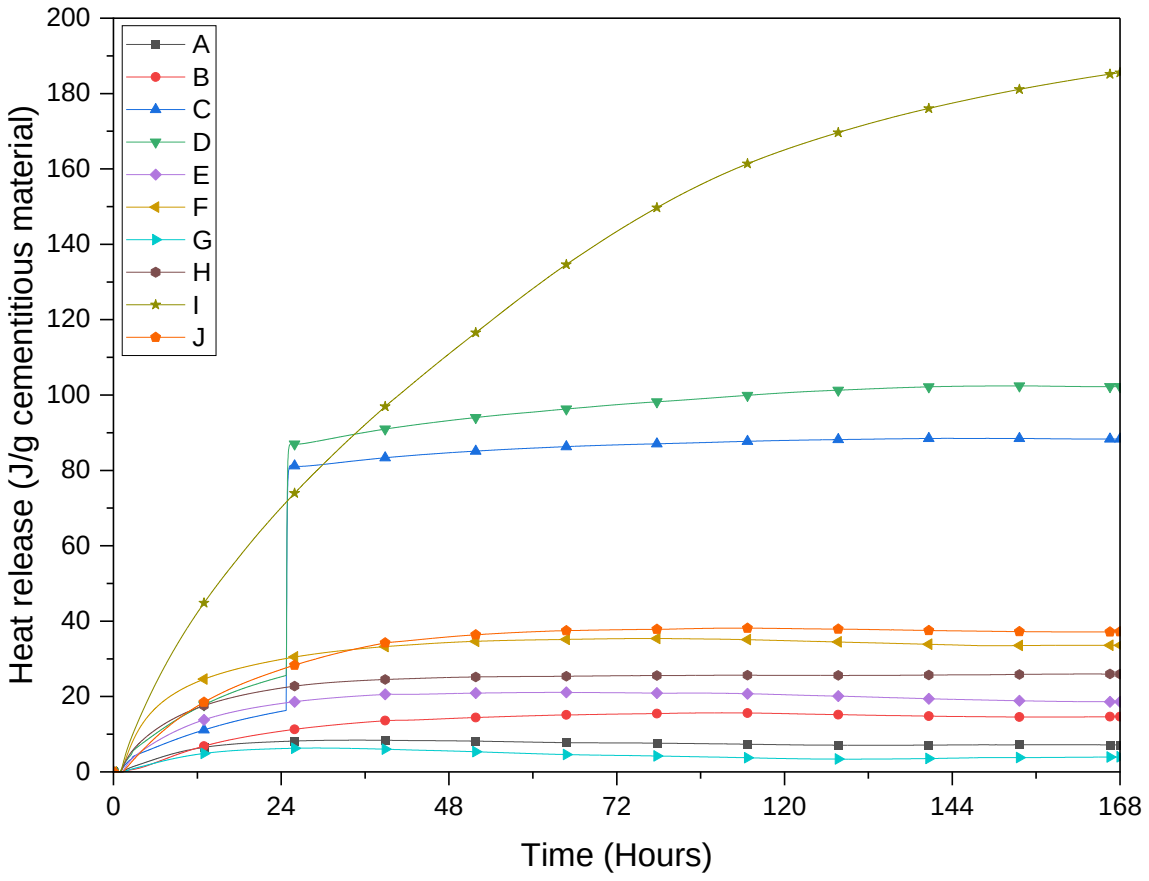

Figure 30 *Cumulative heat release (J/g) of model systems using legacy iron and steel slag during isothermal calorimetry at 50°C.*

Heat release results were between 6-185 J/g of SCM for samples A to J and are presented on Figure 31.

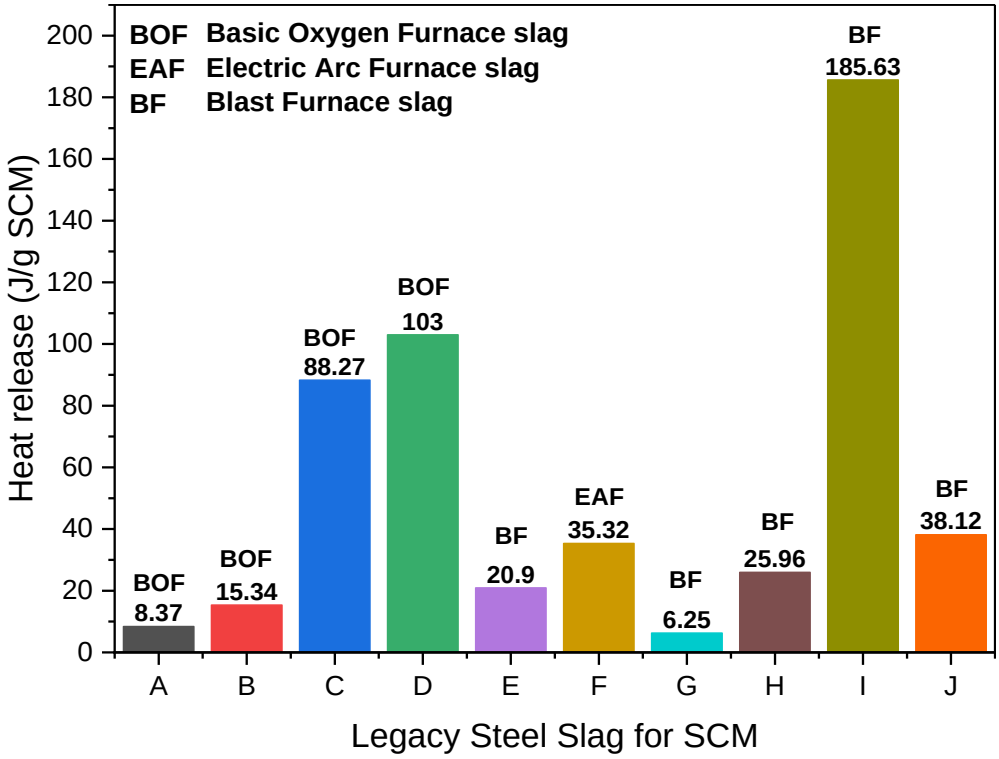

Figure 31 *Maximum values of heat release (J/g) of legacy iron and steel slag from isothermal calorimetry at 50°C.*

4.4.3 Thermogravimetric analysis (TGA).

Calcium hydroxide consumption was measured on model systems using legacy iron and steel slag as a potential supplementary material. Overall results from thermogravimetry indicate low reactivity from the tested cementitious blends with $Ca(OH)_2$ formation on 60% of the cementitious models. A ±5% to ±10% relative error was applied to the experimental procedure performed, following the documented methods from Scrivener et al. (2016) and Lothenbach et al. (2016) for the model system preparation and TGA performance.

Figure 32 shows the evolution of the cementitious paste across temperature rising resulted from the thermogravimetry test, showing similarity between samples in the weight percentage loss curves (Figure 32a) and dihydroxylation peaks (Figure 32b), with the only notable difference being in sample C (BOF) where a low reactivity was recorded in the experiment. Section (a) of the figure indicates the $Ca(OH)_2$ weight loss in terms of molecular H_2O of the ten legacy iron and steel slag model systems tested occurred between 350-550°C, consistent to data recorded in Suraneni et al. (2019),Suraneni & Weiss (2017) and Wang & Suraneni (2019).

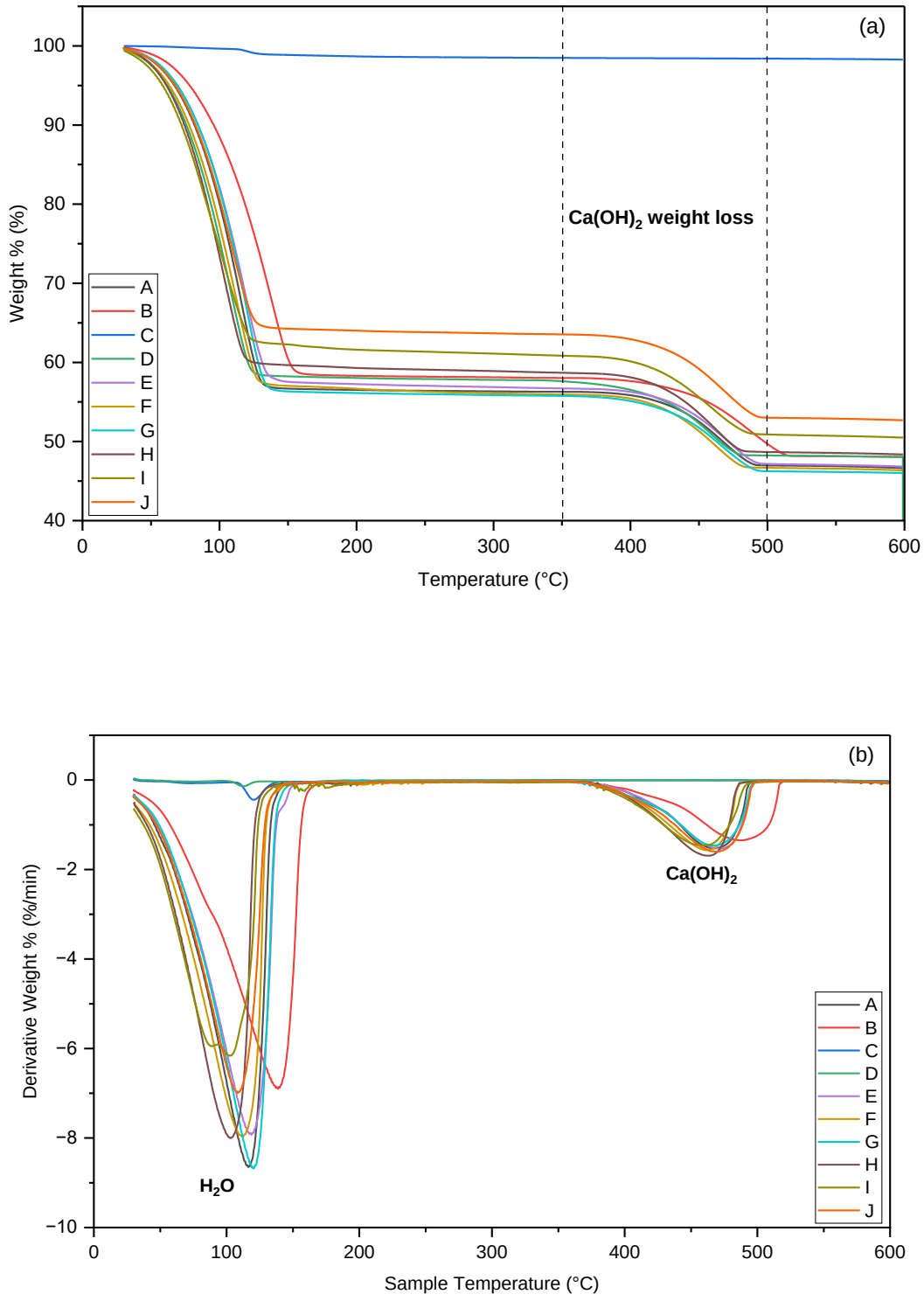

Figure 32 *Thermogravimetric analysis of model systems using legacy iron and steel slag, Ca $(OH)_2$ weight loss between 250-550°C (a); dihydroxylation peaks (H_2O/Ca $(OH)_2$) (b).*

Model systems using Blast Furnace iron slag as cementitious components presented higher weight loss measurements with an average of 10.05%, followed by the model system using Electric Arc Furnace slag (average weight loss= 9.38%) with Basic Oxygen Furnace slag model systems as the lowest dehydroxylated classified with an average of 7.16%. Section (b) of Figure 32 shows the derivative weight calculated per minute across temperature from TGA, where dihydroxylation peaks of the cementitious model systems indicate weight loss related to pore H_2O at 100-130°C and molecular H_2O bound to calcium hydroxide at 350-550°C.

Percentage of weight loss differential was calculated as delta “Y” using Pyris V.13.4.0 operative software, where the mass difference expressed in percentage units at 350-550°C were between 0.144% to 10.674%. The recorded data are summarised in Table 11.

	A	B	C	D	E	F	G	H	I	J
Delta Y	9.128%	9.790%	0.1444%	9.595%	9.680%	9.375%	9.619%	10.130%	10.159%	10.674%

Table 11. Weight loss percentage between 350-550°C on ten model systems after TGA.

Thermogravimetric analysis for each of the model systems (A-J) are presented on Figure 33, where inflection peaks over the 1st derivative weight loss curves denoted pore and molecular H_2O bound to $Ca(OH)_2$.

Delta "Y" represents the differential percentage of weight loss observed in the thermogravimetric analysis (TGA), calculated using Pyris V.13.4.0 software. It refers to the change in mass, expressed in percentage units, across the temperature range of 350-550°C, which is associated with the decomposition of calcium hydroxide ($Ca(OH)_2$) and the release of molecular H_2O bound to it. This calculation allows for quantifying the weight loss due to dihydroxylation and is important for analysing the hydration and thermal stability of the cementitious model systems. In this study, the delta "Y" values for the slag samples ranged from 0.144% to 10.674%, as shown in Table 11. These values provide insight into the variability of the $Ca(OH)_2$ content and hydration characteristics among the different slag samples tested.

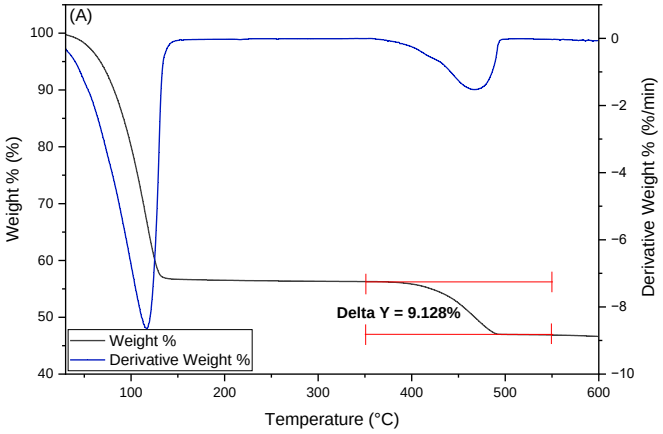
(A)
Weight % (%)
Derivative Weight % (%/min)
Temperature (°C)
Delta Y = 9.128%
Weight %
Derivative Weight %

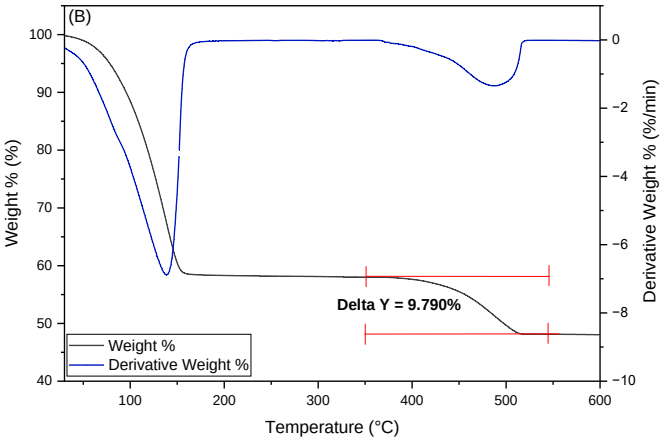
(B)
Weight % (%)
Derivative Weight % (%/min)
Temperature (°C)
Delta Y = 9.790%
Weight %
Derivative Weight %

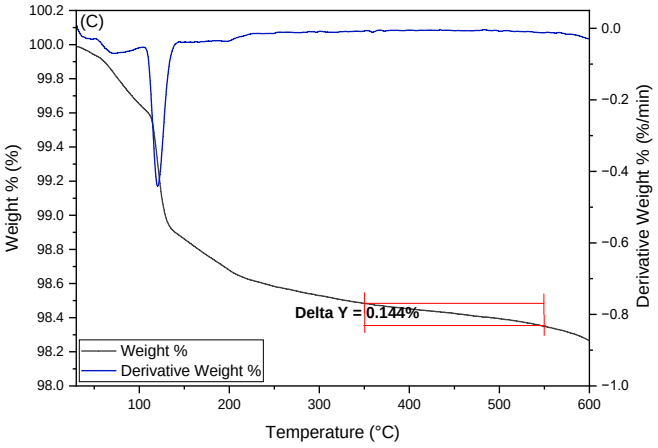
(C)
Weight % (%)
Derivative Weight % (%/min)
Temperature (°C)
Delta Y = 0.144%
Weight %
Derivative Weight %

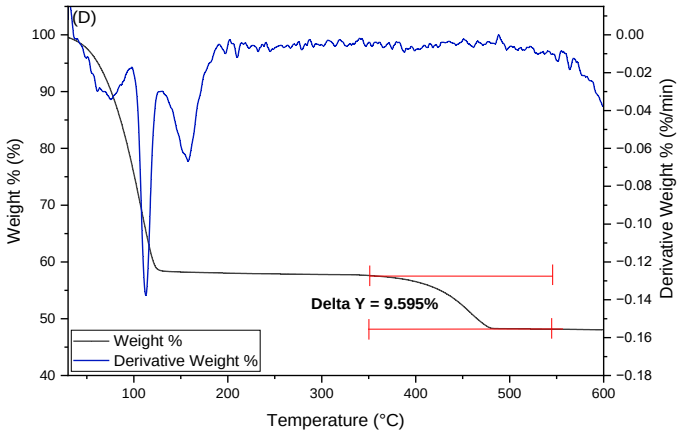
(D)
Weight % (%)
Derivative Weight % (%/min)
Temperature (°C)
Delta Y = 9.595%
Weight %
Derivative Weight %

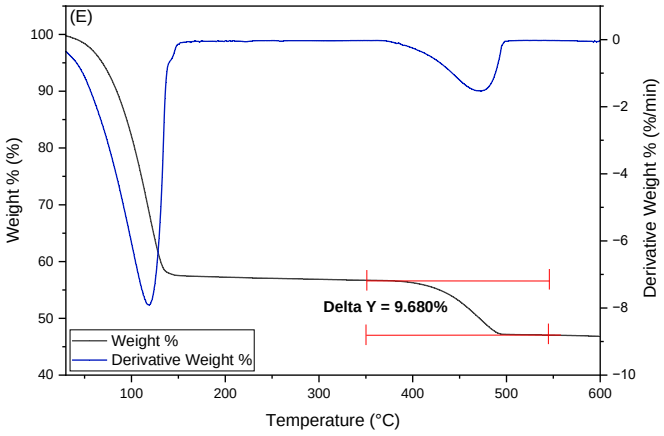
(E)
Weight % (%)
Derivative Weight % (%/min)
Temperature (°C)
Delta Y = 9.680%
Weight %
Derivative Weight %

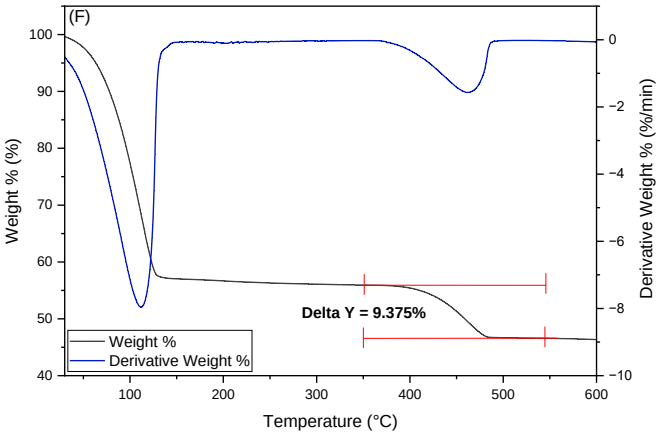
(F)
Weight % (%)
Derivative Weight % (%/min)
Temperature (°C)
Delta Y = 9.375%
Weight %
Derivative Weight %

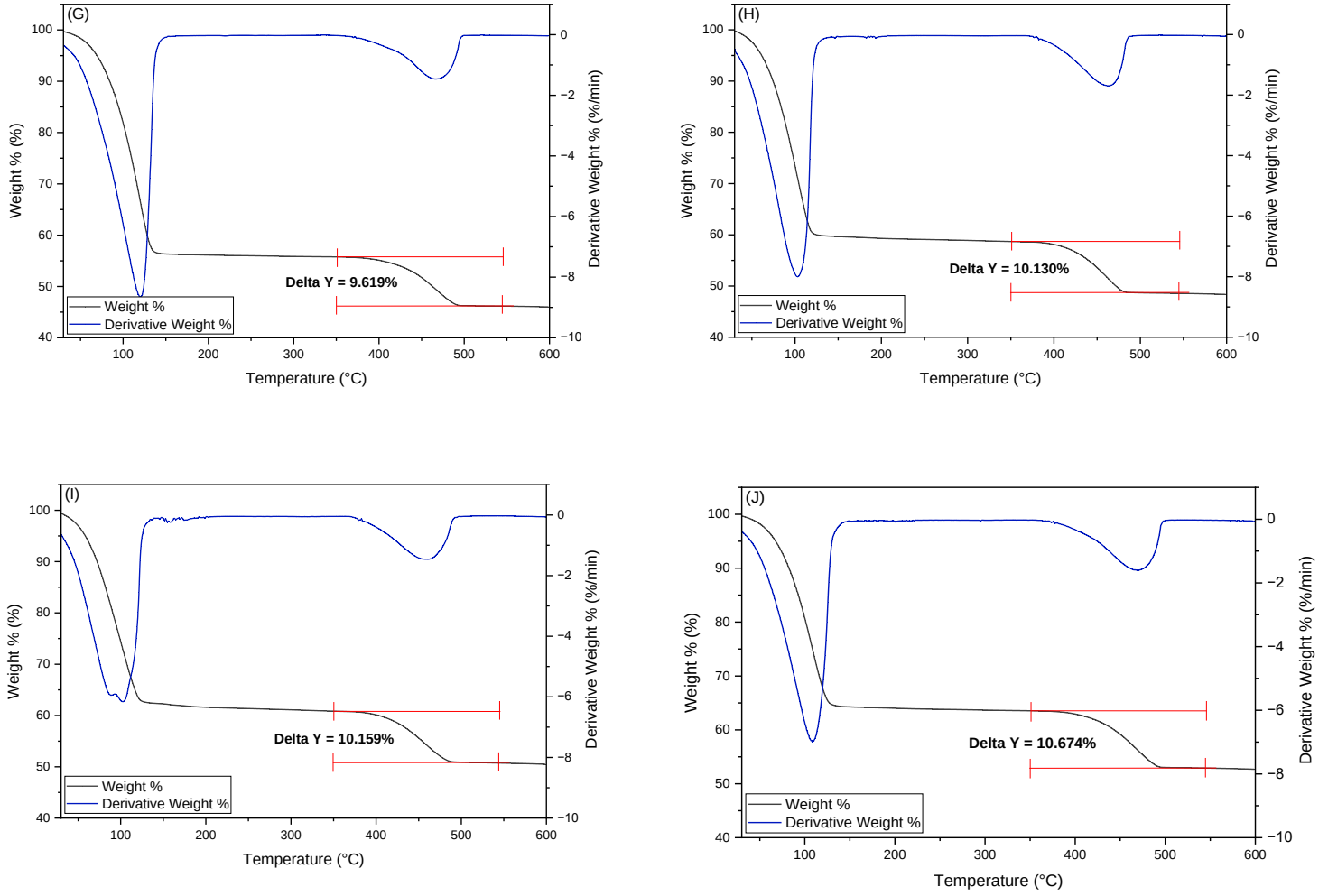

Figure 33 *Thermogravimetric analysis of legacy iron and steel slag. Tangential method applied on weight loss %.*

Table 12 summarises the calcium hydroxide consumed after thermogravimetry on the ten model systems (A-J) using legacy iron and steel slag as supplementary material.

Table 12. Calcium hydroxide consumption of the ten model systems using legacy iron and steel slag.

	A	B	C	D	E	F	G	H	I	J
CH for the ten samples. In g/100g of SCM	14.82	-5.852	295.5	0.228	-2.432	7.068	-0.532	-16.492	-17.404	-33.5312

4.4.4 Heat release and calcium hydroxide consumption on model systems using legacy iron and steel slag as a potential cementitious material.

Classification of the results involved the scheme proposed by various authors, such as: Suraneni & Weiss (2017), Suraneni et al. (2019) and Wang & Suraneni (2019), where five studied segments (*inert-not reactive, pozzolanic less reactive, pozzolanic more reactive, latent hydraulic less reactive or latent hydraulic more reactive*) provide the boundaries for the results to be organised based on the heat released, and using calcium hydroxide consumption as a secondary parameter. The ranges and reactivity generalities for supplementary cementitious materials classification are observed on Table 13.

Table 13. Pozzolanic classification parameters based on heat release and calcium hydroxide consumption (Suraneni et al., 2019; Suraneni & Weiss, 2017; Wang & Suraneni, 2019).

Classification	Reactivity	Calcium hydroxide consumption (g/100g SCM)	Heat release (J/g SCM)
Inert	Not reactive	0-50	0-120
Pozzolanic	Less reactive	40-100	200-370
	More reactive	100-180	400-750
Latent hydraulic	Less reactive	0-20	150-250
	More reactive	20-50	370-550

Figure 34 show the response of legacy iron and steel slag to pozzolanic tests (*isothermal calorimetry + thermogravimetry*) evaluating potential cementitious properties for its utilisation in sustainable concrete. Heat released and consumed calcium hydroxide of the ten model systems using BOF, EAF and BF iron and steel slag were plotted to better understand the pozzolanic behaviour of the legacy slags. Inert conditions were found on 8 of 10 model systems (*A, B, D, E, F, G, H, J*) where heat release was between 6 to 103 J/g SCM. Calcium hydroxide consumption was variable, with negative values on samples B, E, G, H, I, J, meaning $Ca(OH)_2$ was generated during the pozzolanic test. Sample F, the single Electric Arc Furnace slag was classified as inert (not reactive) although it had $Ca(OH)_2$ consumption (*7.068 g/100g SCM*) during the analysis, but heat released under isothermal calorimetry was lower (*35.32 J/g SCM*). Sample D was also considered inert, although reactivity on the model system was found; heat released was ~103 J/g of SCM, above the average measurement from the ten samples and within the three high-exothermic model systems analysed, calcium hydroxide consumption was low with 0.228 g/100 g SCM.

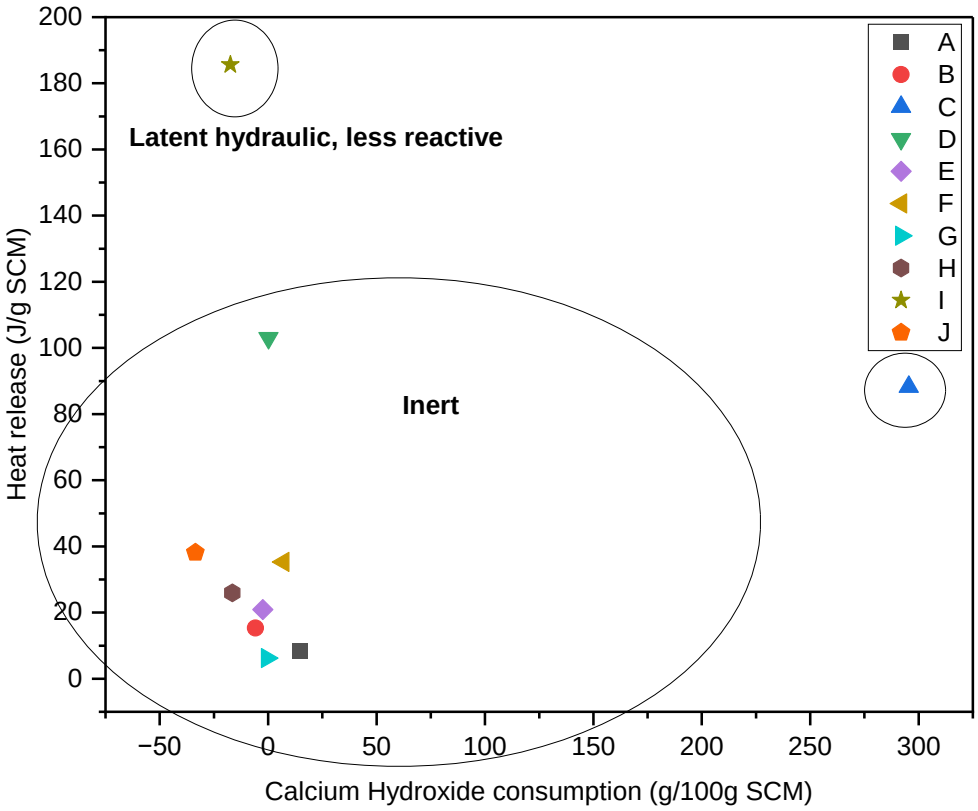

Figure 34 *Results of pozzolanic test on model systems using legacy iron and steel slag for SCM utilisation. Circles and labels show classification in terms of Wang et al. (2019) work.*

Sample C showed out-of-the-boundaries behaviour in terms of calcium hydroxide consumption with 295.5 g/100g of SCM, as expected ranges suggested 180 g/100g SCM as the higher limit (Suraneni et al., 2019). However, heat release on the sample was under the classification boundaries with 88.27 J/g SCM. Although the model system using sample I (*Hodbarrow, England*) generated calcium hydroxide during TGA (*-17.404 g/100g SCM*), the system was classified as “latent hydraulic, less reactive” based on the higher exothermic reactivity with a heat release of 185.63 J/g SCM during calorimetry test.

4.5 Discussion.

The aim of this section is to contextualize the findings presented in section 4.4.4 of this chapter to determine if hydraulic behaviour and pozzolanic potential of the legacy iron and steel slag studied is determined by their backgrounds. Results presented in section 4.4.4 in reference to model systems made using three types of legacy iron & steel slag, Basic Oxygen Furnace slag (*samples A, B, C, D*), Electric Arc Furnace slag (*sample F*) and Blast Furnace slag (*sample E, G, H, I, J*) indicated limited pozzolanic properties and poor hydraulic characteristics on 8 out of 10 of the model systems using legacy iron and steel slag; this enabled a discussion around how isothermal calorimetry, thermogravimetry and x-ray diffraction analysis were key to evaluate if representative legacy slags from England, Mexico and Scotland were suitable for sustainable concrete utilisation.

4.5.1 Evaluation of crystalline nature of BOF, BF and EAF iron and steel slag using x-ray diffraction.

Qualitative x-ray diffraction was performed to understand the mineralogy of legacy iron and steel slag as the resulting abundance on crystalline peaks on the diffraction patterns indicated possible expansive behaviour and hydration tendance (Wang & Suraneni, 2019), deteriorative properties that directly impact the strength of the concrete blend. When studying cementitious properties on possible supplementary materials, amorphous behaviour on XRD patterns is expected (Wang & Suraneni, 2019); in this way less porosity is assured, and strength parameters are fulfilled. Figure 29 indicates crystalline behaviour over BOF, BF and EAF peaks analysed, implying further quantitative XRD is needed to determine the relative concentration of each crystalline phase within the slag samples. Knowledge on the quantity of each crystalline phase in the samples would enable better understanding of the mineralogy of the slags, and to further compensate potential structural limitations like crystal structure, porosity or particle size distribution (Jiang et al., 2018; Mattila et al., 2012). Addressing these limitations would avoid poor hydraulic and pozzolanic properties when the iron and steel slags (*BOF, BF, EAF*) are in mixtures for sustainable construction materials.

4.5.2 Does the age of BOF, BF and EAF slag determine cementitious properties when used on concrete blends?

Age influences the cementitious characteristics of iron and steel slag when used on concrete blends, as a longer exposure of stockpiled slag under outdoor conditions might originate inner chemistry reactions interfering with initial properties of the slag after being produced (Akhil & Singh, 2023). An example of age influencing chemistry of iron and steel slag is mineral weathering (Mayes et al., 2018), where leachates are generated over extensive periods of close contact between pluvial sources and piled slag, enabling metal release and causing environment modifications (Petitjean et al., 2021). Therefore, discussion of pozzolanic and hydraulic reactivity data is needed to better understand if cementitious characteristics of steel slag might be determined by the material age when used on concrete blends.

Historical records from sample collection sites, indicating the year of production for each slag, were used to categorize the results from the pozzolanic assessment performed on the ten model systems (A-J) and to identify correlations between the age of the slag and its cementitious properties when studied as an SCM. As a result, the tested model systems were categorized from older to newer: [*J (1846-1929) > I (1867-1968) > G (1864-1980) > E (1860-1983) > H (1841-1985) > A & B (1964-1990) > F (1975-1991) > C (1999) > D (2009)*].

A correlation between age and slag production method was found, as model systems using samples J, I, G, E and H were classified as the older from the study (*the 5 of them originated on 20th century*) and were produced using blast furnaces. This indicates similarities on the slag properties and homogeneous behaviour when tested for pozzolanic characteristics. In fact this was shown as a comparative between the BF slag in terms of calcium hydroxide consumption, with results indicating that BF samples J (*-33.53 g/100g of SCM*), I (*-17.40 g/100g of SCM*), G (*-0.53 g/100g of SCM*), E (*-2.43 g/100g of SCM*) and H (*-16.49 g/100g of SCM*) showed negative consumption patterns of calcium hydroxide after analysing TGA results; this behaviour on cementitious blends containing BF slag is not uncommon and is associated with the presence of $Ca(OH)_2$ crystals bounded to the slag, derived from production method and material exposure over time to outdoor conditions (Akhil & Singh, 2023). This could be indicative of age influencing slag properties when tested for pozzolanic and hydraulic reactivity, as 4 out of 5 model systems prepared with less aged slag (*A, C, D, F*) presented $Ca(OH)_2$ consumption consistent to Suraneni et al. (2017).

4.5.3 The use of Isothermal calorimetry and thermogravimetry to evaluate pozzolanic properties of three types (*BOF, BF and EAF*) of legacy iron and steel slag for cementitious application.

Although iron and steel slags are derived from steel making, each slag type has their own inherent mineralogical properties and composition based on the production method used (*BF, BOF, EAF*), cooling conditions or post-processing actions; these characteristics make each type of slag behave differently when wider applications are studied, e.g., the cementitious capacity of BOF, BF or EAF when mixed with a binder element for a concrete blend. In this regard, the following section explored the results from section 4.4.4 and the influence of slag type and their pozzolanic characteristics.

4.5.3.1 Basic Oxygen Furnace slag.

While heat release from Basic Oxygen Furnace slag samples A, B, C and D was expected to be around 217 J/g SCM as found by Wang et al. (2019) for other BOF slags, the results observed were below the cited amount, as the released heat by the model systems was recorded between 8-15 J/g SCM for samples A and B, BOF slag collected in Ravenscraig, Scotland with over ~ 50 years of age. Also originated on a Basic Oxygen Furnace, sample D showed a 103 J/g of SCM of released heat. Lower heat release values in mortars using iron and steel slags can be attributed to their chemical composition and reactivity (Pang et al., 2022). In this case, samples A, B, and D might contain higher amounts of crystalline phases and lower amorphous content, as shown in the XRD results. A higher amorphous content directly influences a faster hydration process, resulting in higher heat release values, such as those recorded by Wang et al. (2019). Another factor that might contribute is the slower hydration kinetics (Weise et al., 2021). Contrary to sample A and B, sample D was collected at Monclova, Mexico where it was stockpiled for only ~10 years. Steel slag sample C from Monclova, Mexico (*aged 20 years*), showed results on heat release tested within the three top model systems with 88.27 J/g SCM and showed the highest calcium hydroxide consumption of the ten model systems with 295.5 g/100g SCM.

The amount of calcium hydroxide consumed by sample A and D did not meet the required levels for concrete utilisation, but was within the boundaries found by Suraneni et al., (2019) where average $Ca(OH)_2$ consumption on studied BOF was around 5 g/100g SCM. Sample B presented a formation of Ca $(OH)_2$ during thermogravimetric analysis, which is common for BOF slag (Wang & Suraneni, 2019), meaning poor compressive strength characteristics gained when used for concrete blends (Avet et al., 2016).

Consumption of calcium hydroxide correlates to compressive strength gain, and higher $Ca(OH)_2$ consumption equates to higher compressive strength of the concrete mixture (Snellings et al., 2023; Wang & Suraneni, 2019). In this case as calcium hydroxide was generated instead of consumed, the compressive strength of the mixture is poor, resulting in a low-quality rating for being implemented as a supplementary cementitious material.

Environmental conditions, age and manufacturing process seem to influence the contrasting exothermic performance from the BOF slags studied. This was also shown over the heat flow recorded with two major hydration peaks observed in samples C and D (*Figure 29*). The first hydration peak was documented within the first three hours of isothermal calorimetry, following a similar performance as other steel manufacturing slag analysed (Suraneni & Weiss, 2017; Wang & Suraneni, 2019). The second hydration peak was noted 29-31h after the experiment commenced, where a dominant peak was observed for both model systems (C, D). As mentioned early in section 4.4.2, this might be derived from an excess of $C_{12}A_7$ impacting silicate dissolution, generating a sulfate imbalance, which was evident as retardation in hydration with higher peaks (Wang & Suraneni, 2019).

4.5.3.2 Electric Arc Furnace slag.

Sample F, a ~70-year-old slag, presented the 2nd highest value (W/g of cementitious material) of measured heat flow within the first 2 hours of the test; showing a higher initial exothermic nature than other model systems using BOF and BF slags; hydration peaks of the EAF slag were just below the overall top-three samples (*D>C>I>**F***) with the highest heat flow measured during 168h at 50°C.

Contrary to the initial data recorded during isothermal calorimetry, when the test was completed, sample F presented inert characteristics, low reactivity and poor heat released (*35.32 J/g SCM*); those results indicated the low potential of EAF for sustainable concrete use, as a correlation between accumulated heat and heat flow influence characteristics of compressive strength in a concrete blend (Cristelo et al., 2021). Consistent with these reported results, Electric Arc Furnace slag tested for potential concrete utilisation by Rojas et al. (2004) presented null pozzolanic activity, indicating low potential of EAF for sustainable concrete use.

Findings on sample F (*EAF slag collected in Clydesdale, Scotland*) during thermogravimetric analysis also indicated poor hydraulic capacity and lower pozzolanic performance, as TGA results indicate calcium hydroxide consumption was 7.09 g/100 of SCM, suggesting it was unsuitable as a cementitious element on a concrete blend.

On the other hand, some studies including Muhmood et al. (2009) and Bernardo et al. (2007) have shown a positive perspective on the use of EAF slag for concrete mixtures if the slag is pretreated to remove Fe-oxide, as this action modifies the chemistry of the slag and increases hydraulic properties of the alkaline material, suitable for concrete utilisation.

4.5.3.3 Blast Furnace slag.

Model systems using Blast Furnace slag (*E, G, H, I, J*) presented a common trend of negative calcium hydroxide consumption over the TGA test, meaning portlandite [Ca $(OH)_2$] was produced during the weight loss reaction; this outcome is commonly associated with potential corrosion and durability impacts on cement strength. Registered CH consumption values from lowest to highest are expressed in grams per 100g of SCM: G= -0.532, E= -2.432, H= -16.492, I= -17.404, J= 33.53. Although it is commonly known that calcium hydroxide on concrete might have a negative impact, it is also adequate to maintain an alkaline environment within the composite blend and might be beneficial for sulfate control and to promote carbonation reactions (Z. Li et al., 2023).

The thermo-kinetics of cementitious paste I (*Hodbarrow, England*) were the highest of all legacy slags analysed with 185.63 J/g SCM, indicating latent hydraulic reactivity. The remaining BF samples (*E, G, H, J*) were classified as inert-not reactive, based on the low or almost null reactivity recorded in the calorimetry assessment. These results were expected as literature indicates an average of 19 J/g SCM for Blast Furnace slag (Suraneni et al., 2019). Sample G, collected in Consett, England, with a pre-1980 age had the lowest amount of released heat (*6.25 J/g SCM*). Samples E and H, with similar age range (pre-1985) collected at Barrow, England and Glengarnock, Scotland respectively, were between 20 to 26 J/g SCM in calorimeter measurements. Sample J (*Warton, England*) with an aging period above 80 years, presented a released heat of 38.12 J/g SCM, which was above the measured heat released of samples E and H, which in terms of age, had half of the carbonation period of sample J.

While suitable pozzolanic characteristics were found on sample I, the implementation of Blast Furnace slag for cement replacement is less common than the utilisation of other slag types, for instance Ground Granulated Blast Furnace Slag (*GGBFS*). GGBFS has shown better pozzolanic affinity compared to BF, mainly because of the amorphous nature and stable composition of GGBFS, which is defined during the post-processing and cooling stage.

BF and GGBFS derived from the same steel making process, however the velocity of the cooling process, which is slower for BF defines their crystalline nature, while a rapid contact with water or steam influences the physical and chemical characteristics of GGBFS (Ghorbani et al., 2023). Another key differentiator between BF and GGBFS is particle size, as hydraulic characteristics are highly dependent on the slag particle fineness, but not particularly keen for superfine slags (any slag type) as there is a correlation between powdered slag and compressive strength. Studies like Pang et al. (2022) revealed that although Ground Granulated Blast Furnace Slag is suitable for cementitious aims, superfine GGBFS slag when mixed for concrete might increase the hydraulic capacity of the mixture but will decrease compressive strength after long setting periods. Overall, up to now GGBFS seems to be the most reliable slag type to replace Ordinary Portland Cement in concrete mixtures and generate sustainable concrete.

4.5.3.4 Summary: the use of Isothermal calorimetry and thermogravimetry to evaluate pozzolanic properties of three types (BOF, BF and EAF) of legacy iron and steel slag for cementitious application.

Within the three types of slag analysed, only one model system using blast furnace slag (sample I) presented suitable characteristics for cementitious implementation; the model system using sample I produced between 1867-1968 in Hodbarrow Steel Works (*England*), which was classified as latent hydraulic following the parameters proposed by Wang et al. (2019). Heat released measured was 185.63 J/g SCM and calcium hydroxide consumption was -17.404 g/100g of SCM.

Samples A (*BOF*), B (*BOF*), D (*BOF*), E (*BF*), F(*EAF*), G (*BF*), H (*BF*), and J(*BF*) were classified as inert, meaning low heat released was measured during isothermal calorimetry and calcium hydroxide consumption (*TGA*) either was poor or negative [($Ca(OH)_2$ produced during test]. Sample C (*BOF*) stockpiled at Monclova, Mexico in 1999 showed heat released (180 g/100g SCM) consistent with literature in Wang et al. (2019) but calcium hydroxide consumption was outside the boundaries expected for BOF. However, this sample can be considered as pozzolanic, less reactive, because pozzolanic, as a concept, is mainly related to whether Ca ($OH)_2$ can be consumed and converted into C-S-H gel (N. Li & Unluer, 2023; Wang, 2016b; Wang & Suraneni, 2019); in this case calcium hydroxide consumption was high, thus sample C present pozzolanic characteristics.

4.5.4 Wider implications for slag reutilisation.

Iron and steel slag can often be reutilized, particularly in the construction industry, where, depending on the slag composition, it can be used as an aggregate or as supplementary cementitious material for Ordinary Portland Cement replacement (Wang et al., 2023). Evidence has also shown iron and steel slag can be effective as rail ballast or in road pavement based on durability and cost-effective characteristics (Chen & Wang, 2023).

There are more specific fields like agriculture or soil remediation that might find steel slag a suitable compound to resolve nutrient shortage on lands used for agroindustry, this being based on the elements and minerals the slag can provide (O'Connor et al., 2021; Oh et al., 2023). Another possible reutilisation is mineral carbonation of atmospheric CO_2, as explored in Chapter II.

Material cost savings, decreased environmental impact, and feasible chemical composition for cementitious aims are some of the benefits of cement replacement in concrete mixtures (Xu et al., 2023), a gap that iron and steel slag could cover. As well as current production there are billions of tonnes of legacy iron and steel making slags stockpiled in heaps. Riley et al. (2020) estimated there was ~190 Mt of legacy slag in the UK alone, while the results in Chapter III showed an estimated 273, 612.5 tonnes of legacy iron and steel slag in Mexico.

This chapter aimed to assess the potential of some legacy slags from Scotland, England and Mexico for use as supplementary cementitious materials. Based on this, the findings from the experimental work described in this chapter aimed to gain knowledge on the pozzolanic characteristics of legacy EAF, BOF and BF slags for concrete utilisation.

The performance of 8 out of 10 model systems (*A, B, D, E, F, G, H, J*) using legacy iron and steel slag tested, might not reflect the expected results on calcium hydroxide consumption or hydraulic behaviour to reinforce their potential use as a partial binder in concrete, but what the results did provide was a wider perspective on mineralogy, hydraulic capacity and pozzolanic performance of the three types of legacy slag tested in concrete blends. As referenced in the chapter and based on the results of sample I and the uncommon behaviour of sample C, there is evidence of pozzolanic and hydraulic properties on legacy BOF and BF slags. These findings are consistent with Wang et al. (2019) and Suraneni et al. (2017), where Basic Oxygen and Blast Furnace slags react positively during calcium hydroxide consumption testing and hydraulic heat release evaluations.

Both of these parameters are key indicators for determining whether steel-making by-products can contribute to compressive strength, durability, and feasible setting times when partially replacing Ordinary Portland Cement as a binder in concrete mixes.

Inherent interpretation of the results and discussion around the limitations of pozzolanic potential of the model systems studied was addressed in the context of the research aim to promote iron and steel slag utilisation for sustainable concrete blends. Whereas the use of BOF and BF is viable, cementitious properties of legacy iron and steel slag are unpredictable. Therefore, plausible modifications of the mass ratio of the steel manufacturing slag can be implemented as the addition of alkaline activators (*NaOH, $CaCl_2$, $CaSO_4 \cdot H_2O$*) or high silica content compounds (*silica fume, fly ash*) improves the slag composition resulting from the reaction with excessive calcium hydroxide (Suraneni et al., 2019). For EAF slag in particular, which is expected to become the dominant slag type in the coming decades (Andersson et al., 2023), future research on chemical characteristics is required to enhance its utilisation on construction materials.

While the results presented here suggest that legacy slag is typically not suitable in its current form for utilisation as SCMs, addition of alkaline activators as highlighted above could overcome this. There are, however, additional factors to consider before more widespread re-utilisation of legacy slags as SCMs. In the UK, Riley et al. (2020) found that many legacy slag deposits were protected due to their nature conservation value, i.e. the presence of rare species of plants, insects and nesting birds. Factors such as these would also need to be considered before excavation of legacy slag deposits for potential reutilisation as SCMs.

4.6 Conclusion.

4.6.1 Conclusion.

The use of iron and steel slag as supplementary cementitious material is in general a well-documented process for some slag types like GGBFS, showing evidence on the positive workability of GGBFS to partially replace Ordinary Portland Cement in sustainable concrete and its widespread acceptance in the construction industry. There are other iron and steel slag types (*BOF, BF, EAF*) which are less documented regarding their behaviour as a cementitious material and the study of internal and external conditions influencing the performance of the slag when used as SCM. Hundreds of millions of tonnes of these slags are produced every year globally (World Steel Association, 2023), as well as many billions of tonnes of stockpiled legacy slag, thus representing a major potential resource for use as SCMs. Therefore, data is needed on the pozzolanic and hydraulic characteristics of iron and steel slag influenced by post-processing, environment and aging periods. This will give a better understanding of the performance and wider implications of legacy BOF, BF and EAF iron and steel slag when implemented as cementitious material in sustainable concrete.

This chapter presented the findings recorded during the evaluation of cementitious properties of ten model systems (*A-J*) using legacy BOF, BF and EAF iron and steel slag samples from sites in Scotland, England and Mexico, examining their reactivity, pozzolanic characteristics and hydraulic behaviour by using x-ray diffraction, isothermal calorimetry and thermogravimetric analysis. The key findings are summarised below, and provide better understanding of the cementitious potential of the tested steel slag:

1) Qualitative x-ray diffraction analysis completed on BOF (*Basic Oxygen Furnace*), EAF (*Electric Arc Furnace*), and BF (*Blast Furnace*) slags showed mostly crystalline phases over XRD peaks analysed. This indicates potential poor pozzolanic characteristics of the slags when used as part of cementitious blends. Quantitative XRD could provide a better understanding on crystallographic limitations of the legacy slags, enabling compensation mechanisms like addition of alkaline activators such as NaOH, $CaCl_2$, or $CaSO_4 \cdot H_2O$, or the increase of silica content through the addition of silica fume or fly ash, to improve the slag composition.

2) Eight out of ten model systems analysed using legacy BOF, EAF and BF slag presented low hydraulic heat release and poor or negative calcium hydroxide consumption, categorizing them as inert under the pozzolanic classification provided by Wang et al.(2019). These are therefore not suitable in their current form as SCMs.

3) Latent hydraulic behaviour was identified in one out of ten model systems tested, following the classification method of Wang et al. (2019); the model system with feasible pozzolanic characteristics was made using legacy blast furnace iron slag (*aged ~ 100 years*), in this case the age of the blast furnace iron slag might not have a negative influence on the hydraulic and pozzolanic properties of the alkaline compound when used for partial cement replacement on sustainable concrete. Further research is needed to better understand how slag composition changes over time and how external conditions influence the development of its cementitious mechanisms.

4) Out-of-boundaries pozzolanic behaviour was found in one of ten model systems tested, a slag sample originated in Mexico in 1999. This presented excessive calcium hydroxide consumption, an indicator of the slag to convert Ca $(OH)_2$ into C-S-H gel, which is a key parameter for cement-based materials utilisation (N. Li & Unluer, 2023; Wang, 2016b; Wang & Suraneni, 2019). This sample was categorized as pozzolanic less reactive under the classification proposed by Wang et al. (2019).

Overall, legacy iron and steel slag tested in this chapter showed poor performance and low pozzolanic characteristics for being implemented as supplementary cementitious materials. However, a viable reutilisation approach is their use as a carbon removal technology through mineral carbonation, which was addressed in chapter II of this thesis.

References.

Akhil, & Singh, N. (2023). Microstructural characteristics of iron-steel slag concrete: A brief review. *Materials Today: Proceedings*. https://doi.org/10.1016/j.matpr.2023.03.548

Andersson, A., Isaksson, J., Lennartsson, A., & Engström, F. (2023). Insights into the Valorization of Electric Arc Furnace Slags as Supplementary Cementitious Materials. *Journal of Sustainable Metallurgy*. https://doi.org/10.1007/s40831-023-00778-y

Avet, F., Snellings, R., Alujas Diaz, A., Ben Haha, M., & Scrivener, K. (2016). Development of a new rapid, relevant and reliable (R3) test method to evaluate the pozzolanic reactivity of calcined kaolinitic clays. *Cement and Concrete Research*, *85*, 1–11. https://doi.org/10.1016/j.cemconres.2016.02.015

Baker, R. (2023, August). *Iron and Steel*. Historical Industry of Cumbria.

Barabanshchikov, Y., Usanova, K., Akimov, S., & Bílý, P. (2020). Low heat concrete with ground granulated blast furnace slag. *IOP Conference Series: Materials Science and Engineering*, *896*(1). https://doi.org/10.1088/1757-899X/896/1/012098

Beaudoin, J., & Odler, I. (2019). Hydration, Setting and Hardening of Portland Cement. In *Lea's Chemistry of Cement and Concrete* (pp. 157–250). Elsevier. https://doi.org/10.1016/B978-0-08-100773-0.00005-8

Bernardo, G., Marroccoli, M., Nobili, M., Telesca, A., & Valenti, G. L. (2007). The use of oil well-derived drilling waste and electric arc furnace slag as alternative raw materials in clinker production. *Resources, Conservation and Recycling*, *52*(1), 95–102. https://doi.org/10.1016/j.resconrec.2007.02.004

Brand, A. S., & Fanijo, E. O. (2020). A review of the influence of steel furnace slag type on the properties of cementitious composites. In *Applied Sciences (Switzerland)* (Vol. 10, Issue 22, pp. 1–27). MDPI AG. https://doi.org/10.3390/app10228210

Chen, G., & Wang, S. (2023). Research on macro-microscopic mechanical evolution mechanism of cement-stabilized steel slag. *Journal of Building Engineering*, *75*. https://doi.org/10.1016/j.jobe.2023.107047

Cristelo, N., Garcia-Lodeiro, I., Rivera, J. F., Miranda, T., Palomo, Á., Coelho, J., & Fernández-Jiménez, A. (2021). One-part hybrid cements from fly ash and electric arc furnace slag activated by sodium sulphate or sodium chloride. *Journal of Building Engineering*, *44*. https://doi.org/10.1016/j.jobe.2021.103298

Cumbria Archive and Local Studies Centre, B.-F. (2018, March 20). *Iron and Steel Works, Barrow-in-Furness*. Exploring Morecambe Bay.

Del Strother, P. (2019). Manufacture of Portland cement. In *Lea's Chemistry of Cement and Concrete* (pp. 31–56). Elsevier. https://doi.org/10.1016/B978-0-08-100773-0.00002-2

Donatello, S., Tyrer, M., & Cheeseman, C. R. (2010). Comparison of test methods to assess pozzolanic activity. *Cement and Concrete Composites*, *32*(2), 121–127. https://doi.org/10.1016/j.cemconcomp.2009.10.008

Durham County Council. (2020, September 12). *Looking back at Consett Steel Works*. Durham County Record Office.

Ghorbani, S., Stefanini, L., Sun, Y., Walkley, B., Provis, J. L., De Schutter, G., & Matthys, S. (2023). Characterisation of alkali-activated stainless steel slag and blast-furnace slag cements. *Cement and Concrete Composites*, *143*. https://doi.org/10.1016/j.cemconcomp.2023.105230

Herfort, D., & Macphee, D. E. (2019). Components in Portland. In *Lea's Chemistry of Cement and Concrete* (pp. 57–86). Elsevier. https://doi.org/10.1016/B978-0-08-100773-0.00003-4

Historic Environment Scotland. (2018). *Bellshill, Clydesdale Street, Clydesdale Tube Works*. Steel Works (19th Century) - (20th Century).

Hume, J. (2007, August 7). *Motherwell, Ravenscraig Steelworks*. National Record of the Historic Environment.

Jiang, Y., Ling, T. C., Shi, C., & Pan, S. Y. (2018). Characteristics of steel slags and their use in cement and concrete—A review. In *Resources, Conservation and Recycling* (Vol. 136, pp. 187–197). Elsevier B.V. https://doi.org/10.1016/j.resconrec.2018.04.023

Kurdowski, W. (2014). *Cement and Concrete Chemistry*. Springer Netherlands. https://doi.org/10.1007/978-94-007-7945-7

Li, Ling, T. C., & Pan, S. Y. (2022). Environmental benefit assessment of steel slag utilization and carbonation: A systematic review. In *Science of the Total Environment* (Vol. 806). Elsevier B.V. https://doi.org/10.1016/j.scitotenv.2021.150280

Li, N., & Unluer, C. (2023). Development of high-volume steel slag as cementitious material by ethylenediamine tetraacetic acid induced accelerated carbonation. *Powder Technology*, *428*. https://doi.org/10.1016/j.powtec.2023.118899

Li, Z., Zhou, X., Ma, H., & Hou, D. (2023). *Advanced concrete technology*.

Liska, M., Wilson, A., & Bensted, J. (2019). Special cements. In *Lea's Chemistry of Cement and Concrete* (pp. 585–640). Elsevier. https://doi.org/10.1016/B978-0-08-100773-0.00013-7

Lothenbach, B., Durdziński, P., & De Weerdt, K. (2016). *Thermogravimetric analysis*.

Mattila, H. P., Grigaliu-naite, I., & Zevenhoven, R. (2012). Chemical kinetics modeling and process parameter sensitivity for precipitated calcium carbonate production from steelmaking slags. *Chemical Engineering Journal*, *192*, 77–89. https://doi.org/10.1016/j.cej.2012.03.068

Mayes, W. M., Riley, A. L., Gomes, H. I., Brabham, P., Hamlyn, J., Pullin, H., & Renforth, P. (2018). Atmospheric CO2 Sequestration in Iron and Steel Slag: Consett, County Durham, United Kingdom. *Environmental Science and Technology*, *52*(14), 7892–7900. https://doi.org/10.1021/acs.est.8b01883

McCarthy, M. J., & Dyer, T. D. (2019). Pozzolanas and pozzolanic materials. In *Lea's Chemistry of Cement and Concrete* (pp. 363–467). Elsevier. https://doi.org/10.1016/B978-0-08-100773-0.00009-5

Moranville-Regourd, M., Kamali-Bernard, S., & Hewlett, P. (2019). Cements made from blastfurnace slag. In *Lea's Chemistry of Cement and Concrete* (pp. 469–507). Elsevier. https://doi.org/10.1016/B978-0-08-100773-0.00010-1

Muhmood, L., Vitta, S., & Venkateswaran, D. (2009). Cementitious and pozzolanic behavior of electric arc furnace steel slags. *Cement and Concrete Research*, *39*(2), 102–109. https://doi.org/10.1016/j.cemconres.2008.11.002

North Lanarkshire Council. (2023a). *Ravenscraig: Making Steel*. Culture and Leisure NL Ltd.

North Lanarkshire Council. (2023b). *Steelmaking at Ravenscraig*.

O'Connor, J., Nguyen, T. B. T., Honeyands, T., Monaghan, B., O'Dea, D., Rinklebe, J., Vinu, A., Hoang, S. A., Singh, G., Kirkham, M. B., & Bolan, N. (2021). Production, characterisation, utilisation, and beneficial soil application of steel slag: A review. *Journal of Hazardous Materials*, *419*. https://doi.org/10.1016/j.jhazmat.2021.126478

Oh, S. J., Irshad, M. K., Kang, M. W., Roh, H. S., Jeon, Y., & Lee, S. S. (2023). In-situ physical and chemical remediation of Cd and Pb contaminated mine soils cultivated with Chinese cabbage: A three-year field study. *Journal of Hazardous Materials*, *459*. https://doi.org/10.1016/j.jhazmat.2023.132091

Pang, L., Liao, S., Wang, D., & An, M. (2022). Influence of steel slag fineness on the hydration of cement-steel slag composite pastes. *Journal of Building Engineering*, *57*. https://doi.org/10.1016/j.jobe.2022.104866

Petitjean, Q., Choulet, F., Walter-Simonnet, A. V., Mariet, A. L., Laurent, H., Rosenthal, P., de Vaufleury, A., & Gimbert, F. (2021). Origin, fate and ecotoxicity of manganese from legacy metallurgical wastes. *Chemosphere*, *277*. https://doi.org/10.1016/j.chemosphere.2021.130337

Piatak, N. M., Parsons, M. B., & Seal, R. R. (2015). Characteristics and environmental aspects of slag: A review. In *Applied Geochemistry* (Vol. 57, pp. 236–266). Elsevier Ltd. https://doi.org/10.1016/j.apgeochem.2014.04.009

Reade, L. (2013). *The Red-Wud Kilburnie Blastie*. Wordpress.

Riley, A. L., MacDonald, J. M., Burke, I. T., Renforth, P., Jarvis, A. P., Hudson-Edwards, K. A., McKie, J., & Mayes, W. M. (2020). Legacy iron and steel wastes in the UK: Extent, resource potential, and management futures. *Journal of Geochemical Exploration*, *219*. https://doi.org/10.1016/j.gexplo.2020.106630

Rojas, M. F., & Sánchez De Rojas, M. I. (2004). Chemical assessment of the electric arc furnace slag as construction material: Expansive compounds. *Cement and Concrete Research*, *34*(10), 1881–1888. https://doi.org/10.1016/j.cemconres.2004.01.029

Scrivener, K., Snellings, R., & Lothenbach, B. (2016). *A practical guide to microstructural analysis of cementitious materials*.

Sims, I., Lay, J., & Ferrari, J. I. (2019). Concrete aggregates. In *Lea's Chemistry of Cement and Concrete* (pp. 699–778). Elsevier. https://doi.org/10.1016/B978-0-08-100773-0.00015-0

Snellings, R. (2016). *X-ray powder diffraction applied to cement*. www.crystallography.net

Snellings, R., & Scrivener, K. L. (2016). Rapid screening tests for supplementary cementitious materials: past and future. *Materials and Structures/Materiaux et Constructions*, *49*(8), 3265–3279. https://doi.org/10.1617/s11527-015-0718-z

Snellings, R., Suraneni, P., & Skibsted, J. (2023). Future and emerging supplementary cementitious materials. *Cement and Concrete Research*, *171*. https://doi.org/10.1016/j.cemconres.2023.107199

Suraneni, P., Hajibabaee, A., Ramanathan, S., Wang, Y., & Weiss, J. (2019). New insights from reactivity testing of supplementary cementitious materials. *Cement and Concrete Composites*, *103*, 331–338. https://doi.org/10.1016/j.cemconcomp.2019.05.017

Suraneni, P., & Weiss, J. (2017). Examining the pozzolanicity of supplementary cementitious materials using isothermal calorimetry and thermogravimetric analysis. *Cement and Concrete Composites*, *83*, 273–278. https://doi.org/10.1016/j.cemconcomp.2017.07.009

Thomas, C., Rosales, J., Polanco, J. A., & Agrela, F. (2018). Steel slags. In *New Trends in Eco-efficient and Recycled Concrete* (pp. 169–190). Elsevier. https://doi.org/10.1016/B978-0-08-102480-5.00007-5

Tironi, A., Trezza, M. A., Scian, A. N., & Irassar, E. F. (2013). Assessment of pozzolanic activity of different calcined clays. *Cement and Concrete Composites*, *37*(1), 319–327. https://doi.org/10.1016/j.cemconcomp.2013.01.002

Trout, E. A. R. (2019). The history of calcareous cements. In *Lea's Chemistry of Cement and Concrete* (pp. 1–29). Elsevier. https://doi.org/10.1016/B978-0-08-100773-0.00001-0

Vélez, N. L. J., Zamora, G. Hervey., De León, Homero., & Flores, V. F. A. (2002, November 1). *Experiencias y resultados alcanzados en los BOF´s de AHMSA al fabricar en casa sus propias escorias sintéticas*. Simposio Nacional de Siderurgia Instituto Tecnológico de Morelia.

Wang. (2016a). Environmental aspects of slag utilization. In *The Utilization of Slag in Civil Infrastructure Construction* (pp. 131–153). Elsevier. https://doi.org/10.1016/b978-0-08-100381-7.00007-0

Wang. (2016b). Slag use in cement manufacture and cementitious applications. In *The Utilization of Slag in Civil Infrastructure Construction* (pp. 305–337). Elsevier. https://doi.org/10.1016/b978-0-08-100381-7.00013-6

Wang, H., Gu, X., Liu, J., Zhu, Z., Wang, S., Xu, X., & Meng, J. (2023). Enhancement mechanism of micro-iron ore tailings on mechanical properties and hydration characteristics of cement-steel slag system. *Journal of Building Engineering*, *79*. https://doi.org/10.1016/j.jobe.2023.107882

Wang, & Suraneni. (2019). Experimental methods to determine the feasibility of steel slags as supplementary cementitious materials. *Construction and Building Materials*, *204*, 458–467. https://doi.org/10.1016/j.conbuildmat.2019.01.196

World Steel Association. (2023). *Steel industry co-products*.

Xu, Y., Lv, Y., & Qian, C. (2023). Comprehensive multiphase visualization of steel slag and related research in cement: Detection technology and application. In *Construction and Building Materials* (Vol. 386). Elsevier Ltd. https://doi.org/10.1016/j.conbuildmat.2023.131572

Yates, P. ; W. J. (2022). *The Carnforth Iron Works Trail*. Lancaster Civic Vision.

Chapter V. Conclusions and future work.

5.1 Introduction.

The work completed in this thesis was based in the context of the current global environmental overview, where the excess of greenhouse gases, particularly CO_2, demand innovative strategies for emissions reductions and carbon dioxide removal. Carbon dioxide removal is important in sectors and industries which are difficult to decarbonise, and where CO_2 may be removed alongside better management of industrial waste (Crippa et al., 2023; Li et al., 2022; Thonemann et al., 2022). The original research presented in this thesis was in the three practical chapters (*II-IV*). An exploration of the use of iron and steel slags from Mexico and Scotland for the sequestration of CO_2 was conducted in *Chapter II "Potential for the utilisation of mineral carbonation using steel slag as a solution to decrease atmospheric CO_2 levels"*. In the same chapter, it was also explored if external conditions could have influenced the amount of carbon dioxide quantified within the slag heaps studied: Monclova in Mexico and Ravenscraig in Scotland. In *Chapter III "Geospatial evaluation of legacy iron and steel slag sites in Mexico for CO_2 sequestration"*, the focus was to complete a volume estimation on the existent iron and steel slag deposits in Mexico, to generate a repository of the tonnage of the stockpiled slags in the country, to explore their potential re-utilisation in Mexico. Given the properties of iron and steel slags for their use as supplementary cementitious materials, in *Chapter IV "Utilisation of legacy iron and steel slag as sustainable construction material"*, the research was focused on the use of slag samples from England, Mexico and Scotland, to assess their hydraulic and pozzolanic properties and to measure their capacity to be used as a replacement material in sustainable concrete blends.

This chapter summarizes the original research presented in these three chapters and a discussion on the findings is given. By revisiting the aims initially set, the chapter aims to discuss if the findings of the practical work done were aligned to the initial plan and how this reflects any limitations found, and where future work could be completed to better understand the use of iron and steel slags for CO_2 sequestration or other reutilisation, in the context of Mexico and the United Kingdom.

5.2 Summary of Findings.

Original research presented in Chapters II, III and IV of this thesis involved the study of iron and steel slags to better understand their passive mineral carbonation, and to what extent local conditions might be implicated in their potential to sequestrate CO_2. Mexican slag deposits were studied and measured to have a current overview of the amount of iron and steel slags within the country and better develop strategies for their utilisation, related to local industries or needs. Within a further utilisation of iron and steel slags, an evaluation of the hydraulic and pozzolanic properties of these materials was completed, aiming to test their capacity to be a cementitious material replacement in sustainable concrete mixtures.

5.2.1 Findings review from Chapter II "Potential for the utilisation of mineral carbonation using steel slag as a solution to decrease atmospheric CO_2 levels".

Detailed in Chapter II are the methods to quantify the volume of CO_2 mineralised in legacy steel slags from Monclova, Mexico and Ravenscraig, Scotland. X-ray computed tomography was used on the slag samples, obtaining scanned versions of carbonated slags to further conduct a component segmentation and a volume fraction quantification of the components of interest: *Slag, Calcite* and *Pores*. Where the *Calcite* component represented the CO_2 precipitated as calcite ($CaCO_3$) within the slags, the *Slag* component grouped any other solid constituent of the samples tested and the *Pores* component included any empty spaces within the slags e.g., porosity or unfilled spots within the scans. Results from volume fraction quantification within the sixteen samples tested indicated contrasting amounts of CO_2 between both slag sets, where Scottish samples presented twice the amount of carbonated CO_2 measured in Mexican samples.

The differences in mineralised CO_2 volume between Mexican and Scottish steel slags enabled consideration of the impact of certain parameters related to the local context of where the slags carbonated, such as: carbonation time, humidity, pressure, temperature, pH or physical and chemical properties. Documented findings from the assessment were:

- Humidity was interpreted to be the most important parameter influencing mineral carbonation reactions within both slag sets studied. The abundance of rainfall in Scotland

potentially resulted in higher volumes of CO_2 carbonated in Scottish slags and the limited availability of humidity in Monclova, Mexico resulted in limited CO_2 sequestration in the slag samples from there.

- Although temperature conditions are markedly different between both locations where slags were passively carbonating, after the results assessment, this parameter was deemed to play a lesser role in determining the volume of CO_2 precipitated as calcite within the steel slags from Mexico and Scotland.

- Whereas further research is needed to better understand the relation between time, pressure and pH and the mineralisation of CO_2, after the assessment it can be said that these parameters did not play a major part in determining the amounts of CO_2 carbonated, when compared to humidity.

- Physical or chemical characteristics of the slags were not part of the assessment, however further analysis of their impact within passively carbonated slags would be merited.

5.2.2 Findings review from Chapter III "Geospatial evaluation of legacy iron and steel slag sites in Mexico for CO_2 sequestration".

Chapter III presented a volume estimation of slag deposited in Mexico, and also provided an overview of the land use in the proximities of the studied sites. The methods followed involved archival research of various historical records, shared by government agencies in Mexico, for site identification and contextual data recovery on each confirmed site. The volume estimation of the slag heaps involved the use geospatial tools, primary using the *Raster Surface Volume* mechanism from QGIS (2024) over the Digital Elevation Models (*DEM*) corresponding to the areas where the slag deposits were identified. Location data was corroborated by using Google Maps (2024) and Google Earth Pro (2024).

- Findings from the chapter detailed the identification of 16 slag deposits in Mexico, with a total estimated volume of ~273612.5 tonnes of slag. Most of the slag quantified was distributed in the vicinity of two of the largest steel manufacturing companies of the country. The site with the largest slag deposit (173117 tonnes) is located within Altos

Hornos de Mexico in Monclova, Coahuila; 72523.5 tonnes of slag are located in Lazaro Cardenas, Michoacan on the Pacific coast of Mexico within the industrial site of the company ArcelorMittal.

- Capturing potential of the slag sites was assessed through an empirical route as outlined in Chapter II of this thesis, and was calculated that Mexican slag heaps could capture around 5,745,862.5 Kg of CO_2 per tonne of steel slag. In an additional approach, projections on carbonation potential based on the work from Riley et al. (2020) and Pullin et al. (2019), were also completed, where the projected CO_2 sequestration through direct carbonation was between 80.9 – 92.2 Kt of CO_2, while enhanced carbonation could capture between 115.4 – 159.7 Kt of CO_2 if further developed in Mexico.

- Within the land use of slag deposits studied, the lack of conservation designations offers the chance for reusing slag heaps, potentially for CO_2 sequestration or sustainable concrete production. Repurposing legacy iron and steel slags in Mexico holds economic and environmental benefits, especially in the production of supplementary cementitious materials. As explored in Chapter IV of this thesis, Mexican slags might be useful for this aim, however further research is needed to better understand their properties within concrete blends. The repurposing of the slags could reduce greenhouse emissions and mitigate the environmental impact from the iron and steel industry, while used for sustainable concrete production, as construction material production is a key industry for Mexico.

5.2.3 Findings review from Chapter IV "Utilisation of legacy iron and steel slag as sustainable construction material".

Within Chapter IV, the reactivity of Basic Oxygen Furnace, Blast Furnace and Electric Arc Furnace slags from a selection of sites across the UK and Mexico was analysed through x-ray diffraction, isothermal calorimetry and thermogravimetry to evaluate their pozzolanic and hydraulic characteristics so as to investigate their potential to be used as supplementary cementitious materials in concrete blends. Documented findings were:

- Overall, limited pozzolanic characteristics were interpreted from an initial x-ray diffraction analysis, which determined that the BOF, BF and EAF slags tested showed almost null amorphous humps, which are indicative of potential cementitious properties. Slags

tested primarily showed a crystalline nature within the XRD spectra evaluated. Quantitative XRD may allow further understanding of the slag phases tested.

- Inert pozzolanic properties were determined in 8 out of 10 slags samples tested prepared with BF, BOF and EAF slags, based on lower measurements of heat released and poor consumption of calcium hydroxide, using the classification of Wang et al. (2019).

- Pozzolanic characteristics were found in one of the ten model systems studied, indicating feasibility for using as a cementitious material. The model system was made of a ~100 years aged Blast Furnace slag, and presented latent hydraulic properties within the classification proposed by Wang et al. (2019), used to categorize materials with a potential utilisation as concrete replacement.

- One model system presented pozzolanic, less reactive characteristics according to the Wang et al. (2019) method of classification; although this showed a potential use as cementitious material, further analysis is advised to assess if the excessive calcium hydroxide consumption measured would not represent a drawback when in concrete blends.

5.3 Discussion.

The summary of findings previously described might indicate individual results derived from the experimental work within chapters II, III and IV, however there is a correlation between the findings of the three chapters and the aims of the thesis defined in Chapter I, where the focus to increase knowledge on environmental remediation methods using iron and steel slags is key to mitigate excessive CO_2 from the atmosphere. Additionally, the research can feed into better waste management for steel industry waste and the potential utilisation of slags as construction materials in a circular economy approach.

The exploration of legacy iron and steel slags from contrasting geographical locations (*Mexico and the United Kingdom*) shapes the connection within the results from this research. In Chapter II, it was documented how much CO_2 could be captured within decadal timescales by legacy steel slags from Mexico and Scotland using x-ray computed tomography as a base to segment the phases integrating the slag samples and quantify the CO_2 mineralised as calcite within. The outcomes enabled further exploration of why the amounts of CO_2 were so different, with humidity interpreted as a key parameter in passive mineral carbonation of steel slags. This aspect has been studied from laboratory-based experiments where its impact was reported as higher CO_2 uptake within controlled conditions, as documented in Ragipani et al. (2021), Huijgen & Comans (2006) or Baras et al. (2023). This parameter has also been approached during passive carbonation in the work from Mayes et al. (2018), where the presence of water increased mineral weathering within the slag heaps, promoting the growth in the amount of carbonated CO_2 through mineral sequestration.

While the use of x-ray computed tomography was highly effective as a non-destructive method for assessing CO_2 mineralisation within the slags, its accuracy in quantifying the exact volume of mineralised CO_2 could benefit from further corroboration with complementary techniques. To address the limitations of the experimental approach used, it is important to recognize that while XCT was central to quantifying CO_2 mineralization in legacy slags, there are inherent limitations in relying solely on this method for accuracy. XCT is highly beneficial as a non-destructive tool, allowing for internal structural assessment without sample damage, and permitting further analyses on the same sample. In this study, XCT was used to segment rock samples and assess CO_2 mineralisation; however, complementary methods such as X-ray diffraction (XRD) were essential to validate that the segmented phases were indeed calcite (mineralised CO_2). While the XCT-based segmentation approach remains robust and effective, future work could incorporate additional techniques such as thermogravimetric analysis (TGA) or scanning electron microscopy (SEM) to further corroborate CO_2

quantification. Nevertheless, the approach undertaken here demonstrates a reliable and solid framework for investigating CO_2 mineralisation in iron and steel slags.

A more focused discussion on the parameters influencing CO_2 mineralisation in both slag deposits could provide an opportunity for deeper assessment. While the exploration of legacy iron and steel slags from Mexico and the United Kingdom offered valuable insights, certain limitations outside the scope of this research may have impacted the results. For example, that controlled laboratory experiments may not fully replicate real-world environmental conditions. Factors like temperature fluctuations, pollutant exposure, and long-term humidity changes could significantly affect carbonation rates in natural settings, as highlighted by Ragipani et al. (2021), Huijgen & Comans (2006) and Baras et al. (2023).

Overall Chapter II fulfilled the aim to provide some underpinning knowledge on the CO_2 sequestration potential of legacy iron and steel slags from Mexican and Scottish samples. To utilise legacy slags for CO_2 sequestration, it is essential to know the volumes/tonnages of legacy slag available, their geographical locations, and any constraints to their reutilisation. Riley et al. (2020) conducted research of this type for the UK (including Scotland) but this data was not available for Mexico. This limitation impacted the ability to develop a fully integrated analysis of the potential for slag reutilization across both regions. To addressed this, Chapter III focused on mapping legacy slag deposits in Mexico, but the lack of historical and geographical data on slag volumes restricted the completeness of the analysis. Future studies should focus on collecting this data to enable a more precise and strategic plan for slag reutilization. Another potential limitation or area of opportunity involved the DEM (Digital Elevation Model) resolution used for the volume measurement of the slag deposits. As only one resolution was available for this study, the accuracy of the results may have been impacted. In future work, the availability of DEMs with different or more accurate resolutions could provide a broader perspective and improve the precision of volume estimations. While a certain margin of error is expected in any experimental work, the absence of comparable data or previous studies in this area makes it difficult to fully evaluate the precision of the measurements. As such, reliance on the methodology, which was validated by similar studies in other locations, was necessary.

The aim, as in Chapter III, was to conduct a geospatial evaluation of legacy slag heaps, quantify the deposited slag, estimate the amount of atmospheric CO_2 sequestered through passive mineral carbonation, and compare these results to other enhanced CO_2 sequestration methods from the literature. Building on this knowledge gap, Chapter III focused on mapping legacy iron and steel slag deposits remaining unused in Mexico, and investigated how this could represent an opportunity for CO_2 sequestration. While CO_2 sequestration is an essential

task given the current climate crisis, legacy slag can be reutilised in other ways which ultimately help to offset global carbon emissions. Chapter IV explored the potential of samples from a range of sites in the UK and Mexico to be repurposed for the sustainable production of concrete, by evaluating the supplementary cementitious capacity of the slags in experimental concrete blends. The representativeness of these samples may not fully capture the diversity of slag materials available in the two countries, and further experimentation with a broader range of samples would strengthen the findings. Additionally, the laboratory-based nature of the experiments did not account for the potential scale-up challenges in industrial settings, such as variability in mixing conditions, long-term durability of slag-blended concretes, or the influence of external environmental factors on concrete performance.

Looking beyond the findings presented in Chapters II-IV, there are other uses for existent slag deposits in Mexico. For example, slag could be reprocessed and used as a source of metals, or for soil remediation in agribusiness, another key industry in the country. By knowing the estimated volume of slags in Mexico calculated in Chapter III, a general evaluation of how to utilise them, as documented for the UK in the work of Riley et al. (2020), could be developed as part of a remediation plan for decreasing industrial wastes in Mexico. Delimiting potential challenges within this implementation or any other implications of land use, for instance sites accessibility or safety reasons, could also be addressed. In this line, potential limitations include challenges in reprocessing slag for alternative uses, such as metal recovery or soil remediation in agribusiness, as noted in the conclusion. While Chapter III suggested the potential for these applications, the lack of experimental validation for these processes within this research indicates a need for further studies to assess the feasibility and environmental impacts of these alternative uses.

Beyond individual assessments completed within the three practical chapters, these converge with a shared objective, to address the pressing need for effective solutions in mitigating atmospheric CO_2 emissions and improving waste management practices within the steel industry. The limitations discussed above highlight the need for more extensive real-world testing, broader data availability, and consideration of scale-up challenges. These aspects must be addressed in future research to fully realize the potential of slags as a tool for climate mitigation and sustainable waste management. Even so, despite these limitations and the need for further research, the experimental work completed in this study has been valuable in highlighting the potential of steel manufacturing by-products for passive CO_2 sequestration and repurposing them into other applications, such as supplementary cementitious materials.

5.4 Suggestions for Future Work.

Based on the findings previously described and the knowledge gained while developing the three practical chapters of this thesis, there is a suggestion for developing research in addition of the work already completed in Chapters II, III and IV.

Suggestion for future work, Chapter II:

To extend the scope of the chapter and further explore Mexican steel slags in their capacity to sequestrate CO_2, by selecting new locations across the country (*from the mapping provided in chapter III of this thesis*) and conduct an evaluation towards CO_2 mineralisation capacity, to then extend it to analyse other components contained in the slags, apart from carbonated CO_2, in this approach other industrial fields might be beneficiated, for instance, by metal recovery from the slags.

Suggestion for future work, Chapter III:

Time constraints may be a challenge in promoting carbon capture initiatives with existing slag deposits in Mexico. However, the estimated volumes of slags can offer alternative opportunities for their utilization. One approach might involve the use of slags in agribusiness for soil remediation purposes. Another option could be within the construction industry, as these materials can serve as valuable supplementary cementitious materials or as components of construction aggregates, providing sustainable solutions while addressing environmental concerns.

Suggestion for future work, Chapter IV:

A further step in the study of legacy iron and steel slags as supplementary cementitious, might be to assess their long-term properties as construction material mortars. This would require controlled conditions emulating local environments from the place of disposal or assessing their progressive behaviour in a recreated lab-scale scenario with the conditions of a location where the construction materials mortars could be implemented. This would evaluate how the materials would change across time and their exposure to rough environments.

5.5 Closing Remarks.

Overall, the objectives of the thesis were fulfilled and the outcomes highlighted the need to develop further research within mineral carbonation of iron and steel slags, better understanding the passive carbonation approach and the parameters involved. This not only is applicable for Mexico and the United Kingdom; the idea could be extended to other locations with deposits of iron and steel slags.

From this thesis, it was seen that there exists a significant potential for CO_2 sequestration using iron and steel slags as highlighted in Chapter II. However, to further progress these efforts, future research could focus on optimizing carbonation techniques and exploring innovative methods for enhancing CO_2 capture efficiency.

In Chapter III, the utilization of slag heaps in Mexico can provide a dual opportunity for environmental sustainability and economic development. However, is needed to investigate the feasibility of utilizing slag heaps for other industrial applications beyond concrete production, such as in road construction or soil stabilization, as this could expand their potential benefits.

Furthermore, Chapter IV explored the application of iron and steel slags for supplementary cementitious utilisation. However further research in the area is needed to expand the understanding of long-term properties of different slag types.

Overall, it was considered that exploring and developing policy frameworks and incentive structures in the use of industrial wastes at global scale would encourage greater collaboration between steel manufacturers, governmental agencies, and other stakeholders, facilitating the sustainable utilization of slag heaps while addressing regulatory and economic challenges. By pursuing these avenues for future work, we can harness the full potential of slag heaps as valuable resources for environmental remediation and economic growth, not only for Mexico or the United Kingdom, but for many other regions in the world.

References.

Baras, A., Li, J., Ni, W., Hussain, Z., & Hitch, M. (2023). Evaluation of Potential Factors Affecting Steel Slag Carbonation. *Processes*, *11*(9), 2590. https://doi.org/10.3390/pr11092590

Crippa, M., Guizzardi, D., Schaaf, E., Monforti-Ferrario, F., Quadrelli, R., Risquez Martin, A., Rossi, S., Vignati, E., Muntean, M., Brandao De Melo, J., Oom, D., Pagani, F., Banja, M., Taghavi-Moharamli, P., Köykkä, J., Grassi, G., Branco, A., San-Miguel, J., & European Commission. Joint Research Centre. (2023). *GHG emissions of all world countries : 2023.*

Google Earth Pro. (2024). *Google Earth Pro*.

Google Maps. (2024). *Google Maps*.

Huijgen, W. J. J., & Comans, R. N. J. (2006). Carbonation of steel slag for CO2 sequestration: Leaching of products and reaction mechanisms. *Environmental Science and Technology*, *40*(8), 2790–2796. https://doi.org/10.1021/es052534b

Li, Ling, T. C., & Pan, S. Y. (2022). Environmental benefit assessment of steel slag utilization and carbonation: A systematic review. In *Science of the Total Environment* (Vol. 806). Elsevier B.V. https://doi.org/10.1016/j.scitotenv.2021.150280

Mayes, W. M., Riley, A. L., Gomes, H. I., Brabham, P., Hamlyn, J., Pullin, H., & Renforth, P. (2018). Atmospheric CO2 Sequestration in Iron and Steel Slag: Consett, County Durham, United Kingdom. *Environmental Science and Technology*, *52*(14), 7892–7900. https://doi.org/10.1021/acs.est.8b01883

Pullin, H., Bray, A. W., Burke, I. T., Muir, D. D., Sapsford, D. J., Mayes, W. M., & Renforth, P. (2019). Atmospheric Carbon Capture Performance of Legacy Iron and Steel Waste. *Environmental Science and Technology*, *53*(16), 9502–9511. https://doi.org/10.1021/acs.est.9b01265

QGIS. (2024). *QGIS*.

Ragipani, R., Bhattacharya, S., & Suresh, A. K. (2021). A review on steel slag valorisation: Via mineral carbonation. In *Reaction Chemistry and Engineering* (Vol. 6, Issue 7, pp. 1152–1178). Royal Society of Chemistry. https://doi.org/10.1039/d1re00035g

Riley, A. L., MacDonald, J. M., Burke, I. T., Renforth, P., Jarvis, A. P., Hudson-Edwards, K. A., McKie, J., & Mayes, W. M. (2020). Legacy iron and steel wastes in the UK: Extent, resource potential, and management futures. *Journal of Geochemical Exploration*, *219*. https://doi.org/10.1016/j.gexplo.2020.106630

Thonemann, N., Zacharopoulos, L., Fromme, F., & Nühlen, J. (2022). Environmental impacts of carbon capture and utilization by mineral carbonation: A systematic literature review and meta life cycle assessment. In *Journal of Cleaner Production* (Vol. 332). Elsevier Ltd. https://doi.org/10.1016/j.jclepro.2021.130067

Wang, & Suraneni. (2019). Experimental methods to determine the feasibility of steel slags as supplementary cementitious materials. *Construction and Building Materials*, *204*, 458–467. https://doi.org/10.1016/j.conbuildmat.2019.01.196

Appendix A.

Supplementary Materials for Chapter III: Geospatial evaluation of legacy iron and steel slag sites in Mexico for CO_2 sequestration.

The geospatial data of the 16 slag deposits studied in Chapter III. Geospatial evaluation of legacy iron and steel slag sites in Mexico for CO_2 sequestration, along with other supplementary materials contained within this folder for consultation. If further questions, please contact

Access:

https://gla-my.sharepoint.com/:f:/g/personal/j_del-angel-lozano_1_research_gla_ac_uk/EgNCSbMF8RVJomtMIzxvZdUBw1168mq8QIhh8PpkcFOHdQ?e=Ohyb1I

Password: *ChapterIII*16SlagDepositMexico*